UNIVERSIDADE FEDERAL DO CEARÁ
CENTRO DE CIÊNCIAS
DEPARTAMENTO DE BIOQUÍMICA E BIOLOGIA MOLECULAR
PROGRAMA DE PÓS-GRADUAÇÃO EM BIOQUÍMICA

ANTÔNIO WILLAME DA SILVA ALVES

Codium isthmocladum LECTIN 1 (CIL-1): INTERACTION WITH *N*-GLYCANS EXPLAINS ANTINOCICEPTIVE AND ANTI-INFLAMMATORY ACTIVITIES IN ADULT ZEBRAFISH (*Danio rerio*)

FORTALEZA
2021

ANTÔNIO WILLAME DA SILVA ALVES

Codium isthmocladum LECTIN 1 (CIL-1): INTERACTION WITH *N*-GLYCANS EXPLAINS ANTINOCICEPTIVE AND ANTI-INFLAMMATORY ACTIVITIES IN ADULT ZEBRAFISH (*Danio rerio*)

Tese apresentada ao Programa de Pós-Graduação em Bioquímica da Universidade Federal do Ceará, como requisito parcial à obtenção do título de Doutor em Bioquímica. Área de concentração: Bioquímica Vegetal.

Orientador: Prof. Dr. Bruno Anderson Matias da Rocha.

Coorientador: Prof. Dr. Celso Shiniti Nagano.

FORTALEZA

2021

Dados Internacionais de Catalogação na Publicação
Universidade Federal do Ceará
Biblioteca Universitária
Gerada automaticamente pelo módulo Catalog, mediante os dados fornecidos pelo(a) autor(a)

A477c Alves, Antônio Willame da Silva.
Codium isthmocladum lectin 1 (CiL-1): Interaction with N-glycans explains antinociceptive and anti-inflammatory activities in adult zebrafish (Danio rerio) / Antônio Willame da Silva Alves. – 2021.
84 f. : il. color.

Tese (doutorado) – Universidade Federal do Ceará, Centro de Ciências, Programa de Pós-Graduação em Bioquímica , Fortaleza, 2021.
Orientação: Prof. Dr. Bruno Anderson Matias da Rocha.
Coorientação: Prof. Dr. Celso Shiniti Nagano.

1. Macroalga marinha verde. 2. Lectina de ligação à galactose. 3. Ácido siálico. 4. Canais TRP. 5. Espécies reativas de oxigênio. I. Título.

CDD 572

ANTÔNIO WILLAME DA SILVA ALVES

Codium isthmocladum LECTIN 1 (CIL-1): INTERACTION WITH *N*-GLYCANS EXPLAINS ANTINOCICEPTIVE AND ANTI-INFLAMMATORY ACTIVITIES IN ADULT ZEBRAFISH (*Danio rerio*)

Tese apresentada ao Programa de Pós-Graduação em Bioquímica da Universidade Federal do Ceará, como requisito parcial à obtenção do título de Doutor em Bioquímica. Área de concentração: Bioquímica Vegetal.

Aprovada em: 30/06/2021.

BANCA EXAMINADORA

_____
Prof. Dr. Bruno Anderson Matias da Rocha (Orientador)
Universidade Federal do Ceará (UFC)

_____
Prof. Dr. Claudener Souza Teixeira
Universidade Federal do Ceará (UFC)

_____
Profa. Dra. Ana Lúcia Pontes Freitas
Universidade Federal do Ceará (UFC)

_____
Prof. Dr. Eridan Orlando Pereira Tramontina Florean
Universidade Estadual do Ceará (UECE)

_____
Prof. Dr. Ito Liberato Barroso Neto
Centro Universitário Christus (UNICHRISTUS)

A Deus e à minha família.

AGRADECIMENTOS

A Deus que cuida de mim e das pessoas que amo.

À minha mãe Francisca por todo amor e educação e ao meu pai Francisco, por todo apoio, até mesmo nos momentos mais difíceis.

Ao Prof. Bruno da Rocha, pelo acolhimento, orientação e conhecimento compartilhado.

Ao Prof. Celso Nagano e ao Prof. Alexandre Sampaio, pelo acolhimento, conhecimento compartilhado e parceria.

Ao Prof. Eridan Florean pelo suporte e contribuições fundamentais para a realização desse trabalho.

A Profa. Izabel Guedes pela parceria e contribuições.

A todos os autores do artigo produzido a parir desse estudo. Grato por todas as contribuições.

A todos do Grupo de Biotecnologia Molecular e Estrutural (GBME) com quem tenho o prazer de conviver e trabalhar. Aos colegas do Departamento de Bioquímica e Biologia Molecular, que sempre me ajudaram.

A todos do Laboratório de Biotecnologia Marinha por todos os esforços e parceria.

Aos animais que passaram pelas minhas mãos em prol da ciência.

Aos professores e funcionários do Departamento de Bioquímica e Biologia Molecular - UFC.

Ao CNPq, a CAPES e a UFC por financiamento de bolsa e projetos que auxiliaram no desenvolvimento da pesquisa.

De modo geral, a todos que direta ou indiretamente contribuíram com a realização deste trabalho e conclusão desta importante etapa de minha vida.

Gratidão.

“Ninguém nasce pronto. A vida é para quem é corajoso o suficiente para ariscar e humilde o bastante para aprender”

Clarice Lispector

RESUMO

A inflamação e o estresse oxidativo são processos associados a diferentes doenças humanas. São tratadas com o uso de drogas que apresentam vários efeitos colaterais. As macroalgas marinhas são fontes de compostos naturais potencialmente relevantes para uso como tratamento terapêutico dessas desordens. As lectinas têm capacidade de interagir reversivelmente com carboidratos complexos e modular os receptores glicosilados da membrana celular por meio dessa interação. Este estudo teve como objetivo determinar o potencial antinociceptivo e antiinflamatório de CiL-1 em peixes-zebra adultos pela modulação do TRPA1 por meio da ligação lectina-glicano. A nocicepção foi induzida por formalina e a inflamação foi induzida por carragenina. O conteúdo de ROS foi determinado usando DCFH-DA. A possível neuromodulação pelo canal TRPA1 também foi avaliada por pré-tratamento com cânfora. CiL-1 foi eficaz em todas as doses testadas, revelando efeitos antinociceptivos e antiinflamatórios em peixes-zebra adultos. Esta lectina de ligação à galactose também foi capaz de reduzir o conteúdo de ROS no cérebro e no fígado. Análises in silico mostraram interações de CiL-1 com ambos os ligantes testados. Oligossacarídeo-1 (LacNac2) apresenta a energia de ligação mais favorável com a proteína. A interação ocorre em 4 subsites como uma conformação estendida no site. O oligossacarídeo-2 (LacNac2-Sia) teve a curva de interação energética menos favorável. Com base nas previsões feitas para os oligossacarídeos, um glicano putativo tetra-antenato foi esquematicamente construído, ilustrando uma interação entre TRPA1 N-glicano e CiL-1. Essa ligação parece estar relacionada à atividade antiinflamatória da CiL-1 como resultado da modulação do receptor.

Palavras-chave: Macroalga marinha verde. Lectina de ligação à galactose. Ácido siálico. Canais TRP. Espécies reativas de oxigênio.

ABSTRACT

Inflammation and oxidative stress are processes associated with different human diseases. They are treated using drugs that have several side effects. Seaweed are sources of potentially relevant natural compounds for use as a therapeutic treatment of these disorders. Lectins are able to reversibly interact with complex carbohydrates and modulate cell membrane glycosylated receptors through this interaction. This study aimed to determine the antinociceptive and anti-inflammatory potential of CiL-1 in adult zebrafish by modulation of TRPA1 through lectin-glycan binding. Nociception was induced by formalin, and inflammation was induced by carrageenan. ROS content was determined using DCFH-DA. Possible neuromodulation by TRPA1 channel was also evaluated by camphor pretreatment. CiL-1 was efficacious at all tested doses, revealing anti-nociceptive and anti-inflammatory effects in adult zebrafish. This galactose-binding lectin was also able to reduce the content of ROS in brain and liver. *In silico* analyses showed CiL-1 interactions with both ligands tested. Oligosaccharide-1 (LacNac2) presents the most favorable binding energy with the protein. The interaction occurs at 4 subsites as an extended conformation at the site. Oligosaccharide-2 (LacNac2-Sia) had a less favorable curved-shape interaction energy. Based on the predictions made for the oligosaccharides, a tetra-antenate putative glycan was schematically constructed, illustrating an interaction between TRPA1 *N*-glycan and CiL-1. This binding seems to be related to CiL-1 anti-inflammatory activity as result of receptor modulation.

Keywords: Green seaweed. Galactose-binding lectina. Sialic acid. TRP channels. Reactive oxygen species.

LISTA DE ILUSTRAÇÕES

SUMÁRIO

1 INTRODUÇÃO

1.1 Alga

A definição clássica de algas classifica um grupo heterogêneo de organismos fotossintetizantes que habitam ambientes marinhos, de água doce e terrestres úmidos, apresentando formas de vida planctônica, como microalgas, e bentônica, como macroalgas (SZE, 1997). O termo alga é usado para designar um imenso grupo polifilético, no qual os organismos podem ou não compartilhar linhas evolutivas e ancestrais em comum. Devido à complexidade, ao grande número de organismos e a diferentes origens evolutivas das espécies, a classificação das algas é constantemente atualizada (GUIRY; GUIRY, 2020). Avanços como a utilização de técnicas de microscopia eletrônica de transmissão e de varredura e o sequenciamento de nucleotídeos permitem a comparação de características moleculares e morfológicas que objetivam reforçar a segurança na identificação e classificação das espécies (SILVA, 2008).

As macroalgas, por sua vez, compreendem um grupo de organismos fotossintetizante que habitam ambientes marinhos e de água doce, com representantes do dodomínio *eucarya* (KIDGELL et al., 2019).

As macroalgas marinhas habitam ambientes salinos e apresentam grande relevância ecológica por contribuírem com a produção primária, fixando carbono e produzindo oxigênio que é solubilizado na água marinha e usado pelos demais organismos aquáticos, atuarem na mineralização e no ciclo dos principais elementos químicos, constituírem a base da cadeia alimentar para animais herbívoros e onívoros, e ao morrerem, seus constituintes químicos sofrem transformações no sedimento, sendo solubilizados e reciclados na água (KIDGELL et al., 2019).

As semelhanças biológicas e ecológicas das macroalgas marinhas com plantas aquáticas superiores são notáveis, porém, por não apresentarem tecidos especializados (talófitas) e não compartilharem aspectos evolutivos, as macroalgas são classificadas em um grupo distinto (MORAIS et al., 2020).

As macroalgas marinhas têm distribuição na zona eufótica da coluna de água e a abundância dos diferentes tipos são dependentes de:

1. Fatores físicos, tais como marés, disponibilidade de luz, tipo de substrato, dessecação, exposição às correntes marítimas e temperatura.

2. Fatores químicos, como o pH, disponibilidade de nutrientes e salinidade.

3. Fatores biológicos, como a competição, herbivoria e ação antrópica. Muitas

espécies apresentam variação sazonal de distribuição, sendo mais abundantes quando as condições ambientais são favoráveis (PHANG et al., 2016).

As algas são classificadas em três grupos com base na abundância da pigmentação. Existem aproximadamente 10.000 espécies classificadas em: Ochrophyta, rhodophyta e chlorophyta (MORAIS et al., 2020).

Ochrophyta (algas pardas) com aproximadamente 1.800 espécies, é o grupo menos abundante. Apenas 1% das espécies conhecidas são de água doce. A cor marrom está relacionada aos pigmentos carotenóides e fucoxantinas. Além desses, caroteno, violaxantina, diatoxantina e clorofila são encontrados (CHERRY et al., 2019).

Rhodophyta (algas vermelhas) com aproximadamente 6.100 espécies, das quais, apenas 150 são de água doce (PHANG et al., 2016). É o grupo mais adaptado a maiores profundezas, onde sua fotossíntese é mais eficiente. A cor vermelha resulta da presença de pigmentos, ficoeritrina e ficocianina. Além desses, caroteno, luteína, zeaxantina e clorofila são encontrados (CORINO et al.,2019).

Chlorophyta (algas verdes) é o grupo mais diversificado, com mais de 13.000 espécies. Estima-se que cerca da metade são de macroalgas marinhas. A cor verde se deve à presença das clorofilas a e b, pigmento utilizado durante o processo fotossintético. Sua cor geralmente depende do equilíbrio entre essas clorofilas e outros pigmentos, tais como carotenos e xantofilas. O amido é o principal polissacarídeo de reserva, estocado dentro dos cloroplastos. A parede celular da maioria das algas verdes é formada por celulose e uma matriz extracelular de polissacarídeos sulfatados rica em arabino-galactanas, ramnanas e ulvanas. Pode ainda ocorrer o depósito de carbonato de cálcio em algumas espécies. As algas verdes são comuns em áreas com luz abundante, como águas rasas e poças de maré. Os principais gêneros incluem *Ulva, Codium, Chaetomorpha e Cladophora* (CORINO et al.,2019).

1.2 Gênero *Codium*

O gênero *Codium* possui aproximadamente 144 espécies e pertencem ao Filo *Chlorophyta*, Sub-filo *Tetraphytina*, a Classe *Ulvophyceae* e Família *Codiaceae*. Morfologicamente são constituídas por talo cenocítico, filamentos tubulares contínuos sem divisão celular, se comportando como uma célula gigante com vários núcleos e cloroplastos dispostos livremente em citosol compartilhado (BARSANTI; GUALTIERI, 2014). Geograficamente são distribuídas em ambientes tropicais e temperados. Podem ser comumente encontradas na América do Sul, Central e do Norte, Europa e África. Devido sua adaptação de eficiência fotossintética, costuma se distribuir em regiões do mesolitoral em zonas de poças de maré (KEITH; KERSWELL; CONNOLLY, 2014). As populações de *Codium* são, geralmente, dioicas com um ciclo de vida diploide com meiose gamética, com a reprodução sexuada efetuada pela fusão de gametas haploides em zigotos. Os seus picos de reprodução e de crescimento coincidem, ocorrendo quando as condições ambientais são propícias, geralmente no fim do Verão e princípio do Outono (KANG et al., 2008).

A costa marinha nordestina abriga uma considerável variedade de *Codium ssp.* A praia de Paracuru – CE apresenta extenso banco natural, lar de diversas espécies de macroalgas marinhas, dentre elas *Codium isthmocladum*, a espécie alvo deste estudo que teve duas lectinas purificadas e caracterizadas recentemente. Esta, é uma macroalga com variação sazonal, apresentando cor verde-escura, talo esponjoso, que pode atingir até 40 cm de comprimento e 8 a 10 mm de diâmetro, tendo como epífitas típicas espécies dos géneros *Ulva, Ceramium, Ectocarpus e Chaetomorpha*. É fixada ao substrato por uma estrutura denominada opressório na forma de um pequeno disco, tem ramificação dicotómica, e apresenta forma cilíndrica (Figura 1).

De modo geral, as macroalgas marinhas, bem como a espécie *C. isthmocladum*, apresentam grande abundância de proteínas. Dentre elas destacam-se as lectinas, uma classe de proteínas que vêm sendo estudada há mais de seis décadas e apresenta grande importância biotecnológica.

Figura 1- Exemplar de *Codium isthmocladum*.

Reino: *Plantae;*

Divisão: *Chlorophyta;*

Classe: *Ulvophyceae;*

Orden: *Bryopsidales;*

Família: *Codiaceae;*

Gênero: *Codium;*

Espécie: *Codium isthmocladum Vickers 1905.*

Fonte: Google imagens; Algae Base.

1.3 Lectinas

Etimologicamente a palavra lectina vem do latim *Legere* e significa selecionar ou escolher. O termo foi proposto por Boyd e Shapleigh no ano de 1954 ao descrever uma classe de aglutininas de plantas superiores. As lectinas possuem ampla distribuição na natureza e já foram isoladas em vírus, bactérias, fungos, algas, plantas superiores e animais (WELCH et al., 2020). Devido à grande diversidade estrutural forma um grupo heterogêneo de proteínas ou glicoproteínas que teve sua definição atualizada ao longo de todo histórico de pesquisa. A definição mais clássica assume que as lectinas apresentam como características gerais a grande variedade em tamanho, estrutura e organização molecular, contudo, não apresentam origem imune e tem a capacidade de reconhecer e interagir de forma específica com carboidratos ou glicoconjugados (MANNING et al., 2017; PEUMANS; VAN DAMME, 1995). Possuem a propriedade de aglutinar células sanguíneas devido a interação com glicoconjugados presentes na membrana celular, e por esse motivo também são denominadas de aglutininas (FEIZI; HALTIWANGER, 2015). A definição mais recente classifica uma lectina como uma proteína ou glicoproteína com pelo menos um domínio não catalítico que pode se ligar específica e reversivelmente a monossacarídeos ou oligossacarídeos (CHEN et al., 2019; WANG et al., 2019). Dessa forma proteínas de origem imune (a partir da nova

classificação incluída no grupo) e não imune que podem apresentar ou não domínios catalíticos passaram a ser classificados como lectinas, aumentando consideravelmente a diversidade dessas moléculas.

Historicamente, a primeira aglutinina descrita na literatura data de 1860, e foi isolada do veneno da espécie *Crotalus durissus,* comumente conhecida como cascavel. Duas décadas depois, em 1888, a primeira lectina de origem vegetal foi descrita, sendo isolada da semente da mamona *Ricinus communis.* (MITCHEL, 1860; WORBS et al., 2015). Em 1966 a primeira lectina de alga foi descrita, a partir da determinação da atividade hemaglutinante de eritrócitos humanos do extrato de algas marinhas (BOYD; ALMODÓVAR, 1966). No Brasil, o primeiro estudo com lectinas de espécies coletadas localmente se deu em 1991, com o *screening* de hemaglutininas marinhas brasileiras (AINOUZ; SAMPAIO, 1991). Atualmente várias lectinas já foram caracterizadas e apresentam grande importância biotecnológica, contudo, ainda são poucas as publicações de lectinas de algas quando comparadas a plantas ou até mesmo animais. Isso acontece devido ao baixo rendimento e relativa dificuldade em se obter material de estudo.

As lectinas são macromoléculas amplamente encontradas em diferentes tecidos dos seres vivos, estando presentes em células de origem animal e vegetal (COELHO et al., 2017) e exibem diversas funções diferentes, podendo atuar em processos de reconhecimento celular, citotoxicidade de patógenos, adesão celular, interações célula-matriz, indução de apoptose, aglutinação de células e bactérias em animais, e ainda, em vegetais atuam como moléculas de defesa, de reserva energética, de controle da homeostase, e participam da simbiose de plantas com bactérias nitrificantes (DANGUY et al., 2002).

Levando em consideração a estrutura, as lectinas são atualmente classificadas de acordo com os domínios de interação com carboidratos e catalíticos em quatro grupos. As lectinas que apresentam somente um domínio de reconhecimento e ligação a carboidratos são classificadas como merolectinas, e por esse motivo, não são capazes de aglutinar células (Figura 02). As que apresentam mais de um domínio de reconhecimento e ligação a um tipo de carboidrato, são classificadas como hololectinas e por esse motivo são capazes de aglutinar células, sendo denominadas também de aglutininas. Essa propriedade é amplamente aplicada em processos de purificação para determinar a presença ou ausência de lectinas em uma solução com diferentes tipos de proteína. A grande maioria das lectinas conhecidas pertencem a esse grupo (Figura 02). As que apresentam mais de um domínio de reconhecimento e ligação independente a diferentes carboidrato, são classificadas como superlectinas (Figura 02). E ainda, há as lectinas que apresentam domínios catalíticos além dos domínios de

reconhecimento e ligação a carboidratos, estas são classificadas como quimerolectinas. Os domínios catalíticos atuam independentemente dos domínios ligantes a carboidratos (Figura 2). A lectina mais conhecida desse grupo é a ricina. Uma proteína altamente tóxica de origem vegetal (mamona) e sua toxicidade está associada a diferentes mecanismos de ação nos diferentes domínios em sua estrutura que combinados permitem a inativação de ribossomos (PEUMANS; VAN DAMME, 1998; RIBEIRO et al., 2018; TSANEVA; VAN DAMME, 2020).

Como dito anteriormente, as lectinas estão presentes em quase todos os organismos vivos, constantemente lectinas de macroalgas marinhas vêm sendo purificadas, caracterizadas e há quase três décadas importantes propriedades têm sido descobertas.

Figura 2- Classificação das lectinas baseado na diversidade estrutural.
Merolactinas: apresentam somente um domínio de reconhecimento e ligação a carboidratos (DRLC). Hololectinas: apresentam mais de um DRLC com apenas um tipo de carboidrato. Quimerolectinas: apresentam domínios catalíticos além dos DRLC. Superlectina: apresentam mais de um DRLC que interagem independentemente com diferentes carboidratos.

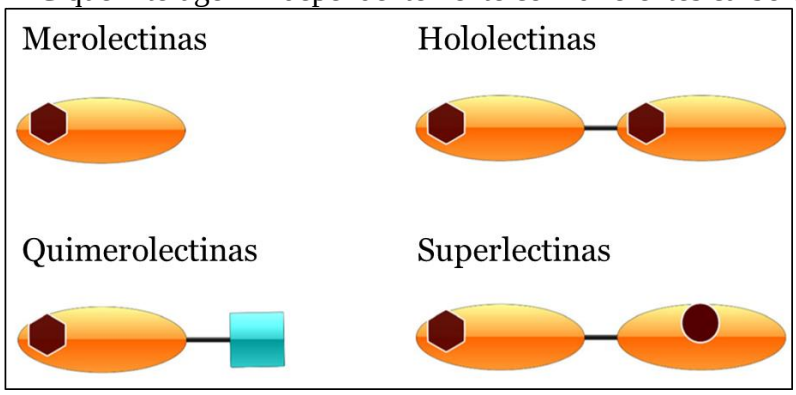

Fonte: TSANEVA; VAN DAMME, 2020 (adaptado).

1.4 Lectinas de macroalgas marinhas

As lectinas de macroalgas marinhas vêm sendo estudadas desde 1996, desde o primeiro estudo com o objetivo de identificar aglutininas, várias propriedades relevantes foram identificadas nessas moléculas (BOYD et al., 1966). Desde então, com o desenvolvimento de técnicas de extração e purificação, representantes dos três grupos de macroalgas já tiveram lectinas purificadas (PLIEGO-CORTÉS et al., 2020). Apesar da grande diversidade estrutural, costumam apresentar baixo peso molecular, apresentam menor afinidade por monossacarídeos e maior afinidade por oligossacarídeos e glicoproteínas. Costumam ter alta proporção de aminoácidos ácidos e aminoácidos essenciais, apresentam pontos isoelétricos também ácidos (entre 4 e 6), são termoestáveis e não dependente de

cátions divalentes. Entretando, algumas lectinas já caracterizadas dos gêneros *Enteromorpha*, *Ulva* e *Codium* tem especificidade por monossacarídeos e são dependentes de Ca^{2+} (PÉREZ; FALQUÉ; DOMÍNGUEZ, 2016; YOON et al., 2008; CARNEIRO et al., 2020).

O primeiro relato de atividade hemaglutinante de macroalgas foi realizado em 1966 e descreveu a atividade em 24 extratos proteicos de espécies nativas do Porto Rico. Desde então, novas lectinas de macroalgas marinhas têm sido purificadas e caracterizadas. No Brasil, os estudos com espécies nativas se iniciaram em 1991, com o *screening* de atividade hemaglutinante de 20 espécies (AINOUZ; SAMPAIO, 1991).

A primeira lectinas do gênero *Codium* foi isolada em 1985 e pertencia a espécie *Codium fragile* (ROGERS; LOVELESS; BALDING, 1986), desde então outras 14 espécies tiveram lectinas purificadas e caracterizadas em diferentes níveis. Estas apresentaram características semelhantes. A especificidade de ligantes costuma ser para os monossacarídeos GalNAc e/ou GlcNAc e para as glicoproteínas mucina e fetuína. Quanto a caracterização bioquímica, costumam apresentar ponto isoelétrico ácido e a maioria não depende de cátions para exibir atividade hemaglutinante, embora haja exceções. Podem apresentar formas monoméricas ou oligoméricas.

Recentemente duas novas lectinas de *C. isthmocladum* foram purificadas através de técnicas de cromatografia de troca iônica e exclusão molecular, e caracterizadas quanto a aspectos físico-químicos. São elas, Lectina de *Codium isthmocladum* 1 e 2 (CiL-1 e CiL-2). As duas lectinas foram capazes de aglutinar eritrócitos humanos e de coelhos. CiL-1 é constituída de uma cadeia monomérica de 12 kDa e apresenta especificidade de ligação a galactosídeos e fetuína. CiL-2 é constituída de um oligômero com cadeias de 12,3 kDa e apresenta especificidade de ligação a GalNAc e mucina do estômago de porco (PSM). CiL-1 juntamente com lectina de *C. barbatum* CBA são as únicas lectinas do gênero *Codium* que tiveram a sequência de aminoácidos elucidada. Foi possível ainda obter o modelo de CiL-1 (PRASEPTIANGGA; HIRAYAMA; HORI, 2012; CARNEIRO et al., 2020). Na tabela 1 estão representadas as espécies de *Codium* que possuem lectinas isoladas e suas principais características físico-químicas.

Tabela 1 - Características de lectinas isoladas de algas marinhas do gênero *Codium*.

Espécie	MM (kDa)	Inibição	Subunidade	Referência
C. adherens	65,8	GalNAc	-	ROGERS et al., 1994
C.arabicum	-	GalNAc/GclNAc	-	DINH; HORI; QUANG, 2009
C. bursa	18,4	GalNAc	1	ROGERS; FLANGU, 1991
C. capitatum	62,9	GalNAc	4	ROGERS et al., 1994
C. effusum	13,9	GalNAc	1	ROGERS et al., 1994
C. fragile ssp atlaticum	60,0	GalNAc	4	ROGERS; LOVELESS; BALDING, 1986
C. fragile ssp tomentosoides	60,0	GalNAc	4	ROGERS; LOVELESS; BALDING, 1986
C. giraffa	17,0	GalNAc	1	ALVAREZ et al.,1999
C. platylobium	12,8	GalNAc	2	ROGERS et al., 1994
C. taylori	-	GalNAc	-	CHILES; BIRD, 1989
C. tomentosum	15,5	GclNAc	2	FABREGAS et al., 1988
C. vermilara	17,8	GalNAc	2	ROGERS; FANGU, 1991
C. isthmocladum	12	GalNAc	1	CARNEIRO et al., 2020

Fonte: RODRIGUES, 2011 (adaptado).

Apesar do crescente número de trabalhos referentes às lectinas de macroalgas marinhas nas últimas décadas, estudos de caracterização bioquímica e estruturais ainda permanecem menos numerosos quando comparado com trabalhos de lectinas de plantas superiores. Na última década houve o aumento de esforços para caracterização estrutural de lectinas de invertebrados e macroalgas marinhas da costa nordestina. Diversas técnicas com aplicação de biofísica como espectrometria de massas, espectroscopia de dicroísmo circular, espectroscopia de fluorescência, cristalografia, difração de raios X e ressonância magnética nuclear, e de biologia molecular, como PCR, clonagem, expressão heteróloga e sequenciamento genético tem sido empregada com sucesso e vem se tornando cada vez mais relevante nessa área. O estudo estrutural a partir da combinação de resultados das técnicas listadas e de ferramentas de bioinformática vêm se tornando cada vez mais relevante para compreender o mecanismo de ação a nível molecular das atividades biológicas, ou ainda fazer alterações moleculares direcionadas com o propósito de aumentar a eficiência ou ainda desenvolver novas drogas (MEIERS et al., 2019; NOTOVA et al., 2020).

Graças aos esforços empregados na aplicação de purificação e caracterização estrutural de CiL-1, um modelo foi proposto e validado (ANEXO A).

1.5 Estrutura de CiL-1

O modelo estrutural da CiL-1 é constituído de 110 resíduos de aminoácidos e apresenta uma estrutura global composta por quatro folhas-β duplas dispostos em um arranjo tridimensional semelhante a um barril, conectados por loops de tamanhos variados. Apresenta um núcleo hidrofóbico bem estruturado composto por resíduos alifáticos e/ou aromáticos pertencentes a cada uma das folhas-β. A estrutura apresenta duas pontes dissulfeto que ligam os resíduos 17 e 65 ao 20 e 68 respectivamente. Essas ligações estabilizam importantes estruturas em loop presente nos sítios de ligação (Figura 3) (CARNEIRO et al., 2020).

CiL-1 apresenta dois sítios independentes de ligação a monossacarídeos, designados como S1 e S2. Esses dois sítios são conectados por um grande sitio estendido dividido em duas partes: E1 e E2. Esses sítios apresentam a arquitetura de ferradura. Esse arranjo permite o reconhecimento de diferentes tipos de complexos e carboidratos simples (Figura 3).

S1 apresenta uma cavidade de aproximadamente 147 Å composta pelos resíduos Ala63, Arg64, Cys65, Asn66, Asn67, Cys68, Trp69, Glu82, Gln86 e Tyr88.

S2 apresenta um bolso de aproximadamente 140 Å composta pelos resíduos Arg64, Ala73, Tyr74, Pro75, Ala77, Asp76, Phe79, Gln109 e Tyr110.

E1 e E2 apresentam um volume total de aproximadamente 220 Å compostos pelos resíduos Leu14, Cys17, Asn18, Tyr25, Asp27, Ser28, Ala29, Thr30, Val31, His32, Ala73, Ala78, Phe79, Val80 e Val105. Análises estruturais evidenciaram uma grande cavidade, que pode ser dividida em oito subunidades para interação com monossacarídeos. Devido a alta complexidade estrutural, possivelmente CiL-1 tem a habilidade de interagir com um largo spectro de oligossacarídeos ramificados, principalmente os que apresentam unidades de galactose e suas variantes na porção terminal (Figura 3) (CARNEIRO et al., 2020).

A estrutura tridimensional e disposição dos sítios de ligação de CiL-1 levantam o questionamento de um possível mecanismo de ação para atividade antinociceptiva e anti-inflamatória alvo do presente estudo.

Figura 3- Estrutura geral e arquitetura de sítios de ligação a carboidratos de CiL-1.
Esquema estrutural composto por quatro folhas-β duplas em arranjo de barril, conectados por loops de tamanhos variados. DRLCs EI, EII, SI e SII seletivos a um largo spectro de oligossacarídeos ramificados, principalmente os que apresentam unidades de galactose e suas variantes na porção terminal.

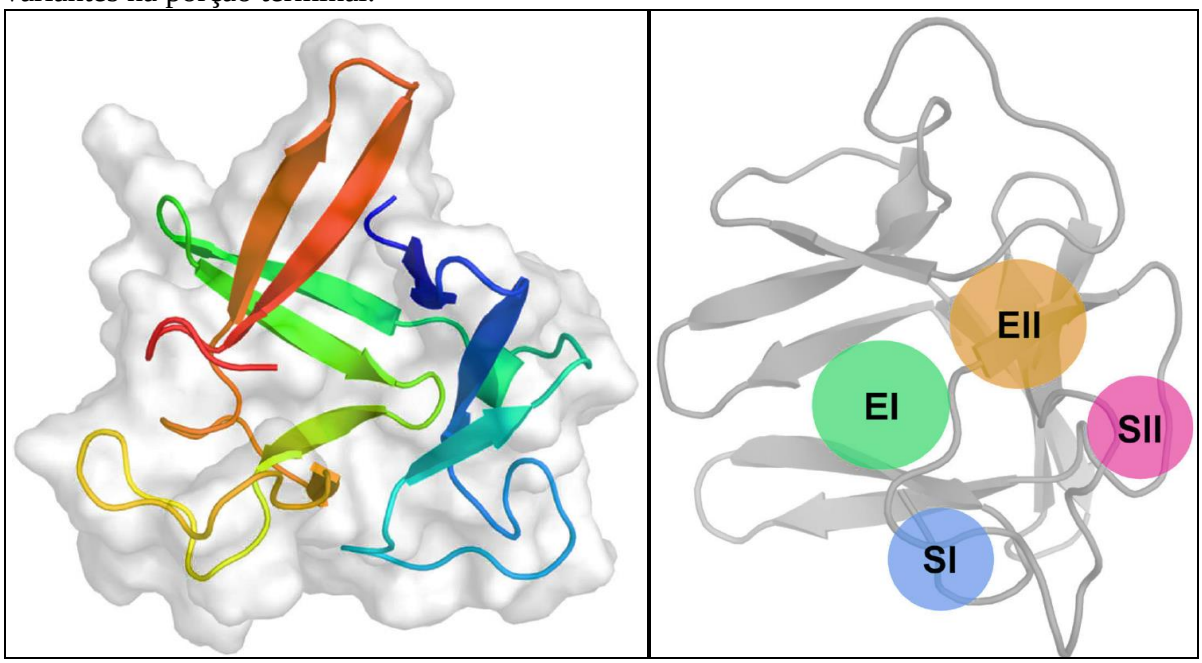

Fonte: CARNEIRO et al., 2020.

1.6 Inflamação

A inflamação é uma resposta natural do organismo quando um tecido vascularizado sofre estímulos nocivos, como dano celular, ação de patógenos, agentes químicos, físicos, microrganismo, lesão térmica ou mecânica. É um processo complexo que envolve diversos eventos. Alguns sinais são evidentes e incluem rubor, aquecimento, edema, dor e perda de função (GRANGER; SENCHENKOVA, 2010). Quando algum tecido sofre uma lesão ocorre a liberação local e imediata de uma variedade de substâncias químicas incluindo citocinas (TNF-α, IL-1β e quimiocinas), leucotrienos (LTB_4), fator de crescimento neural, endotelinas, substância P, cininas, prostaglandinas e aminas simpaticomiméticas que atuam sobre o controle da infamação e ativação dos nociceptores. O estimulo inflamatório pode ainda desencadear respostas como vasodilatação, aumento da permeabilidade vascular, extravasamento de plasma, formação de espécies reativas de oxigênio, ativação de fatores de transcrição e migração de leucócitos. Todos esses ventos citados anteriormente são ativados, modulados e cessados de acordo com o desenvolvimento do processo inflamatório, na maioria dos casos, acontecendo de forma simultânea, por esse motivo recebe o nome de cascata inflamatória (NATHAN; DING, 2010; WONGRAKPANICH et al., 2018).

A inflamação pode ser classificada como aguda ou crônica, dependendo do tempo de permanência do processo inflamatório. A inflamação aguda se caracteriza por curta duração, ocorrendo em horas ou dias com predomínio do envolvimento de neutrófilos. A inflamação crônica se caracteriza por longa duração com predomínio do envolvimentp de linfócitos, macrófagos e plasmócitos (XIAO, 2017).

Eventos vasculares e celulares caracterizam a migração de leucócitos, um importante evento na inflamação. Durante a ativação da cascata inflamatória a vasodilatação aumenta a passagem de leucócitos dos vasos sanguíneos periféricos para o sítio inflamatório, com subsequente produção de espécies reativas de oxigênio e nitrogênio e liberação de citocinas (PATEL et al., 2020). Essa resposta é essencial para evitar infecções, porém quando não modulada adequadamente pode resultar em diversas condições patológicas. A inflamação e seus sintomas é uma das desordens que mais leva as pessoas a procurarem atendimentos médicos. Normalmente está associada a doenças como aterosclerose, obesidade, câncer, doença pulmonar crônica obstrutiva e asma, gerando altos gastos para o sistema de saúde de urgência, emergência e pós operatório (NATHAN; DING, 2010).

O uso de drogas é uma das principais formas de tratamento da inflamação. Os principais grupos de fármacos empregados para este fim são os glicocorticóides e os anti-inflamatórios não-esteroidais (AINEs) (ZHANG; YAN; LI, 2021). Os glicocorticóides são amplamente utilizados em duas situações, na terapia das doenças autoimunes e na prevenção e/ou tratamento da rejeição de transplantes de órgãos. Essa abordagem terapêutica se deve principalmente pela inibição do gene da COX-2 e a indução da proteína lipocortina, a qual inibe a enzima fosfolipase A2. Consequentemente a cascata inflamatória sofre diminuição da produção de citocinas pró-inflamatórias (TNF-α e IL-1β), além da modulação do fator de transcrição NF-kB (SATO et al., 2010). Os principais corticoides usados são prednisona, prednisolona, hidrocortisona, dexametasona, metilprednisolona e beclometasona.

Os anti-inflamatórios não esteroidais (AINEs) são os fármacos mais prescritos e utilizados no mundo, sendo utilizados no tratamento de inúmeras patologias como artrite reumatóide, osteoartrite e outras doenças inflamatórias. Além da ação anti-inflamatória, esses fármacos apresentam também atividade analgésica e antipirética em sua grande maioria. O mecanismo de ação está associado principalmente ao bloqueio da COX, promovendo a inibição de prostaglandinas (SOSTRES et al., 2010).

A inflamação é um dos fenômenos que mais contribui com o congestionamento do atendimento médico em sociedades industrializadas. Embora não seja em si a causa primaria de doenças como aterosclerose, obesidade, câncer, doença pulmonar crônica obstrutiva e

asma, contribui significativamente para suas patogêneses (NATHAN; DING, 2010).

Os glicocorticoides e os AINES podem apresentar toxicidade gastrointestinal e renal como efeitos adversos e devido a possíveis complicações não é indicado em alguns casos (STEINFELD; BJØRKE, 2002).

Processos inflamatórios agudos e crônicos decorrentes da resposta do organismo em diversos quadros, tais como, de infecção bacteriana, necrose de tecidos, trauma, radiação, queimaduras ou por qualquer corpo estranho presente no tecido causam diversas alterações fisiológicas. Uma dessas alterações é o aumento dos níveis de espécies reativa de oxigênio (ROS) a partir de células envolvidas na resposta de defesa imunológica do hospedeiro (CLARK; KUPPER, 2005).

1.7 ROS

ROS do inglês *reactive oxygen species* podem ser definidos como metabólitos parcialmente reduzidos de oxigênio que possuem fortes capacidades de oxidação. Em baixas concentrações tem a função de sinalização com mecanismos complexos no metabolismo. Regulam o crescimento celular, a adesão de células, diferenciação, senescência e apoptose. Porém são deletérios para as células em altas concentrações quando passam a oxidar proteínas e constituintes celulares lipídicos, além de danificar o DNA. A produção prolongada de ROS está associada a progressão de doenças inflamatórias (MITTAL, et al., 2014; VONG et al., 2020).

Os principais agentes redutores são o ânion superóxido ($O_2^{\bullet-}$), radical hidroxila ($OH^{\bullet}$), peróxido de hidrogênio (H_2O_2) e hipoclorito ácido (HClO) (THANNICKAL; FANBURG, 2000). Eles podem ser gerados como subproduto do metabolismo celular através da cadeia de transportadora de elétrons, dentro das mitocôndrias, através do citocromo P450. O metabolismo celular pode gerar ROS a partir de NADPH oxidases que estão presentes em uma grande variedade de células, especialmente os leucócitos e células endoteliais, envolvidos na resposta inflamatória, mas nesse caso não são produzidos como subprodutos e participam da modulação inflamatória (KRAUSE, 2007; LAMBETH, 2004).

ROS pode ter diferentes origens, mas algumas etapas metabólicas de diferentes cadeias de reações podem se sobrepor. $O_2^{\bullet-}$ é gerado pela redução de um elétron de O_2 através da ação das enzimas NADPH oxidase ou xantina oxidase (XO). Ou ainda durante as reações de transferência de elétrons na CTE na mitocôndria. (HANDY; LOSCALZO, 2012). H_2O_2 é gerado a partir da dismutação de $O_2^{\bullet-}$ pela enzima SOD. $OH^{\bullet}$ é gerado a partir da reação de H_2O_2 com Fe^{2+} (BECKMAN, 1996). HClO é gerado a partir da reação de H_2O_2 com íon

cloreto pela enzima MPO produzida por neutrófilos durante a resposta inflamatória. A figura 4 ilustra a formação de ROS e os mecanismos antioxidantes para neutralização desses radicais.

Figura 4- Fontes de espécies reativas de oxigênio e sistema antioxidante (ROS).

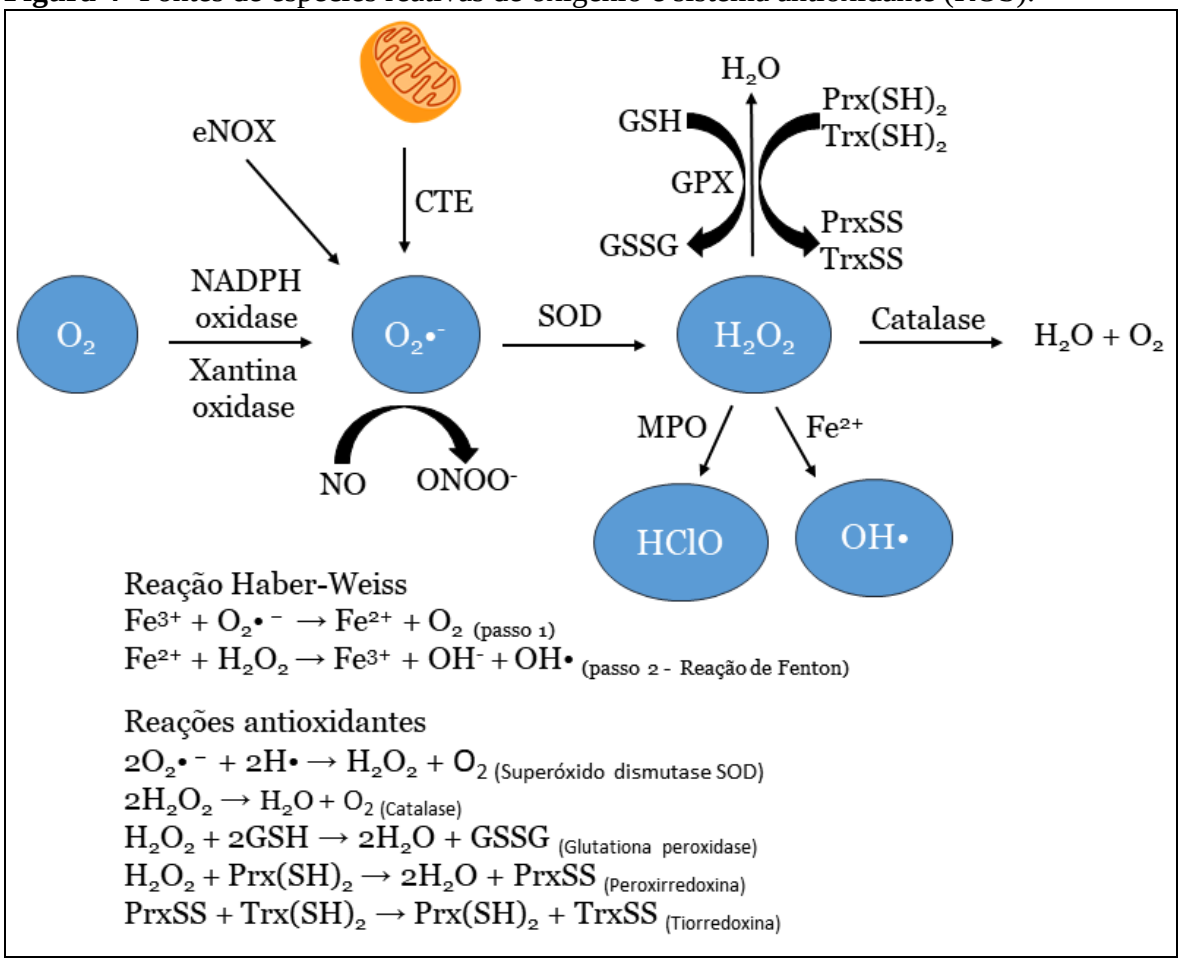

Fonte: MITTAL et al., 2014 (adaptado).

ROS pode atuar de diferentes formas dentro do processo inflamatório. Uma delas é logo após a formação de H_2O_2 nas mitocôndrias. H_2O_2 capaz de atravessar livremente a membrana externa mitocondrial. Ao chegar ao citosol ativa citocinas pró inflamatórias. Esse estresse oxidativo está associado a inflamação crônica e a diversas desordens associadas, como por exemplo a progressão do câncer, diabetes mellitus e aterosclerose. Essa modulação pró inflamatória é gerada a partir da formação de IL-1β, IL-6, and TNF-α (SIMPSON; OLIVER, 2020; XIONG et al., 2019).

Há evidências de que ROS também apresenta envolvimento em processos de extravasamento de leucócitos durante a resposta a um estímulo inflamatório. E que também pode ser regulado pelo estresse oxidativo. A produção de ROS endógeno por células endoteliais é capaz de ativar diretamente moléculas de adesão celular (CAMs) desencadeando processo de diapedese. Ou ainda alterar a expressão de genes sensíveis a alterações redox, tais

como NF-kB e AP-1, desencadeando a cascata inflamatória. Nesse caso, a região promotora de ICAM é modulada a partir de sítios de ligação sensíveis a ROS. Ambos os eventos contribuem para o aumento da migração de leucócitos para a região da inflamação (ZHANG et al., 2018).

Diante do exposto, novos alvos terapêuticos e novas drogas têm sido estudados a fim de desenvolver novos fármacos mais eficientes e com menos ações adversas no tratamento da inflamação, na redução do estresse oxidativo e da dor.

1.8 Dor e nocicepção

A dor é definida como uma experiência sensorial e emocional desagradável que remete ou está diretamente associada a um dano real ou potencial do tecido. O termo dor está ligado a uma definição geral que mescla componentes psicológicos e fisiológicos distintos. Devido ao componente emocional, é percebida de forma individual e pessoal. É influenciada por diversos fatores, seja biológico, psicológico e até mesmo social (RAJA et al., 2020).

A dor faz parte do sistema de defesa e autoproteção, sinalizando para o indivíduo que houve uma lesão tecidual, ativando uma resposta imediata ou ainda protegendo o indivíduo de um perigo inerente, antecipando a reação ao estimulo sem que de fato, ainda não tenha acontecido qualquer tipo de lesão. Embora a dor geralmente desempenhe um papel adaptativo, pode ter efeitos adversos na função e no bem-estar social e psicológico (LEE; ELIZABETH; NECKA, 2020)

A dor também envolve aspectos comportamentais, podendo causar reações emocionais negativas a quem a sente. Quando persistente e intensa, pode tornar-se debilitante e muitas vezes causadora de sofrimento, sendo frequentemente responsável pela diminuição drástica da qualidade de vida dos portadores deste sintoma (FIELDS, 2018; JULIUS; BASBAUM, 2001).

Dor e nocicepção são fenômenos diferentes. A dor não pode ser mensurada pois a sensibilidade é diferente para cada indivíduo. A nocicepção é o componente fisiológico da dor. Está associada ao processo de ativação neural e resposta sensorial. Desta forma, a nocicepção é usada em modelos de experimentação animal de “dor”, onde o objeto de estudo é a sinalização e resposta neural a estímulos nocivos (TJØLSEM et al., 1992; WOO et al., 2017).

A dor pode ser classificada como aguda ou crônica. A dor aguda tem curta duração e normalmente serve como sinalização de algum risco de dano. Fisiologicamente, a dor aguda acontece a partir da ativação direta de estruturas especializadas na detecção de estímulos nocivos (mecânicos, térmicos e químicos) capazes de causar lesão real ou potencial. Essas

estruturas são denominadas nociceptores. A dor crônica, normalmente mais duradoura, persiste mesmo após a resposta de cura ou até mesmo se manifesta na ausência de dano tecidual e parece não servir a um propósito claro (MCDOUGALL, 2011; MCCURDY; SCULLY, 2005). Fisiologicamente a dor crônica resulta de alterações no limiar de ativação dos nociceptores, aumento da síntese e/ou liberação de neurotransmissores, alterações sinápticas e o brotamento de novas fibras nervosas. Quando isso acontece a ativação, transmissão e permanência da sinalização química da dor se torna mais intensa. Desenvolvendo um quadro chamado de hiperalgesia, que se caracteriza por uma resposta exacerbada a qualquer estimulo. Até mesmo estímulos não dolorosos passam a causar dor. A hiperalgesia pode ter efeitos devastadores, chegando a incapacitar o indivíduo afetado. A dor crônica é um dos sinais clássicos de inflamação e é sintoma de muitas desordens clínicas (LOESER; MELZACK, 1999; MILLAN, 1999).

A dor pode ainda ser classificada quanto a origem, quando ocorre devido a ativação direta de nociceptores é denominada dor nociceptiva. Quando o tecido neuronal é lesionado e consequentemente há liberação de neuropeptídeos que induzem à dor, tanto a nível periférico como central, a dor é denominada de neurogênica. Quando há uma lesão ou disfunção do sistema nervoso somatosensorial, a dor é denominada de neuropática. Há ainda a dor que ocorre sem a presença de um fator somático identificável e parece estar relacionada a uma origem de desordem psicossomática, nesse caso a dor é denominada de psicogênica (FORNASARI, 2012).

1.9 Nocicepção

A palavra nociceptor deriva do latim *nocere*, que significa ferir. Por definição, são estruturas especializadas que funcionam como sensores de estímulos nocivos que se comportam como “vigilantes” de qualquer lesão tecidual que ocorra ou que possa ocorrer aos tecidos (MILLAN, 1999).

O conceito de nociceptor foi proposto em 1908, pelo fisiologista britânico Sherrington, que o definiu como uma entidade, um neurônio sensorial primário que seria ativado por um estímulo capaz de causar dano tecidual (JULIUS; BASBAUM, 2001). Esse conceito caracteriza os nociceptores como estruturas especializadas que possuem limiar ou sensibilidade específicos, sendo ativados apenas por estímulos capazes de resultar em lesões teciduais, ou seja, não são sensíveis a estímulos sensoriais não correspondentes a perigo. A partir de então os nociceptores foram classificados de forma independente das fibras nervosas sensoriais, sendo estas, sensíveis a estímulos não-nocivos, como por exemplo o tato (GREER;

HOYT, 1990).

Estudos eletrofisiológicos posteriores demonstraram a existência de neurônios sensoriais primários que podem ser excitados por calor nocivo, pressão intensa ou irritantes químicos. Porém, não são sensíveis a estímulos inócuos, comprovando experimentalmente que a nocicepção é uma sinalização de neurônios especializados. (GREER; HOYT, 1990; JULIUS; BASBAUM, 2001).

Os nociceptores estão presentes nos tecidos cutâneos, ossos, músculos, tecidos conjuntivos, vasos sanguíneos e vísceras. Fazem parte de uma rede de sinalização envolvendo a comunicação entre sistema nervoso central e periférico (SCHAIBLE; RICHTER, 2004; WOOLF, 2004).

O processo fisiológico da dor (nocicepção) compreende três etapas: Transdução, condução e transmissão.

A transdução é a primeira etapa do processo e ocorre quando algum estímulo nocivo é detectado e convertido em atividade elétrica nos neurônios aferentes primários presentes nas terminações nervosas livres. A ativação é alcançada quando o estimulo é suficiente para atingir o limiar de ativação do potencial elétrico (GREER; HOYT, 1990).

Os axônios dos neurônios envolvidos nesse processo podem ou não serem mielinizados e por esse motivo apresentam velocidade de transmissão do sinal nociceptivo mais rápido ou lento respectivamente. Os neurônios de resposta lenta estão presentes nas fibras C e apresentam pequenos corpos celulares. Os de resposta rápida se localizam nas fibras Aδ e apresentam corpos celulares de médio a grande porte. Os neurônios das fibras C e Aδ fazem sinapses com neurônios no corno dorsal da coluna vertebral (Figura 05). A transdução é mediada por canais de cátions não seletivos, como canais de sódio ou cálcio, responsáveis pela despolarização da membrana neuronal (FORNASARI, 2012).

A condução é a segunda etapa do processo e como o próprio nome sugere está relacionado com a condução do estímulo elétrico para terminais centrais de nociceptores presentes na medula espinhal. Na dor inflamatória, substâncias como histamina, bradicinina, serotonina, prostaglandinas e substância P liberada a partir de tecidos lesionados podem facilitar a condução (FORNASARI, 2012).

A transmissão é a terceira etapa do processo e está relacionada com a transmissão do estimulo da medula espimhal para o tronco encefálico. Nessa etapa a sinalização nociceptiva acontece através do lançamento de neurotransmissores de um neurônio a outro a partir do potencial iônico gerado pelo acumulo de Ca^{2+} (Figura 5) (FORNASARI, 2012).

Figura 5- Sistema nociceptivo da dor.
A transdução ocorre quando algum estímulo nocivo é detectado e convertido em atividade elétrica nos neurônios aferentes primários presentes nas terminações nervosas livres. A condução é o envio do estímulo elétrico para terminais centrais de nociceptores presentes na medula espinhal. A transmissão é o envio do estimulo da medula espimhal para o tronco encefálico. Após processado, o estimulo resulta em uma resposta motora que segue o sentido ineverso.

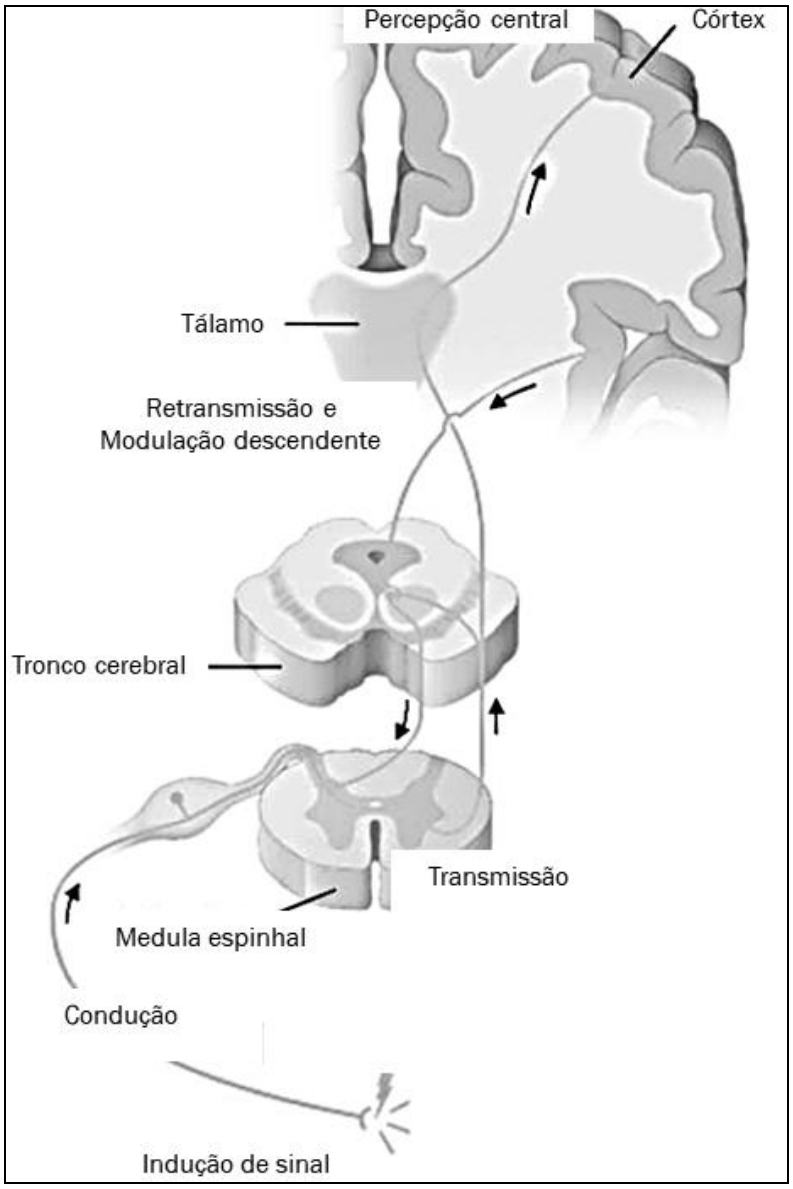

Fonte: FORNASARI, 2012 (adaptado).

Os corpos celulares dos neurônios nociceptivos aferentes primários podem estar localizados nos gânglios da raiz dorsal (GRD) para o tórax, abdome e membros e no gânglio trigeminal (GT) ou gânglio de Gasser para a região orofacial (BEAR; CONNORS; PARADISO, 2006). Os neurônios do GRD e do GT emitem projeções axonais em duas direções. Os neurônios do gânglio GDR emitem projeções para a periferia dos tecidos e para o corno dorsal da medula espinal. Os neurônios do GT emitem seus prolongamentos para a periferia, com a diferença de que seus prolongamentos centrais são emitidos diretamente para regiões do tronco encefálico, sem conexões com a medula espinal (BEAR; CONNORS; PARADISO, 2006).

A sinalização nociceptiva é feita através do sistema glutamatérgico se caracteriza pela presença de diferentes receptores ativados pelo aminoácido glutamato e é amplamente distribuído no sistema nervoso dos vertebrados. O sistema glutamatérgico está associado a diversas funções neuronais básicas. Alterações desse sistema estão diretamente associadas a doenças neurológicas e processos inflamatórios (CRESPO; LEÓN-NAVARRO; MARTÍN, 2021).

1.10 Glutamato

Durante o estimulo nociceptivo várias substâncias são liberadas localmente no tecido lesionado. Essas substâncias são chamadas de mediadores inflamatórios ou mediadores nociceptivos, e podem ser liberadas por mastócitos, células endoteliais, plaquetas, células de Schwann, dentre outras (BESSON,1999; BESSON;DICKENSON,1997). O aminoácido excitatório glutamato é um desses mediadores e é o neurotransmissor mais abundante do sistema nervoso central e pode ser encontrado no encéfalo, na medula espinal e nas enervações periféricas. Durante ativação de nociceptores o glutamato é liberado por vesículas nas sinapses neuronais a partir do aumento dos níveis de Ca^{2+} intracelular. A célula posterior a sinapse recebe o sinal através de receptores presentes na membrana (GRAHAM et al., 1967; MILLER et al., 1988). Existem dois tipos de receptores de glutamato. Os receptores glutamatérgicos ionotrópicos (iGluRs) e receptores glutamatérgicos metabotrópicos (mGluRs).

Os receptores glutamatérgicos ionotrópicos são canais iônicos classificados de acordo com critérios moleculares, eletrofisiológicos e farmacológicos. Essa classificação é feita a partir do agonista pelo qual são seletivamente ativados:

Receptores seletivamente sensíveis ao NMDA (N-metil-D-aspartato).

Receptores seletivamente sensíveis ao AMPA (ácido-amino-3-hydroxi-5-metil-

4-isoxazolepro-pionico).

Receptores seletivamente sensíveis ao ao cainato (ácido caínico) (FUNDYTUS, 2001).

Frequentemente os receptores AMPA e cainato são agrupados em uma subclassificação denominada de receptores não-NMDA. Esses receptores têm maior afinidade por íons Na^+, embora também sejam permeáveis aos íons Ca^{2+} e K^+ e podem apresentar afinidade por diferentes agonistas. Os receptores AMPA e NMDA coexistem nas células neuronais. E são responsáveis pela transmissão sináptica excitatória em diversos eventos neurofisiológicos. O efeito da ativação destes receptores em potenciais de membrana negativos é facilitar a entrada de íons Na^+ na célula e desta forma promover uma despolarização rápida e intensa resultando na transmissão do sinal elétrico entre o sistema nervoso periférico e central (MILLER et al., 1988). Em potenciais de repouso, quando o neurônio não está em atividade excitatória o canal NMDA permanece impermeável aos íons devido ao bloqueio causado pela ligação de íons Mg^{2+}. A saída de Mg^{2+} e a liberação do poro acontece durante a despolarização da membrana. Após a ativação de NMDA ocorre a ativação de canais AMPA (SALTER, 2005).

Os receptores glutamatérgicos metabotrópicos são classificados como um conjunto de receptores acoplados a proteínas G, que diferem estrutural, farmacologica e funcionalmente dos receptores ionotrópicos. Apresentam mecanismo de ação mais lentos e podem ter duas vias de sinalização. A ativação via fosfolipase C, uma enzima que catalisa a produção de inositol trifosfato que, por sua vez, promove a liberação de íons Ca^{2+} dos estoques intracelulares e a ativação via enzima adenilato ciclase com consequente aumento da produção do monofosfato cíclico de adenosina (AMPc) (CONN; PIN, 1997; HAYASHI, 1985).

O influxo de Ca^{2+} para o interior das células presentes nas sinapses é feito através de canais iônicos transmembrana. Quando ativados permitem o fluxo iônico através de um poro central e quando inativados impedem o transporte de ions e a formação do potencial de membrana.

1.11 Canais TRP

Os canais TRP (transient receptor potential) são um grupo de canais iônicos transmembrana receptores de estímulos nocivos. Essa denominação foi dada devido ao comportamento de uma variedade mutante de *Drosophila* que apresentava uma resposta transiente de fotorreceptores ao invés de uma resposta sustentada ao brilho da luz. Esse estudo permitiu concluir que estes canais estavam associados a transdução sensorial (MONTELL; RUBIN, 1989). Esses canais respondem a vários tipos de estímulos e ao serem ativados permitem a entrada de cátions no interior das células nervosas. A ativação dos canais TRP leva à despolarização rápida da membrana, participando da geração de potencial de ação (MORAN, 2018).

Os canais TRP podem ser classificados em seis grupos: anquirina (TRPA), canônico (TRPC), melastatina (TRPM), mucolipina (TRPML), policistina (TRPP) e vaniloide (TRPV). Estruturalmente são compostos por quatro subunidades que podem ou não serem iguais. Há pouca homologia de sequência entre os membros da família e a estrutura geral dos canais pode divergir significativamente. Recentemente o número de trabalhos com elucidação da estrutura dos TRP tem aumentado graças a aplicação de técnicas de criomicroscopia eletrônica (Figura 6). Os TRP são seletivamente expressos nos nociceptores e estão envolvidos em mecanismos chave de processos de detecção e resposta a estímulos nocivos. Apesar de apenas uma pequena cadeia de aminoácidos ser compartilhada entre os diferentes receptores, a estrutura molecular apresenta seis domínios transmembrana (MORAN, 2018; JULIUS; BASBAUM, 2001).

TRP tem se tornado um promissor alvo terapêutico de distúrbios pulmonares, doenças hereditárias, disfunção do sistema nervoso central e no tratamento da dor e inflamação. Devido ao envolvimento comum em diversas desordens e doenças e a melhor compreensão dos mecanismos de ação moleculares, a descoberta dos canais tem aberto uma nova abordagem eficiente e segura para o tratamento de várias doenças (SAKAGUCHI; MORI, 2020; HONG et al.; 2020; YANG; KIM, 2020). Atualmente estudos de mecanismos de regulação têm ganhado destaque em pesquisas com TRPs. Acredita-se que modificações na porção de glicoconjugados presente em sua estrutura estão relacionadas com processos inflamatórios.

Figura 6. Diferentes estruturas de canais TRP elucidadas.

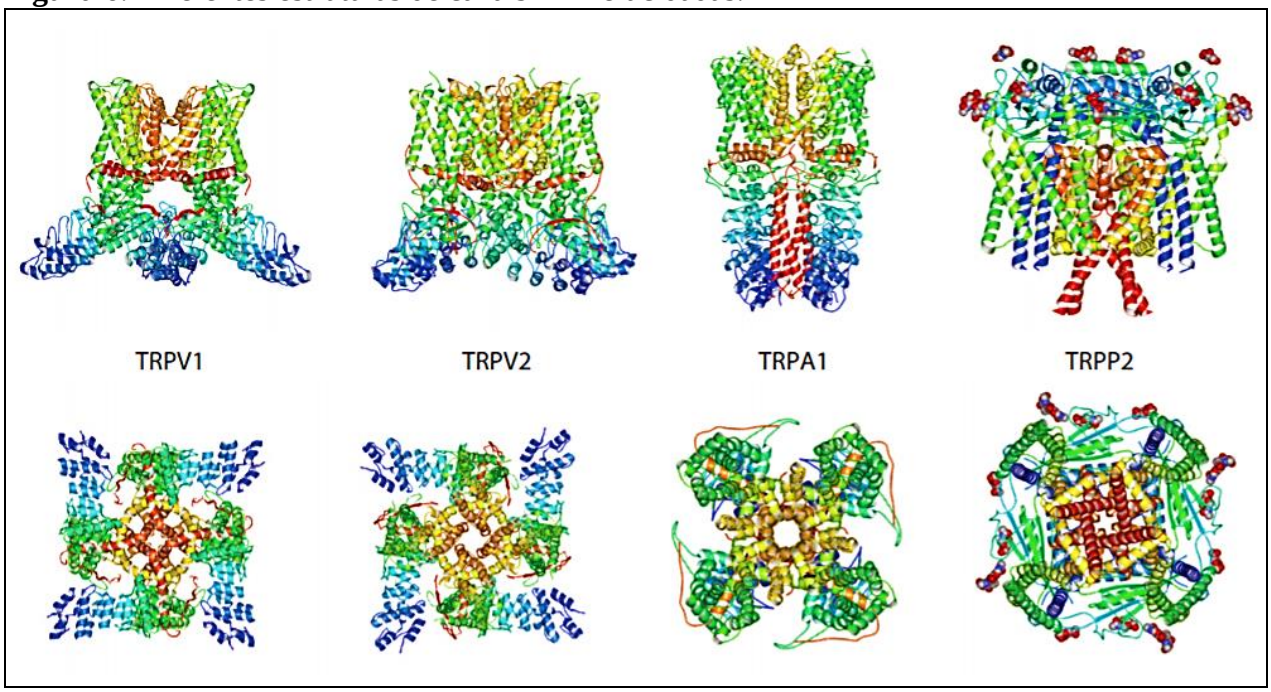

Fonte: MORAN, 2018.

1.12 Glicosilação dos canais TRPs

O termo glicosilação designa a adição covalente de sacarídeos ou glicanos, de cadeia simples ou ramificada, a uma macromolécula por meio de ação enzimática. O padrão de arranjo e de ligação dessas moléculas está associado a importantes funções biológicas e são considerados importantes meios de regulação e sinalização bioquímica (KÁDKOVÁ et al., 2017).

A membrana celular de células animais apresenta grande diversidade de glicoconjugados. Já é sabido que os canais TRPs apresentam sítios de glicosilação em sua estrutura proteica e há evidências de que essa glicosilação tem papel regulatório de sua ativação. As proteínas podem ser ligadas a sacarídeos por ligação do tipo *N*- ou, menos comumente, ligação do tipo *O*-. A *O*-glicosilação consiste na formação de uma ligação glicosídica entre o carbono anomérico presente em um carboidrato com a hidroxila de um resíduo de serina ou treonina presente em uma proteína. Glicosilações do tipo *O*-glicano são muito numerosas e apresentam extensa variedade de substituintes em sua estrutura (COHEN, 2006). Na *N*-glicosilação, um resíduo de *N*-acetilglicosamina (GlcNAc) é ligado por ligação amida a um resíduo de asparagina pertencente a uma sequência consenso, conhecida como sitio de glicosilação. Essa sequência segue a seguinte ordem: Asn – X – Ser/Thr, onde X pode ser qualquer resíduo de aminoácido, exceto a prolina. Oligossacarídeos ligados por ligação do tipo *N*- presentes em células de mamíferos pode assumir várias estruturas, porém, todos são

ramificados e compartilham um motivo pentassacarídeco central, formado por duas unidades GlcNAc e três unidades de manose (Man) (CHAN et al., 2018).

A partir desse núcleo comum unidades de ramificação se prolongam, essas prolongações de cadeias sacarídicas são denominadas antenas. Os *N*-glicanos são classificados em três tipos dependendo da composição das antenas em sua estrutura:

Oligomanosídico: Somente moléculas de man são ligadas ao núcleo comum.

Complexo: As ramificações antenas ligadas ao núcleo comum apresentam moléculas de GlcNAc.

Híbrido: Moléculas de *man* são ligadas ao resíduo de man do núcleo comum e uma ou duas ramificações antenas são ligadas ao resíduo de manose do núcleo comum (EGAN et al., 2016).

As cadeias lineares na estrutura das antenas servem como sinalizadores específicos de proteínas de reconhecimento e de ligação a sacarídeos. Lectinas que ligam-se a polissacarídeos lineares são classificados como exo- ou endo- lectinas, dependendo da porção de interação a qual se ligam:

Exolectinas: Interagem com unidades terminais de polissacarídeos. As lectinas deste tipo ligam-se especificamente à estrutura do *cap* terminal.

Endolectinas: Interagem com unidades internas de polissacarídeos. As lectinas desse tipo são comumente capazes de interagir com um número maior de unidades sacarídicas (NAGAE; YAMAGUCHI, 2014).

Um importante mecanismo de regulação de canais TRPs já foi descrito a partir da adição ou remoção de unidades de ácido siálico em resíduos de galactose presentes no *cap* de antenas de oligossacarídeos do tipo LacNAc (Figura 7). A presença do ácido siálico na glicosilação dos canais TRPs inativa o transporte iônico. Canais ativos no transporte iônico, por sua vez, não apresentam ácido siálico em suas antenas (NAGAE et al., 2009; CHA, et al., 2008).

Figura 7- Típico *N*-glicano tetra-antenado presente na superfície de células de mamíferos. O *N*-glicano é ancorado a proteína através de uma ligação amida entre uma unidade de *N*-acetilglicosamina (GlcNAc) e um resíduo de asparagina presente eum um sitio de glicosilação com a seguinte sequência: Asn – X – Ser/Thr, onde X pode ser qualquer resíduo de aminoácido, exceto a prolina. Um núcleo pentassacarídeco central é formado por duas unidades GlcNAc e três unidades de manose. Prolongações de cadeias sacarídicas LacNAc formam um compexo tetra-antenado com a presença de um *cap* de ácido siálico.

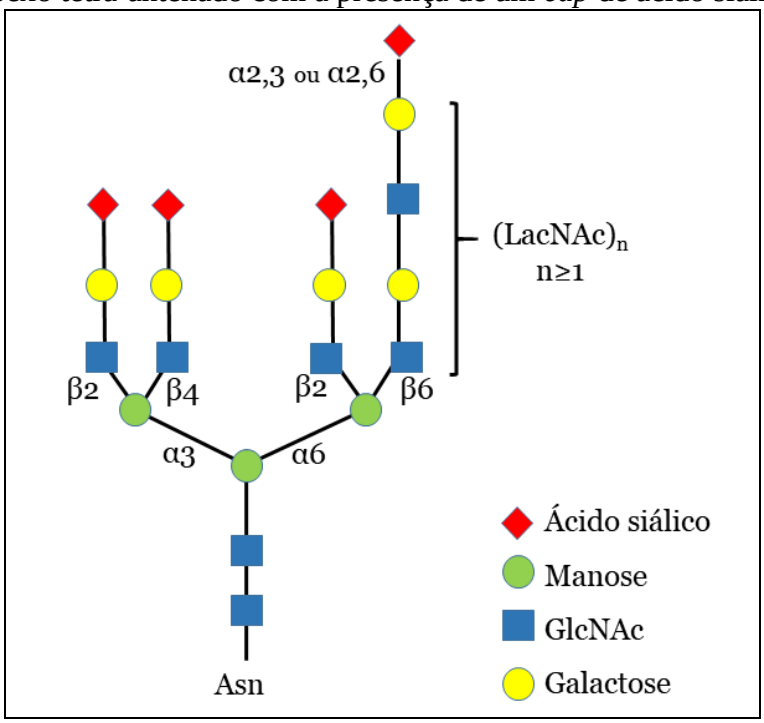

Fonte: CHA et al., 2008 (adaptado).

Dentre os canais TRPs glicosilados conhecidos, o canal TRPA1 vêm ganhando destaque como alvo no tratamento da dor e da inflamação (EGAN et al., 2016).

1.13 Receptor TRPA1

TRPA1 é um canal iônicos sensível a uma grande variedade de estímulos, entre eles, substâncias químicas nocivas, frio intenso, espécies químicas reativas e de sinais endógenos associados a danos celulares. Essa diversidade funcional e o fato de sua expressão acontecer somente em fibras nervosas nociceptivas presentes no epitélio e em uma ampla variedade de tecidos vascularizados, tem dispertado o interesse para estudos associados a múltiplas doenças (EARLEY; BRAYDEN, 2015; DIETRICH; STEINRITZ; GUDERMANN, 2017).

O gene TRPA1 já foi identificado. Nos humanos apresentam uma única sequência e está localizado no cromossomo 8, compreendendo 73.635 bases e 29 éxos. Genes homólogos já foram identificados em outros mamíferos, incluindo primatas, roedores, cães,

porcos, ursos e outras espécies. Estão presentes ainda em pássaros, peixes, anfíbios, insetos e nematoides. Ao contrário dos mamíferos, alguns deles contêm mais de um gene homólogo, como a *Drosophila melanogaster* (mosca da fruta) que possui 4 homólogos e *Danio rerio* (zebrafish) que possui 2 homólogos (VIANA, 2016; MEENTS; CIOTU; FISCHER, 2019).

O gene TRPA1 codifica uma proteína grande, que apresenta ~1100 resíduos de aminoácidos em sua estrutura primária. Mais especificamente 1119 resíduos na proteína humana e 1120 resíduos na proteína de zebrafish. Dentre as diversas espécies a massa molecular estimada varia entre 120 e 130 kDa (TALAVERA et al., 2020).

Estruturalmente, TRPA1 é um homotetrâmero (CVETKOV et al., 2011). Sua conformação contém um núcleo transmembrana conservado entre os membros da família TRP, consistindo em seis hélices transmembrana (TM1-6) com um loop de poro direcionado a porção interna da molécula entre TM5 e TM6. Esses dois domínios TM convergentes são responsáveis por formar e estabilizar a cavidade central do canal e apresentam ainda dois sítios de restrição que possuem a função de controlar o fluxo iônico. Esse controle depende de interações com resíduos D915 opostos, contribuindo para a permeação de Ca^{2+}. Há ainda dois centros hidrofóbicos presentes no fundo do poro, formados pelos resíduos I957 e V961, que são capazes de restringir a permeação de cátions reidratados. Essa interação produz um estreitamento em forma de funil de ~6 Å. Ainda no poro voltado a face intracelular, o canal apresenta duas hélices carregadas negativamente que podem atuar exclusivamente na repulsão de ânions na entrada do poro (Figura 8) (MEENTS; CIOTU; FISCHER, 2019; TALAVERA et al., 2020)

As porções NH_2 e COOH terminais são cadeias longas voltadas para o interior das células, juntas compreendem ~80% da massa molecular da proteína. O terminal NH_2 apresenta de 14 e 18 domínios de repetição de anquirina (ARDs), cada um constituído em 33 resíduos de aminoácidos. O terminal COOH apresenta ainda domínios de regulação alostérica do canal. Outra característica distintiva do TRPA1 é a presença de uma estrutura cilíndrica no centro do canal, abaixo do poro de permeação. Esta estrutura é estabilizada pela interação de resíduos carregados positivamente no exterior da superfície do cilindro com polifosfatos de inositol. Essas interações são essenciais para a funcionalidade do canal. A presença de cisteínas na região pré-TM1 estão envolvidas na ativação do canal por compostos eletrofílicos através de modificações covalentes, esse se caracteriza como um dos mecanismos de regulação do canal (JAQUEMAR; SCHENKER; TRUEB, 1999; JULIUS, 2013; NILIUS; PRENEN; OWSIANIK, 2011).

Figura 8- Diferentes domínios estruturas do canal TRPA1.
TRPA1 é um homotetrâmero cuja conformação contém um núcleo formado por seis hélices transmembrana (TM1-6) com um loop de poro direcionado a porção interna da molécula entre TM5 e TM6. As porções NH_2 e COOH terminais são cadeias longas voltadas para o interior das células e compreendem ~80% da massa molar doTRPA1. O terminal NH_2 apresenta de 14 e 18 domínios de repetição de anquirina (ARDs). O terminal COOH apresenta ainda domínios de regulação alostérica do transporte iônico. Dois sítios de glicosilação estão presentes no loop entre TM1 e TM2.

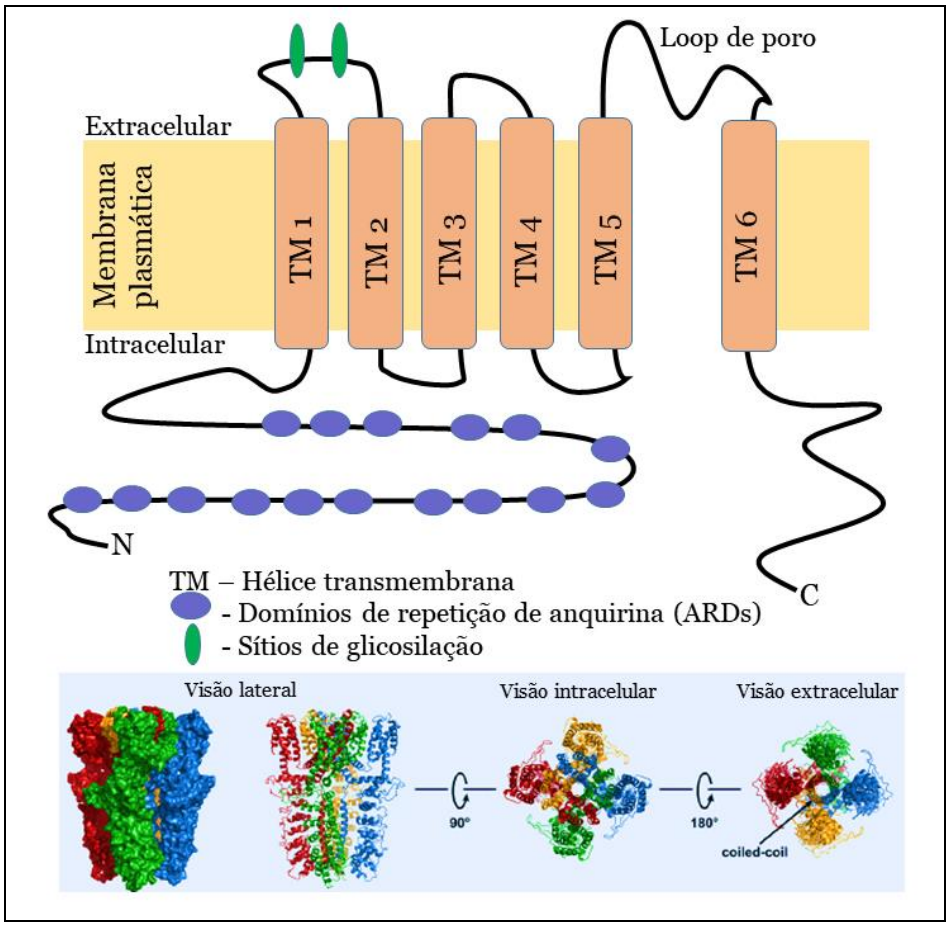

Fonte: MEENTS; CIOTU; FISCHER, 2019 (adaptado).

Nos últimos anos, o interesse no canal TRPA1 como alvo terapêutico tem aumentado constantemente. O fato de TRPA1 estar envolvido em diversos processos associados a desordens clinicas ou doenças é o principal fator desse interesse. Especialmente em processos de dor e inflamação, o bloqueio do canal em neurônios nociceptivos têm se destacado e os estudos dos mecanismos de ação são fundamenteis para desenvolvimento de novos fármacos (BALEMANSet al., 2019; CONKLIN, et al., 2019; BARALDI et al., 2010). Atualmente os modelos animais com zebrafish têm sido frequentemente empregados como *screening* para detecção de modulação de canais TRP.

1.14 Zebrafish

Zebrafish (*Danio rerio*) também conhecido popularmente como paulistinha, é um teleósteo ornamental de água doce, tropical, onívoro, originário da Índia, pertence à família *Cyprinidae*. Quando adulto pode atingir 6 cm. Atinge a maturidade sexual entre três e seis meses, sendo sua fecundação externa. Além de apresentar importância econômica, a espécie vem se estabelecendo nas últimas décadas como modelo de experimentação animal alternativo no estudo de diversas doenças. Muitos modelos de estudos com ratos e camundongos têm sido adaptados e substituídos por modelos com zebrafish. Essa substituição de modelos é mais adequada aos princípios dos 3Rs (redução, substituição e refinamento) na bioética de experimentação animal. Isso se deve a algumas vantagens tais como curto ciclo de vida, elevada taxa de fecundidade, rápido desenvolvimento, menor custo e facilidade de manutenção e de manuseio (MEYERS, 2018). O genoma da espécie já foi totalmente mapeado e apresenta homologia genética de 70% com os seres humanos (HOWE et al., 2013) e ainda apresentam características moleculares, bioquímicas, celulares e fisiológicas muitos semelhantes aos mamíferos (LIESCHKE; CURRIE, 2007). Durante a reprodução os embriões e larvas são transparentes, permitindo a visualização direta dos órgãos internos. Essas características tonam a espécie ideal para investigação da organogênese e de aspectos do desenvolvimento embrionário.

O zebrafish tem metabolismo nociceptivo e inflamatório semelhante ao humano e vários canais TRP, incluindo o receptor TRPA1, estão presentes nesses organismos. Nas últimas décadas o desenvolvimento e a adaptação de novas metodologias têm criado uma nova tendência em estudos de dor e inflamação.

2 OBJETIVO

2.1 Objetivo geral

Avaliar os efeitos de CiL-1 na nocicepção e inflamação utilizando modelos animais de zebrafish adulto (*Danio rerio*).

2.2 Objetivos específicos

- Purificar CiL-1;
- Avaliar os efeitos de CiL-1 na atividade locomotora e toxicidade;
- Avaliar atividade antinociceptiva de CiL-1;
- Avaliar o envolvimento do canal TRPA1 na atividade antinociceptiva de CiL-1;
- Avaliar atividade anti-inflamatória de CiL-1;
- Avaliar o efeito de CiL-1 sobre o estresse oxidativo inflamatório;
- Avaliar a interação CiL-1 *N*-Glicano TRPA1

ARTIGO DE TESE

Codium isthmocladum lectin 1 (CiL-1): Interaction with *N*-glycans explains antinociceptive and anti-inflammatory activities in adult zebrafish (*Danio rerio*)

Antônio Willame da Silva Alves[1], Bruno Lopes de Sousa[4]; Luiz Francisco Wemmenson Gonçalves Moura[3]; Emanuela de Lima Rebouças[3]; Marnielle Rodrigues Coutinho[3]; Antonio Wlisses da Silva[3]; Renata Pinheiro Chaves[2]; Rômulo Farias Carneiro[2]; Eduardo Henrique Salviano Bezerra[5]; Maria Izabel Florindo Guedes[3]; Eridan Orlando Pereira Tramontina Florean[3]; Celso Shiniti Nagano[2]; Alexandre Holanda Sampaio[2]; Bruno Anderson Matias da Rocha[1*].

[1] Laboratório de Biocristalografia –LABIC,
Departamento de Bioquímica e Biologia Molecular, Universidade Federal do Ceará,
Campus do Pici s/n, bloco 907, Av. Mister Hull.
Fortaleza, Ceará 60440-970, Brazil

[2] Laboratório de Biotecnologia Marinha - BioMar-Lab,
Departamento de Engenharia de Pesca, Universidade Federal do Ceará,
Campus do Pici,
Fortaleza, Ceará, Brazil

[3] Laboratório de Biotecnologia e Biologia Molecular - LBBM,
Centro de Ciências da Saúde, Universidade Estadual do Ceará,
Campus do Itaperi,
Fortaleza, Ceará, Brazil

[4] Faculdade de Filosofia Dom Aureliano Matos,
Universidade Estadual do Ceará,
Av. Dom Aureliano Matos, 2060,
Limoeiro do Norte, Ceará 62930-000, Brazil

[5]Laboratório Nacional de Biociências - LNBio,
Centro Nacional de Pesquisa em Energia e Materiais,
Rua Giuseppe Máximo Scolfaro, Cidade Universitária,
Campinas, São Paulo, Brazil

* To whom all correspondence should be addressed:
Professor Dr. Bruno Anderson Matias da Rocha
Bruno Anderson Matias da Rocha (brunoanderson@gmail.com)
Mister Hull Avenue s/n. Campus do Pici, Bloco 907.
Fortaleza, CE, Brazil. Zip Code: 60440-970. Phone/Fax: +55 (85) 3366-9401

3 INTRODUCTION

Pain is a classic sign of inflammation and stems from the sensitization of nociceptors. Chronic pain is present as a symptom of many clinical disorders. It is harmful to the patient and has economic repercussions (Ongaro and Kaptchuk 2019). Non-steroidal anti-inflammatory drugs (NSAIDs) and opioid analgesics are the two types of drugs most used in the treatment of pain and inflammation. However, they can cause adverse reactions, such as addiction and gastrointestinal irritation. Furthermore, they become ineffective with continuous use (Toblin et al. 2011; Fornasari 2012).

Seaweeds stand out as natural products with antinociceptive and antiinflammatory properties (Souza et al. 2020; Salehi et al. 2019). Among these products, lectins are important based on their ability to interact reversibly with complex carbohydrates and modulate cell membrane glycosylated receptors through this interaction (Nagae and Yamaguchi, 2014). A galactose-specific lectin (CiL-1) with antibiofilm property was purified from *Codium isthmocladum*, a green seaweed native to the northeastern coast of Brazil (Carneiro et al. 2020). Seaweeds lectins present high biotechnological potential (Praseptiangga, 2015) and it has been reported that some lectins with high affinity for complex glycans can bind to the same glycan target of human galectin-1. This interaction can interfere in the inflammatory process through receptor modulation (Chan et al. 2018; Carneiro et al. 2020).

Transient receptor potential (TRP) channels are a family of nonselective, cationpermeable integral membrane proteins that commonly act as receptors in various sensory processes, such as the perception of harmful stimuli. TRPV1, TRPA1 and TRPM8 have become strategic targets in the treatment of inflammatory pain by the modulation of glutamate in the central nervous system (Egan et al. 2016). TRPs are composed of four subunits, each containing six transmembrane regions (S1–S6), two extracellular domains (E1 and E2) and an ion-permeable pore formed by the S5–S6 regions. These channels present N-linked glycosylation of an oligosaccharide to asparagine side-chain. One or two specific N-X-S/T consensus sequences have been reported. In general, *N*-glycan proteins can exhibit one of three structures: high-mannose, hybrid or complex (Egan et al. 2016).

Transient receptor potential A1 (TRPA1) is an excitatory ion channel that functions as a cellular sensor, detecting a wide range of proalgesic agents such as environmental irritants and endogenous products of inflammation, as well as oxidative stress (Kádková et al. 2017). TRPA1 is also defined as a polymodal nociceptor activated by a wide range of chemical stimuli. It is present in a subpopulation of C-fiber nociceptive neurons in dorsal root, trigeminal and vagal (nodose or jugular) ganglia (Moore et al. 2018).

TRPA1 is structurally distinguished from other members of the TRP family by the ankyrin repeat motifs along its cytosolic N-terminal domain (Paulsen et al. 2015). They possess two putative *N*-linked glycosylation sites at Asn747 and Asn753. It was reported that both of these sites could be modified with an *N*-glycan and that the glycan at position Asn747 modulates agonist sensitivity of TRPA1 *in vitro* (Kádková et al. 2017).

Reactive oxygen species (ROS) play an important role in the pathogenesis of many human degenerative diseases, and excessive oxidative stress is related to chronic inflammation. High levels of ROS can signal mediators of damage to immunity and cell structures, including lipids and membranes, proteins and nucleic acids (Simpson and Oliver 2020). Stimulated macrophages release ROS as proinflammatory mediators. The inhibition of the production of these mediators is an important therapeutic strategy for treating inflammatory diseases (Zhang et al. 2018).

The adult zebrafish (*Danio rerio*) has gained popularity as a predictive model of drugs. Antinociceptive and anti-inflammatory potential have been successfully described as an alternative to rodent tests. In this species, nociceptive physiology is well established, and it is similar to that of mammals (Magalhães et al. 2018; Batista et al. 2018). The present study aimed to determine the antinociceptive and anti-inflammatory potential of CiL-1 in adult zebrafish by modulation of TRPA1 through lectin-glycan binding.

3.1 Materials and methods

3.1.1 Extraction and purification

Collection and lectin purification was carried out according by Carneiro et al. (2020) with some modifications. *C. isthmocladum* specimens were collected on Paracuru Beach, Ceará, Brazil. All collections were authorized through our registration with SISBIO (Sistema de Autorização e Informação em Biodiversidade, ID: 33913-8) and SISGEN (Sistema Nacional de Gestão do Patrimônio Genético e do Conhecimento Tradicional Associado, ID: AC14AF9).

Protein extraction was performed with 50 mM sodium acetate buffer, pH 5, containing 1 M NaCl at a ratio of 1:3 (*w:v*). The mixture was maintained under agitation for 4 h and then filtered and centrifuged at 8000 × g for 20 min at 4 °C. The precipitate was discarded, and the resulting supernatant (crude extract) was submitted to precipitation with ammonium sulfate saturation. Precipitated proteins between 40 and 100% of saturation (F40-100) were recovered by addition of a small volume of 20 mM phosphate buffer, pH 7 (PB).

The sample was dialyzed against PB and centrifuged, followed by loading the supernatant onto a DEAESephacel column (1.0 × 10 cm), which was previously equilibrated with PB. The column was washed with the same buffer and eluted stepwise in NaCl (0.0, 0.3, and 0.5 M) in PB. Chromatography was conducted at a flow rate of 2 mL min^{-1} and monitored by measurement of absorbance at 280 nm. The fraction containing hemagglutinating activity was pooled, dialyzed and freeze-dried.

3.1.2 Biological Assays

3.1.2.1 Zebrafish

Adult wild zebrafish (*D. rerio*) of both genders (short-fin phenotype), aged 60–90 days, of similar size (3.5 ±0.5 cm) and weight (0.3 ±0.2 g) were obtained from Agroquímica: Comércio de Produtos Veterinários LTDA, a supplier located in Fortaleza (Ceará, Brazil). The fish were acclimated for 24 h in a 10-L glass tank (30 x 15 x 20 cm) containing dechlorinated tap water (ProtecPlus®) and air pump with submerged filter at 25° C, pH 7.0, under near-normal circadian 83 rhythm (14:10 h of light/dark cycle). The fish were fed ad libitum 24 h prior to the experiments. After the experiments, the animals were sacrificed by immersion in ice water (2 - 4 °C) for 10 minutes until loss of opercular movements. All experimental procedures were approved by the Ethics Committee on Animal Research of Ceará State University (CEUA-UECE), and the protocol was filed under N. 0277057/2018.

3.1.2.2 Drugs and reagents

The following drugs and reagents were used in the study: formaldehyde (Dinâmica) and saline solution (0.9%; Arboreto). Diclofenac sodium was obtained from Medley. Camphor, carrageenan and DPPH were purchased from Sigma- Aldrich (USA).

3.1.2.3 Experimental design

The protocols were followed according to Batista et al. (2018). On the day of the experiment, zebrafish were randomly selected and then transferred to a wet sponge for treatment with study drugs or controls administered by the intramuscular (*i.m.*) or intraperitoneal (*i.p.*) route. Afterwards, they were placed in individual beakers (250 mL) containing 150 mL of water from the fish tank and allowed to recover. An insulin syringe (0.5 mL; UltraFine® BD) with a 30-gauge needle was used to inject the intraperitoneal treatment.

3.1.2.4 Open-field test

The animals (n=6/group) were pretreated with CiL-1 (0.1; 0.5 or 1.0 mg/mL; 20 µL; *i.p.*), or vehicle (Control, saline; 20 µL; *i.p.*) without the injection of noxious agents and submitted to the open-field test to observe any alteration in fish motor coordination, either through sedation and/or muscle relaxation. A naive group was included. Number of line crossings was counted during 0–5 min.

3.1.2.5 Toxicity to adult zebrafish

The acute toxicity study was carried out in adult zebrafish (*D. rerio*) according to OECD guidelines. CIL-1 (0.1; 0.5 or 1.0 mg/mL; 20 µL; *i.p.*) was injected intraperitoneally (*i.p.*) with a 20-µL volume (dissolved in saline) to six fish in each group. After the injection, the fish were observed for 96 h. The number of animals that died at each concentration from 0 to 96 h was noted.

3.1.2.6 Formalin-induced nociception

The protocol followed Silva et al. (2020). Adult zebrafish (n = 6/group) were treated (20 µL; *i.p.*) with CiL-1 (0.1; 0.5 or 1.0 mg/mL; 20 µL; *i.p.*), vehicle (Control, saline; 20 µL; *i.p.*), or morphine (positive control, 5.0 mg/mL) 1 h before the injection of 0.1% formalin solution (20.0 µL; *i.m.*) by tail. A naive group was also included. In subsequent experiments, animals (n = 6/group) were pretreated intraperitoneally (20.0 µL) with camphor (2.5 mg/mL; *i.p.*) 15 min before the injection of the most effective concentration of CiL-1 (1.0 mg/mL) to verify the possible involvement of TRPA1 in nociception. Antinociceptive activity was calculated individually during both the neurogenic stage (0 - 5 min) and the inflammatory stage (15 - 30 min).

3.1.2.7 Anti-inflammatory activity

Anti-inflammatory activity was performed under carrageenan-induced abdominal edema as described by Silva et al. (2020). Animals (n = 6/group) received CiL-1 (0.1; 0.5 or 1.0 mg/mL; 20 µL; *i.p.*) or vehicle (Control, saline; 20 µL; *i.p.*). The positive control was sodium diclofenac (2.5 mg/mL; 5.0 µL; *i.p.*). After 1 h, adult zebrafish received *i.p.* injection of carrageenan (1.5%; 20.0 µL). The body weight (BW) of the animals was measured before treatment and 4 h after the induction of peritoneal edema. The animals were sacrificed immediately to stop the biological reactions at the end of the experiment.

3.1.2.8 ROS Analysis

Tissues of brain and liver were collected immediately after sacrifice and homogenized in ice-cold 40 mM Tris-HCl, pH 7.4. The homogenates were centrifuged at 500 × g for 15 min at 4 °C to precipitate large particles and centrifuged again at 12,000 × g for 30 min at 4 °C. The supernatants were maintained at 4 °C. ROS content of the animals treated with CiL-1 (1.0 mg/mL), control (saline) and sodium diclofenac (2.5 mg/mL) was determined according to Hye et al. (2004) with modifications, using DCFH-DA. Briefly, DCFH-DA solution was co-incubated at 37 °C for 20 min. DCF fluorescence intensity was measured on an Anthos Multiread 400 Biochrom® with excitation wavelength at 485 nm and emission wavelength 520 nm. Soluble protein content was determined according to the method of Bradford (1976) using bovine serum albumin (BSA) as a standard. Three biological replicates and three technical replicates were used in the analysis.

3.1.2.9 Statistical analysis

The results were expressed as mean ± standard error of the mean for each group of six animals. After confirming the normal distribution and homogeneity of the data, differences between the groups were submitted to analysis of variance (one-way analysis of variance ANOVA), followed by the Tukey test. All analyses were performed using GraphPad Prism v. 6.01. The level of statistical significance used was 5% ($P < .05$).

3.1.3 In silico analysis

3.1.3.1 Protein and oligosaccharide structural preparation

The structural prediction of *C. isthmocladum* lectin (CiL-1), as well as its carbohydrate binding-site identification, was performed as described by Carneiro et al. (2020). On the other hand, the oligosaccharides used for molecular docking calculations were built using Discovery Studio software (BIOVIA) based on the LacNac ligand (oligosaccharide-1) on the crystal structure of human galectin-9 (PDB ID 2ZHK) (Nagae et al. 2009), followed by the addition of a sialic acid terminal residue (oligosaccharide-2), the coordinates of which were obtained from PubChem (https://pubchem.ncbi.nlm.nih.gov/). These oligosaccharides correspond to variations of a longer branch present on the natural oligosaccharide of the human TRPA1 protein (Chan et al. 2018).

3.1.3.2 Molecular docking calculations and structure minimization

The structural basis for oligosaccharide recognition by CiL-1 was explored through molecular docking calculations, performed with AutoDock Vina, version 1.1.2, which applies an iterated local search global optimizer for the optimization procedure whereby the succession of each step consists of a mutation and local optimization (Trott and Olson, 2009). The protein and carbohydrate ligands were treated as rigid and flexible molecules, respectively, and a specific search was performed using a cubic space of 20 Å × 20 Å × 20 Å centered on the carbohydrate-binding site. For each docking, the ten top-ranked generations based on the predicted binding affinity (in kilocalories per mole) were analyzed. Afterwards, the complexes formed by CiL-1 structure and the selected results for both oligosaccharides were minimized through 50.000 steps of molecular dynamics simulations performed by GROMACS v. 5.0 with the CHARMM36 forcefield (Huang et al. 2016). AutoDock Vina was validated for the presented purpose through redocking calculations using the above-mentioned crystal structure of human galectin-9 (PDB ID 2ZHK), and the results were analyzed by the Root Mean Square Deviation (RMSD) of the atomic positions between the crystal and calculated ligands using the RMSD calculator tool of the Visual Molecular Dynamics (VMD) software (Humphrey et al. 1996).

4 RESULTS

4.1 Open-field test and Toxicity to adult zebrafish

The locomotor activity of the adult zebrafish in the open-field test was not altered by any CiL-1 treatments (0.1 or 0.5 or 1.0 mg/mL) (Fig. 1). This indicates that the animals do not have any change of locomotion when treated with CiL-1. The fact that CiL-1 did not interfere with locomotor activities rules out nonspecific CiL-1- induced muscle relaxation action. In addition, CiL-1 (0.1 or 0.5 or 1.0 mg / mL) dissolved in saline did not cause any behavioral changes or death of adult zebrafish for 96 h. These results confirm that CiL-1 does not have acute toxicity at the administered doses.

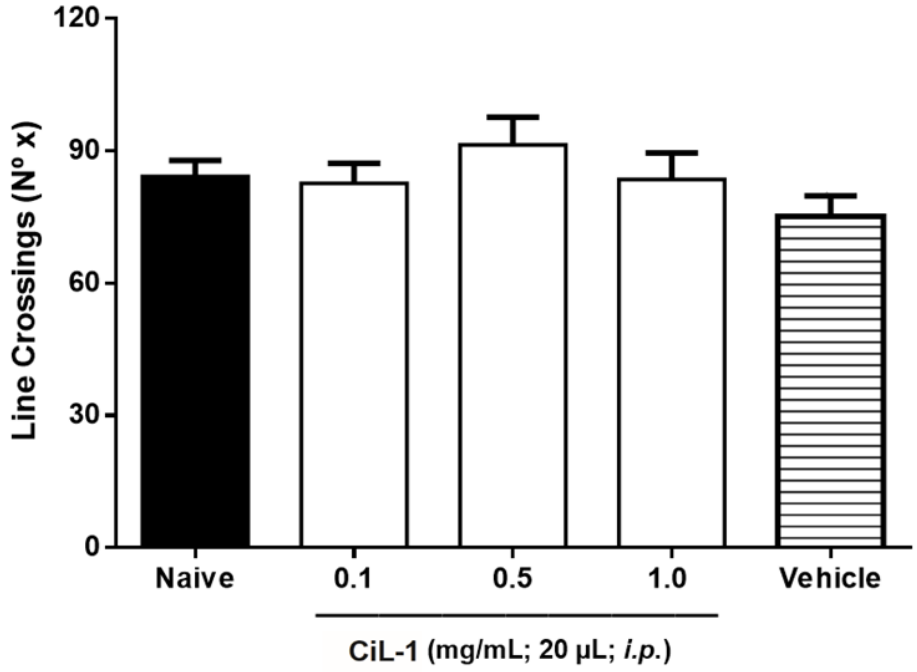

Figure 1. Effect of CIL-1 on locomotor activity of adult zebrafish (*D. rerio*) in the Open Field Test. Each column represents the mean ± standard error of the mean (n = 6/group). Analyzed individually during 0–5 min. Control: vehicle (0.9% saline; 20 µL*i.p.*). CiL-1 (0.1; 0.5 or 1.0 mg/mL; 20 µL; *i.p.*). Naive - untreated animals. One-way ANOVA with Tukey's post-hoc test didn't show any difference between the groups ($p < 0.05$ vs. Control).

4.2 Formalin-induced nociceptive behavior

Pretreatment with CiL-1 or morphine showed significant antinociceptive effect in neurogenic phase (0.1 or 0.5 or 1.0 mg/mL) ($p < 0.05$; $p < 0.01$; $p < 0.001$ vs. Control) and inflammatory phase (0.1 or 0.5 or 1.0 mg/mL) ($p < 0.01$; $p < 0.001$ vs. Control) in 0.1% formalin-induced nociception by decrease of nociceptive behavior. CiL-1 and morphine decreased the nociceptive behavior induced by formalin in the two phases of the test (Fig. 2). The effect was more potent in inflammatory pain, indicating anti-inflammatory action. The antinociceptive effect of CiL-1 (1.0 mg/mL) was diminished in the first stage and completely abolished in the second stage by Camphor (2.5 mg/mL; 20 µL; *i.p.*), which leads to an increase of nociceptive behavior (Fig. 2). Camphor is the TRPA1-specific receptor antagonist, and pretreatment with this compound decreased the CiL-1 effect in both neurogenic and inflammatory phases, but the effect was stronger and significative in the second phase. (Fig. 2). This drug significantly reduced the antinociceptive effect of CiL-1 at a concentration of 1.0 mg/mL, the highest dose tested, indicating that TRPA1 receptor is involved in inflammatory processes and can be modulated by CiL-1.

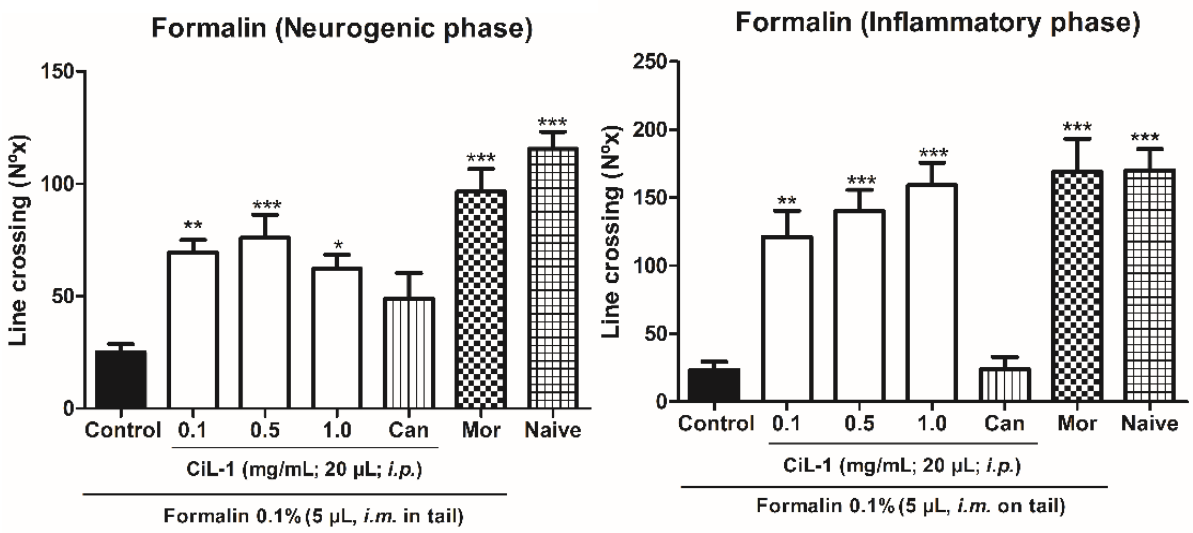

Figure 2. Effect of CiL-1 on formalin-induced nociception in adult zebrafish (*D. rerio*). Analyzed individually during Neurogenic Phase (0- 5 min) and Inflammatory Phase (15-30 min). Each column represents the mean ± standard error of the mean (n = 6/group). One-way ANOVA with post-hoc Tukey's test (* $p < 0.05$; ** $p < 0.01$; *** $p < 0.001$ vs. Control). Control: vehicle (0.9% saline; 20 µL*i.p.*). CiL-1 (0.1; 0.5 or 1.0 mg/mL; 20 µL; *i.p.*). Camphor (2.5 mg/mL; 20 µL *i.p.*) + CiL-1 (1.0 mg/mL; 20 µL *i.p.*). Mormorphine (5.0 mg/mL; 20 µL *i.p.*). Naive: untreated group. Camphor was injected 15 min before the injection of CiL-1 (1.0 mg/mL).

4.3 Anti-inflammatory activity

Pretreatment with CiL-1 (0.5 or 1.0 mg / mL) ($p < 0.01$; $p < 0.001$ vs. Control) or Diclofenac (1.0 mg/mL) ($p < 0.05$ vs. control) significantly reduces the abdominal edema induced by carrageenan, as shown by the decrease in body weight in adult zebrafish (Fig. 3). CiL-1 was able to reduce edema more efficiently than the reference drug, highlighting its potent anti-inflammatory effect. A doseresponse control of abdominal edema by CiL-1 administration can be observed.

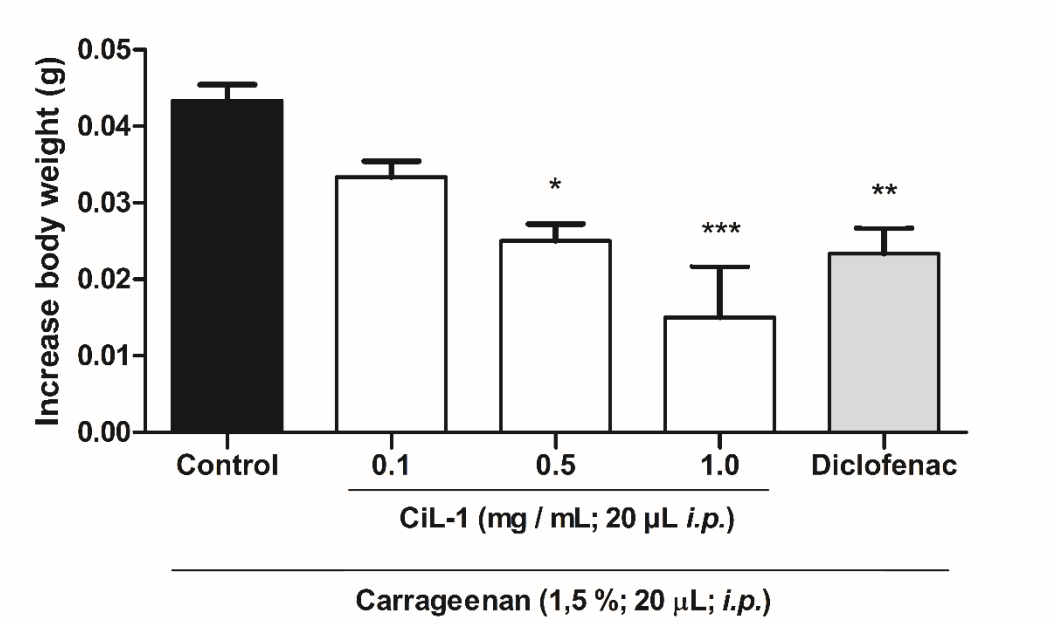

Figure 3. Effect of CiL-1 on carrageenan induced abdominal edema in adult zebrafish (*D. rerio*). Analyzed individually during 0–4 h. Each column represents the mean ± standard error of the mean (n=6/group). One-way ANOVA with post-hoc Tukey's test (* $p < 0.05$; ** $p < 0.01$; *** $p < 0.001$ vs. Control). Control: vehicle (0.9% saline; 20 µL*i.p.*). CiL-1 (0.1; 0.5 or 1.0 mg/mL; 20 µL; *i.p.*). Diclofenac (2.5 mg/mL; 5.0 µL; *i.p.*); Treatment was administered 60 min before injection of carrageenan (1.4%; 20 µL; *i.p.*).

4.4 ROS Analysis

In order to evaluate the possible reduction of ROS inside the cells of the liver and brain, ROS was quantified in animals pretreated with diclofenac and CiL-1 in the most efficient concentration. Pretreatment with the more potent concentration of CiL-1 (1.0 mg/mL) ($p < 0.01$ vs. control) or Diclofenac (2.5 mg/mL) decreased oxidative stress by reducing significantly reactive oxygen species (ROS) in the liver ($p < 0.01$ vs. control) and in the brain ($p < 0.05$ vs. control) (Fig. 4). Diclofenac seems to be more effective, even though the difference between CiL-1 treatment and reference drug was not significant. This systematically corroborates the anti-inflammatory effects from treatment with carrageenan.

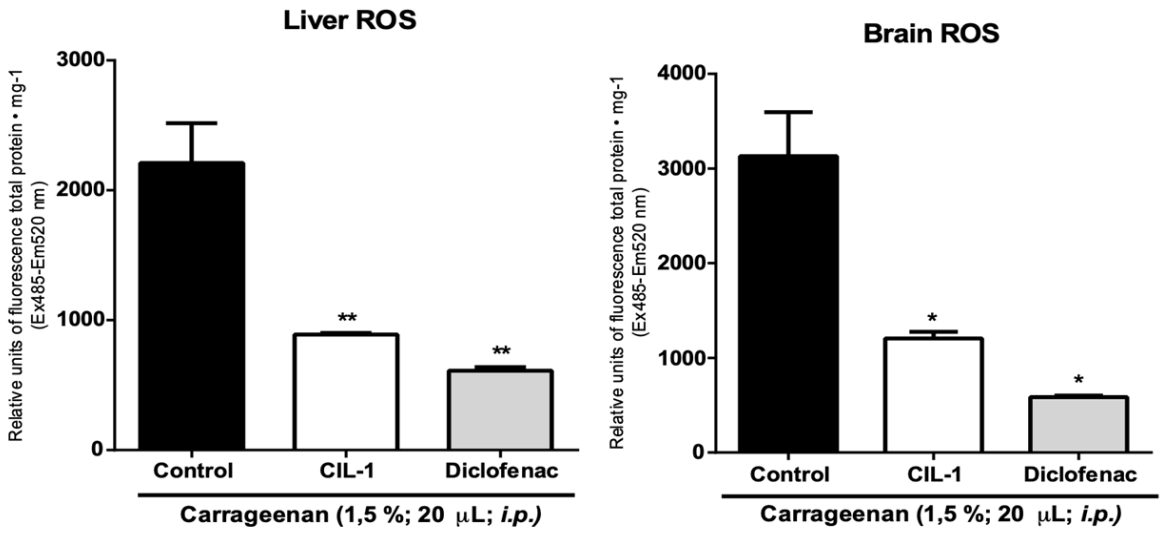

Figure 4. Effect of CiL-1 on the oxidative stress of the liver and brain of zebrafish (*D. rerio*) caused by abdominal edema induced by carrageenan. Each column represents the mean ± standard error of the mean (n = 6/group). One-way ANOVA with post-hoc Tukey's test (* *p <0.05; ** p <0.01* vs. Control). Control: vehicle (0.9% saline; 20 μL*i.p.*). CiL-1 (1.0 mg/mL; 20 μL; *i.p.*). Diclofenac (2.5 mg/mL; 5.0 μL; *i.p.*).

4.5 Molecular docking

Simulations showed that CiL-1 interacts with both ligands tested (Fig. 5). Oligosaccharide-1 (LacNac2), representing the ligand to galectin-1, presents the most favorable binding energy with the protein (-5.8 kcal/mol). The interaction occurs at 4 subsites (S1-S4), and oligosaccharide-1 has an extended conformation at the site (Fig. 5A-B). Oligosaccharide-2 (LacNac2-Sia), which has a sialic acid cap, had a less favorable curved-shape interaction energy (-4.5 kcal/mol) with two residues leaving the site (Fig. 5C-D).

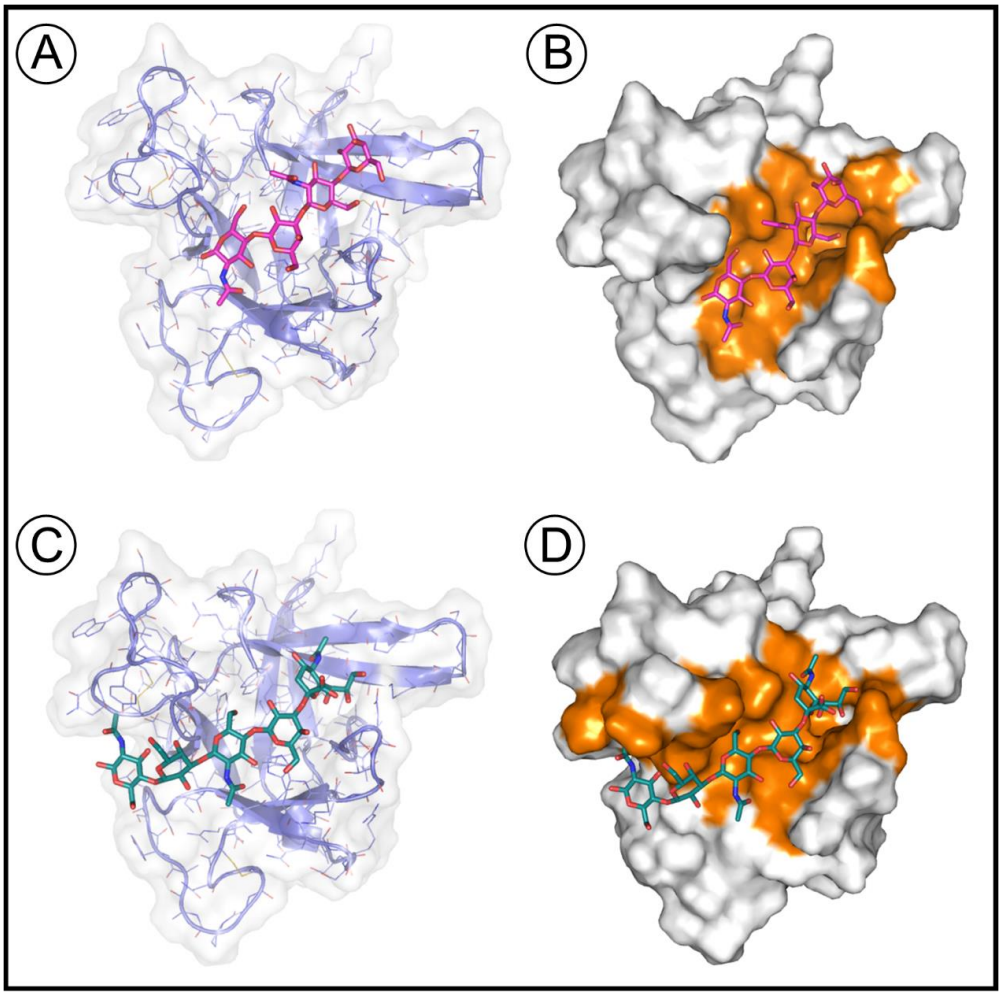

Figure 5. Overall structure of CiL-1 in complex with oligosaccharides 1 and 2. A – Transparent surface representation of CiL-1 in complex with oligosaccharide-1, with the protein structure represented as light blue cartoon and ligand as pink sticks. B – Surface representation of CiL-1 in complex with oligosaccharide-1 with the ligand represented as pink sticks and the surface corresponding to the binding residues colored in orange. C – Transparent surface representation of CiL-1 in complex with oligosaccharide-2, with the protein structure represented as light blue cartoon and ligand as green sticks. D – Surface representation of CiL-1 in complex with oligosaccharide-2, with the ligand represented as green sticks and the surface corresponding to the binding residues colored in orange.

Binding distances are shown in Figure 6 and Supplementary Tables 1-2. The LacNac2 ligand at the CiL-1 site can be arranged in an extended way, occupying 4 subsites. At the distal end (subsite 4) of the oligosaccharide, we have a galactose (GAL4) making a stacking interaction with a histidine such that the sites are occupied in the order S1-NAG1, S2-GAL2, S3-NAG3 and S4-GAL4 (Fig. 6A). Oligosaccharide-2, with salic acid in the distal position, does not have the same form of interaction because salic acid is more bulky than galactose. Consequently, it occupies subsite 3 which, in the first simulation (oligo 1), was occupied by N-acetyl-glucosamine. In this simulation, the sites were occupied alternatively in the order S1-NAG3, S2-GAL4 and S3-5NAC (Fig. 6B).

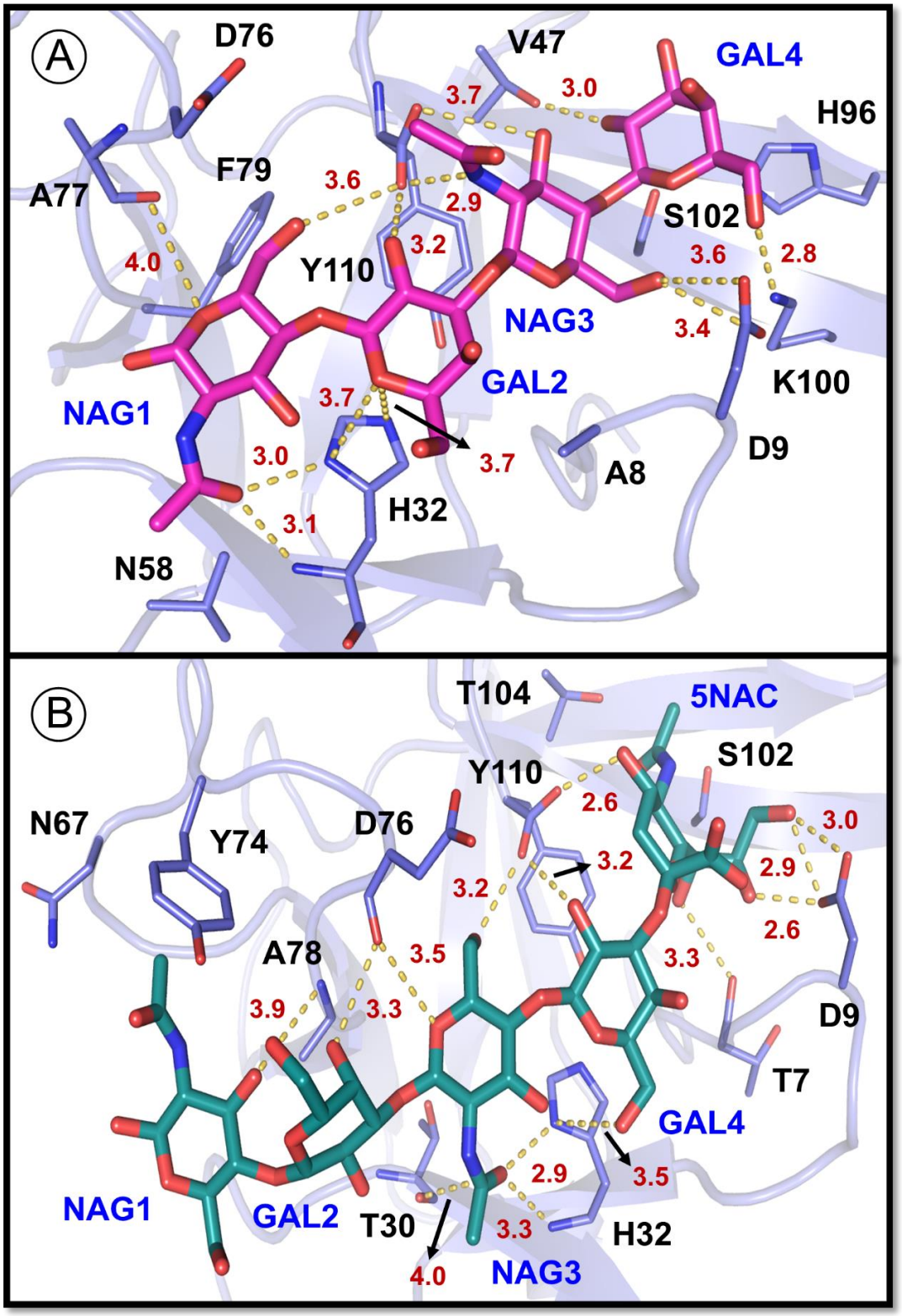

Figure 6. Calculated binding-site interactions between CiL-1 and oligosaccharides 1 and 2. A – Oligosaccharide-1 interaction pattern. B – Oligosaccharide-2 interaction pattern. Protein structure and the interacting amino acid residues are represented as light blue cartoon and sticks, while oligosaccharides 1 and 2 are represented as pink and green sticks, respectively. Polar molecular interactions are represented as yellow dashed lines. For the purpose of clarity, several interactions and residues were omitted.

Based on the predictions made for the oligosaccharides, tetra-antenate putative glycans was constructed, and the interactions were schematically shown in Figures 7A and 7B. In this way, the glycan was added to residue ASN747 of the resolved structure of human TRPA1, illustrating the interactions shown in the docking (Fig. 7C).

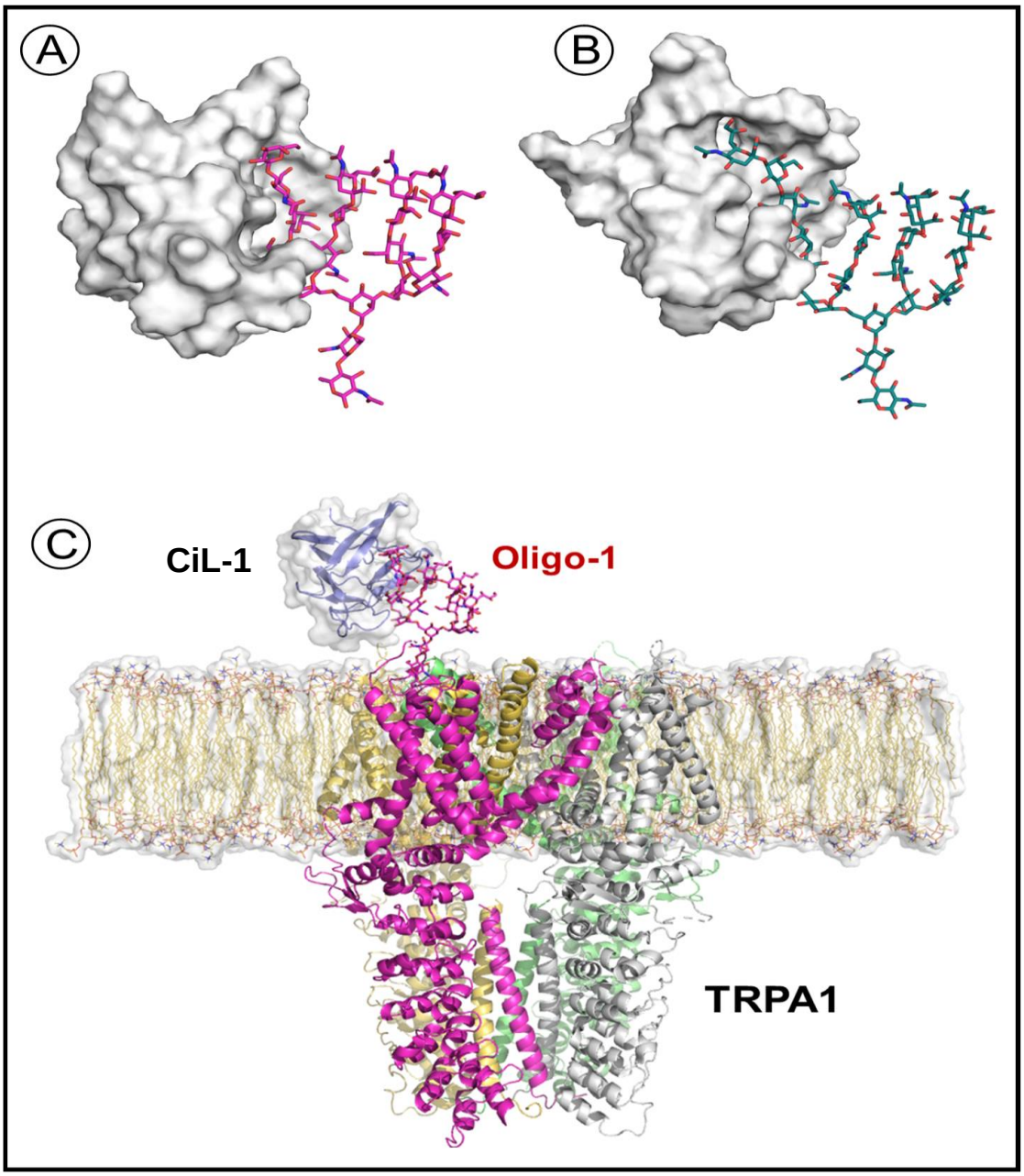

Figure 7. Schematic representation of the complex formed by the recognition of human TRPA1 oligosaccharide-1 by CiL-1. Predicted complex between CiL-1 and oligosaccharides 1 (A) and 2 (B) attached to the complete TRPA1 oligosaccharide. CiL-1 is represented as a white surface, while oligosaccharides 1 and 2 are represented as pink and green sticks, respectively. The complete form of TRPA1 oligosaccharide was built by Discovery studio (BIOVIA). (C) Oligosaccharide-1 and human TRPA1 are represented as pink sticks and multicolored cartoon, while CiL-1 is represented as a light blue cartoon covered by a white surface, respectively. An illustrative lipid bilayer is represented as yellow lines covered by a transparent white surface.

5 DISCUSSION

CiL-1 toxicity was not detected for adult zebrafish, and it did not interfere with locomotor activities in the open-field test. These results indicate the possible safe phytotherapeutic use of this lectin, and carbohydrate-protein interaction often requires affinity enhancement in order to attain biological significance (Nagae and Yamaguchi, 2014). Natural products with neuroprotective effects from seaweed stand out for having few adverse effects (Bălașa et al. 2020). Although some compounds have toxic effects, a wide variety of seaweed compounds have important properties with the potential for therapeutic treatment of diseases and yet have low levels of toxicity (da Silva et al. 2020; Alves et al. 2020).

The formalin injection (TRPA1 agonist) promoted a two-phase nociceptive response, characterized by the decrease in the locomotor activity of adult zebrafish (D. rerio) (Silva et al. 2020). The activation of TRP channels occurs during nociceptive stimulation, especially TRPA1, since formalin is known to be a chemical activator of this ionic transporter. The reduction of inflammatory nociception, known to be more potent than neurogenic nociception, is consistent with peripheral-acting drugs, even though CiL-1 is central-acting, too, and indicates inflammatory neuromodulation (de Góes and Reis 2012; González- Trujano et al. 2019). Formalin also induces nociception through the activation of C fibers and inflammatory reaction. Investigating the modulation of TRPA1 receptors was achieved using adult zebrafish pretreated with the TRPA1-specific receptor antagonist camphor (Alpizar et al. 2013). This drug significantly reduced the antinociceptive effect of CiL-1 at the concentration tested in antinociceptive test. This indicates that TRPA1 is mainly involved in inflammatory responses. The activation of TRPA1 at nerve terminals depolarizes membranes owing to Na^+ influx and induces a local calcium influx through the channel which further releases neuropeptides via Ca^{2+}-dependent exocytosis (Gustavsson et al. 2012). The presence of neuropeptides causes a further amplification of nociception, recruitment of immune cells, vasodilatation and neurogenic inflammation (Geppetti et al. 2008). The nociceptive action is related to the pumping of ion into the nerve cells via TRPA1 and other TRPs increasing the release of glutamate in nerve cell synapses (Batista et al. 2018). Since TRP channels, especially TRPA1 and TRPV1, constitute the largest group of nociceptive ion channels, evidence of codependent action of these channels has been reported (Kichko et al. 2018). It has also been demonstrated that TRPV1 and TRPA1 interact in the bradykinin signaling pathway and that they are extensively coexpressed (Kádková et al. 2017).

The *N*-glycosylation of TRP channels has been occasionally shown to have a profound impact on the levels of cell-surface expression and can modulate the activity of

these channels (Egan et al. 2016). The balance of glycosylation and deglycosylation of ion channels can markedly influence their function and regulation (Dimke et al. 2011). The interaction of lectins with TRP glycan seems to be an important mechanism influencing this regulation (Cha et al. 2008). *N*glycan- mediated binding with galectins is important for regulating the residence time of cell-surface glycoproteins and indicates that other galactose-binding lectins can also act in this modulation. The interaction of CiL-1 with the oligosaccharide-1 is quite similar to that reported to galectin-1 that binds LacNAc and 2,3-sialylated LacNAc, but not 2,6-sialylated LacNAc. The affinity of polymeric LacNAc for galectin-1 is much higher than that of LacNAc monomer (Leppanen et al. 2005). In this work, we evidenced the binding of CiL-1 to a LacNac2 with higher affinity than that of Sialyl-LacNac2. It has been demonstrated that removal of terminal sialic acids from typical complextype asparagine-linked glycans of TRPV5 exposes underlying LacNAc for binding to galectin-1 (Cha et al. 2008).

CiL-1 has anti-inflammatory activity since it can reduce edema. Other seaweed lectins have also had anti-inflammatory activity reported, some from the northeastern Brazilian coast (Fontenelle et al. 2018; Da Conceição Rivanor et al. 2014; Figueiredo et al. 2010). Inflammatory processes, both locally and systemically, are associated with the production of reactive oxygen species (ROS), such as superoxide anions, hydrogen peroxide and peroxynitrite (Fang and Miller 2012). The decrease of ROS in liver and in brain of the treated animals suggests an anti-inflammatory effect that systematically corroborates the results of carrageenan experiments. At the site of inflammation, different cells, including leukocytes, endothelial cells and sensory nerve cells, produce NO. The excess production of NO and neutrophil-derived oxygen radicals cause cytotoxicity and lipid peroxidation. At high levels of NOS, this process causes degradation of membrane lipids and disruption of cell membranes (Loetchutinat et al. 2005). Anti-inflammatory and antioxidant effects of several compounds are related to their ability to protect against oxidative stress (Motterline et al. 2000; Zhang and Tsao, 2016). Evidence shows that systemic anti-inflammatory effect is related to protection from oxidative stress in the brain and liver, as evidenced in the present study (Guo et al. 2017; Xiong et al. 2019). This result corroborates the hypothesis that the experimental reduction of ROS occurs from blocking the TRPA1 channel.

6 CONCLUSION

This study suggested that CiL-1 safely and efficiently decreased the nociception and inflammation in adult zebrafish by TRPA1 modulation and reduction of ROS, thus showing anti-inflammatory potential. Structurally, these effects are related to the binding of CiL-1 to *N*-glycans in TRPA1 channels, mainly those desialyzated, similar to the interactions between galectin-1 and complex glycan, resulting in receptor modulation.

7 DATA AVAILABILITY STATEMENT

The datasets generated during and/or analysed during the current study are available from the corresponding author on reasonable request.

8 ACKNOWLEDGEMENTS

This study was partly funded by Fundação Cearense de Apoio ao Desenvolvimento Científico e Tecnológico (FUNCAP), Coordenação de Aperfeiçoamento de Pessoal de Nível Superior (CAPES), and Conselho Nacional de Desenvolvimento Científico e Tecnológico (CNPq) referring to the Research Productivity grant of BAMR, MIFG, EOPTF CSN, and AHS.

SUPPLEMENTARY TABLES

Table 1. Residues and interaction distances involved in Oligo-1 coordination determined by docking calculations and system minimization (molecular dynamics).

CiL-1		Oligo-1		Distance (Å)*
Residue	**Atom**	**Residue**	**Atom**	
V31	CB	NAG1	C8	4.0
H32	N	NAG1	O7	3.1
H32	ND1	NAG1	O7	3.0
H32	ND1	NAG1	O3	3.0
H32	CE1	NAG1	C3	4.0
H32	CE1	NAG1	C4	3.6
A77	O	NAG1	O5	4.0
D76	O	NAG1	O5	4.0
F79	CE1	NAG1	C6	4.0
Y110	OT1	NAG1	O6	3.6
A8	CB	GAL2	C4	3.9
A8	CB	GAL2	C6	3.7
H32	CG	GAL2	C6	3.8
H32	CD2	GAL2	C6	3.8
H32	CD2	GAL2	C5	3.6
H32	ND1	GAL2	O5	3.7
H32	NE2	GAL2	O5	3.7
H32	CE1	GAL2	C1	3.7
Y110	OT1	GAL2	O2	3.2
D9	OD1	NAG3	O6	3.4
D9	OD2	NAG3	O6	3.6
K100	NZ	NAG3	O6	3.7

Y110	OT1	NAG3	N	2.9
Y110	OT2	NAG3	N	3.1
Y110	OT2	NAG3	O3	3.7
Y110	CD2	NAG3	C3	3.9
H96	CE1	GAL4	C3	3.8
H96	CE1	GAL4	C4	3.9
H96	CE1	GAL4	C5	3.7
K100	NZ	NAG3	O6	2.8
S102	OG	GAL4	O2	3.1
S102	CB	GAL4	C1	4.0
T104	OG1	GAL4	O2	3.0

*** Distance cutoff – 4 Å**

Table 2. Residues and interaction distances involved in Oligo-2 coordination determined by docking calculations and system minimization (molecular dynamics).

CiL		Oligo-2		Distance (Å)*
Residue	**Atom**	**Residue**	**Atom**	
D67	CB	NAG1	C8	3.8
Y74	CB	NAG1	C8	4.0
Y74	CG	NAG1	C8	4.0
A78	N	NAG1	O3	3.9
A78	CB	NAG1	C3	3.8
D76	O	GAL2	O4	3.3
A78	CB	GAL2	C2	4.0
A78	N	GAL2	O4	3.2
T30	O	NAG3	O7	4.0
V31	CG1	NAG3	C8	4.0
V31	CA	NAG3	C8	4.0
H32	N	NAG3	O7	3.3
H32	ND1	NAG3	O7	2.9
H32	ND1	NAG3	O3	3.2
D76	C	NAG3	C6	4.0
D76	O	NAG3	O5	3.5
Y110	OT1	NAG3	O6	3.2
A8	CB	GAL4	C4	3.7
A8	CB	GAL4	C6	3.6
H32	CD2	GAL4	C5	3.6
H32	CD2	GAL4	C6	3.6
H32	ND1	GAL4	O6	3.5
Y110	OT1	GAL4	O1	3.2

T7	O	5NAC	O5	3.3
D9	N	5NAC	O6	3.6
D9	OD1	5NAC	O6	2.6
D9	OD1	5NAC	O7	2.9
D9	OD2	5NAC	O7	3.0
K100	NZ	5NAC	O7	2.8
S102	CB	5NAC	C7	4.0
I103	O	5NAC	O8	3.8
Y110	OT2	5NAC	O3	2.6
Y110	CD2	5NAC	C5	3.9
T104	OG1	5NAC	O8	3.3

*** Distance cutoff – 4 Å**

REFERÊNCIAS

AINOUZ, I.L.; SAMPAIO, A.H. Screening of Brazilian marine algae for hemaglutinins. **Botanica Marina**, Brazil, v.34, p.211-214, 1991.

ALPIZAR, Y.A.; GEES, M.; SANCHEZ, A.; APETREI, A.; VOEST, T.; NILIUS, B.; TALAVERA, K. Bimodal effects of cinnamaldehyde and camphor on mouse TRPA1. **Pflugers Arch Eur J Physiol**, [S.I.], v.465, p.853–864, 2013.

ALVAREZ-HERNANDEZ, S.; DE LARA-ISASSI, G.; ARREGUIN-ESPINOZA, R.; ARREGUIN, B.; HERNANDEZ-SANTOYO, A.; RODRIGUEZ-ROMERO, A. Isolation and partial characterization of geraffine, a lectin from the Mexican endemic alga Codium giraffa Silva. **Botanica Marina**, New York, v.42, p.573–80, 1999.

ALVES, M.F.A.; BARRETO, F.K.A.; VASCONCELOS, M.A.; NETO, G.N.; CARNEIRO, R.F.; SILVA, L.T.; NAGANO, C.S.; SAMPAIO, A.H.; TEIXEIRA, E.H. Antihyperglycemic and antioxidant activities of a lectin from the marine red algae, Bryothamnion seaforthii, in rats with streptozotocin-induced diabetes. **Int J Biol Macromol**, [S.I.], v.158, p.773–780, 2020.

AMBROSIO, A. L. et al. Isolation of two novel mannan- and l-fucose-binding lectins from the green alga Enteromorpha prolifera: biochemical characterization of EPL-2. **Archives of Biochemistry and Biophysics**, USA, v.415, p.245–250, 2003.

BĂLAȘA, A.F.; CHIRCOV, C.; GRUMEZESCU, A.M. Marine biocompounds for neuroprotection- a review. **Mar Drugs**, [S.I.], v.18, p.9–11, 2020.

BALEMANS, D.; AGUILERA-LIZARRAGA, J.; FLORENS, M.V.; JAIN, P.; DENADAI-SOUZA, A.; VIOLA, M.F.; AGUIAR, A.Y.; VAN DER MERWE, S.; VANDEN BERGHE, P.; TALAVERA, K.; VANNER, S.J.; WOUTERS, M.M.; BOECKXSTAENS, G.E. Histamine-mediated potentiation of TRPA1 and TRPV4 signaling in submucosal neurons in IBS patients. **Am J Physiol Gastrointest Liver Physiol**, [S.I.], v.16, p.338–349, 2019.

BARALDI, P.G.; PRETI, D.; MATERAZZI, S.; GEPPETTI, P. Transient receptor potential ankyrin 1 (TRPA1) channel as emerging target for novel analgesics and anti-inflammatory agents. **J Med Chem**, [S.I], v.53, p.5085–5107, 2010.

BARSANTI, L.; GUALTIERI, P. *In:* BARSANTI, L.; GUALTIERI, P. **Algae: Anatomy, Biochemistry and Biotechnology**, CRC Press, Second Edition, [S.I.], 2014, p.362.

BATISTA, F.L.A.; LIMA, L.M.G.; ABRANTE, I.A.; ARAÚJO, J.I.F.; BATISTA, F.L.A.; ABRANTE, I.A.; MAGALHÃES, E.A.; LIMA, D.R.; LIMA, M.C.L.L.; PRADO, B.S.; MOURA, L.F.W.G.; GUEDES, M.I.F.; FERREIRA, M.K.A.; MENEZES, J.E.S.A.; SANTOS, S.A.A.; MENDES, F.R.S.; MOREIRA, R.A.; MOREIRA, A.C.O.M.; CAMPOS, A.R.; MAGALHÃES, F.E. Antinociceptive activity of ethanolic extract of Azadirachta indica A. Juss (Neem, Meliaceae) fruit through opioid, glutamatergic and acid-sensitive ion pathways in adult zebrafish (Danio rerio). **Biomed Pharmacother**, [S.I.], v.108, p.408–416, 2018.

BEAR, M.F.; CONNORS, B.W.; PARADISO, M.A. *In:* BEAR, M.F.; CONNORS, B.W.; PARADISO, M.A. **Neurociências: desvendando o sistema nervoso**, 2. ed. Porto Alegre: Artmed, 2006.

BECKMAN, J.S. Oxidative damage and tyrosine nitration from peroxynitrite. **Chem Res Toxicol**, USA, v.9, p.836–844, 1996.

BESSON, M. J.; DICKENSON, A. *In:* The BESSON, M. J.; DICKENSON, A. **Pharmacology of pain**. Berlin: Springer-Verlag, 1997, cap. 2.

BESSON, M. J. The complexity of physiopharmacologic aspects of pain. **Drugs**, [S.I.], v.53, Supp.2, p.1-9, 1999.

BOYD, W.C.; ALMODÓVAR, L.R. Agglutinin in marine algae for human erythrocytes. **Comparative Biochemistry and Physiology**, [S.I.], v.6, p.82-83, 1966.

BOYD, W.C.; SHAPLEIGH, E. Specific Precipitating Activity of Plant Agglutinins (Lectins). **Science**, [S.I.], v.119, p.419-419, 1954.

BRADFORD, M.M. A rapid and sensitive method for the quantitation of microgram quantities of protein utilizing the principle of protein-dye binding. **Analytical Biochemistry**, [S.I.], v.72, p.248-254, 1976.

CALVETE, J. J. et al. The amino acid sequence of the agglutinin isolated from the red marine alga Bryothamnion triquetrum defines a novel lectin structure. **CMLS Cellular and Molecular Life Sciences**, [S.I.], v.57, p.343-350, 2000.

CARNEIRO, R.F.; DUARTE, P.L.; CHAVES, R.P.; SILVA, S.R.; FEITOSA, R.R.; SOUSA, B.L.; ALVES, A.W.S; VASCONCELOS, M.A.; ROCHA, B.A.M.; TEIXEIRA, E.H; SAMPAIO, A.H; NAGANO, C.S. New lectins from Codium isthmocladum Vickers show unique amino acid sequence and antibiofilm effect on pathogenic bacteria. **Journal of Applied Phycology**, [S.I.], p.01–14, 2020.

CHAN, Y.; LIN, H.; TU, Z.; KUO, Y.; HSU, S.D.; LIN, C. Dissecting the Structure–Activity Relationship of Galectin–Ligand Interactions. **Int J Mol Sci**, [S.I.], v.19, p.1–20, 2018.

CHA, S.; ORTEGA, B.; KUROSU, H.; ROSENBLATT, K.P.; KURO-O, M.; HUANG, H. Removal of sialic acid involving Klotho causes cell-surface retention of TRPV5 channel via binding to galectin-1. **PNAS**, Dallas, v.115, p.9805–9810, 2008.

CHEN, Y.H.; LIU, X.W.; HUANG, J.L.; BALOCH, S.; XU, X.; PEI, X.F. Microbial diversity and chemical analysis of Shuidouchi, traditional Chinese fermented soybean. **Food Res**, [S.I.], v.116, p.1289–1297, 2019.

CHEN, Z.; VONG, C.T.; GAO, C.; CHEN, S.; WU, X.; WANG, S.; WANG, Y. Bilirubin Nanomedicines for the Treatment of Reactive Oxygen Species (ROS)-Mediated Diseases. **Mol. Pharmaceutics**, USA, v.17, p.2260−2274, 2020.

CHERRY, P.; O'HARA, C.; MAGEE, P.J.; MCSORLEY, E.M.; ALLSOPP, P.J. Risks and benefits of consuming edible seaweeds. **Nutr Rev**, [S.I.], v.77, p.307–329, 2019.

CHILES, T.C.; BIRD, K.T. A comparative study of animal erythrocyte agglutinins from marine algae. **Comparative Biochemistry and Physiology**, [S.I.], v.94B, p.107-111, 1989.

CLARK, R.; KUPPER, T. Old meets new: the interaction between innate and adaptive immunity. **J Invest Dermatol**, [S.I.], v.125, p.629–637, 2005.

COHEN, D.M., Regulation of TRP channels by N-linked glycosylation. **Seminars in Cell & Developmental Biology**, [S.I.], v.17, p.630–637, 2006.

CONKLIN, D.J.; GUO, Y.; NYSTORIAK, M.A.; JAGATHEESAN, G.; OBAL, D.; KILFOIL, P.J.; HOETKER, J.D.; GUO, L.; BOLLI, R.; BHATNAGAR, A. TRPA1 channel contributes to myocardial ischemia-reperfusion injury. **Am J Physiol Heart Circ Physiol**, [S.I.], v.316, p.889–899, 2019.

COELHO, L.C.B.B.; SILVA, P.M.S.; LIMA, VLM.; PONTUAL; E.V.; PAIVA; P.M.G.; NAPOLEÃO, T.H.; CORREIA, M.T.S. Lectins, Interconnecting proteins with biotechnological/pharmacological and therapeutic applications. **Evidence-Based Complem and Alt Med**, [S.I.], v.2017, 2017.

CONN, P.J.; PIN, J.P. Pharmacology and functions of metabotropic glutamate receptors. **Pharmacol Toxicol**, [S.I.], v.37, p.205–37, 1997.

CORINO, C.; MODINA, S.C.; DI GIANCAMILLO, A.; CHIAPPARINI, S.; ROSSI, R. Seaweeds in pig nutrition. **Animals**, [S.I.], v.9, p.1126, 2019.

CVETKOV, T.L.; HUYNH, K.W.; COHEN, M.R.; MOISEENKOVA-BELL, V.Y. Molecular architecture and subunit organization of TRPA1 ion channel revealed by electron microscopy. **J Biol Chem**, USA, v.286, p.38168–38176, 2011.

CRESPO, M.; LEÓN-NAVARRO, D.A.; MARTÍN, M. Glutamatergic System is Afected in Brain from an Hyperthermia-Induced Seizures Rat Model. **Cellular and Molecular Neurobiology**, [S.I.], p.01-12, 2021.

DA CONCEIÇÃO RIVANOR, R.L.; CHAVES, H.V.; DO VAL, D.R.; FREITAS, A.R.; LEMOS, J.C.; RODRIGUES, J.A.G.; PEREIRA, K.M.A.; ARAÚJO, I.W.F.; BEZERRA, M.M.; BENEVIDES, N.M.B. A lectin from the green seaweed Caulerpa cupressoides reduces mechanical hyper-nociception and inflammation in the rat temporomandibular joint during zymosan-induced arthritis. **Int Immunopharmacol**, [S.I.], v.21, p.34–43, 2014.

DANGUY, A. et al. Galectins and cancer. **Biochimica et Biophysica Acta**, Belgium, v.1572, p.285-293, 2002.

DA SILVA, A.C.R.; PEREIRA, K.K.G.; CRITCHLEY, A.T.; SANCHEZ, E.F.; FULY, A.L. Potential utilization of a lambda carrageenan polysaccharide, derived from a cultivated, clonal strain of the red seaweed Chondrus crispus (Irish moss) against toxic actions of venom of Bothrops jararaca and B. jararacussu snakes. **J Appl Phycol**, [S.I.], v.32, p.4309–4320, 2020.

DE GÓES, H.G.; REIS, R.P. Temporal variation of the growth, carrageenan yield and quality of Kappaphycus alvarezii (Rhodophyta, Gigartinales) cultivated at Sepetiba bay, southeastern Brazilian coast. **J Appl Phycol**, [S.I.], v.24, p.173–180, 2012.

DIETRICH, A.; STEINRITZ, D.; GUDERMANN, T. Transient receptor potential (TRP) channels as molecular targets in lung toxicology and associated diseases. **Cell Calcium**, [S.I.], v.67, p.123– 137, 2017.

DINH, H.L; HORI,K.; QUANG, N.H. Screening and preliminary characterization of hemagglutinins in Vietnamese marine algae. **Journal of Applied Phycology**, [S.I.], v.21, p.89-97, 2009.

DIMKE, H.; HOENDEROP, J.G.J.; BINDELS, R.J.M. Molecular basis of epithelial Ca2+ and Mg2+ transport: insights from the TRP channel family. **J Physiol, Netherlands**, [S.I.], v.589, p.1535–1542, 2011.

EARLEY, S.; BRAYDEN, J.E. Transient receptor potential channels in the vasculature. **Physiol Rev**, [S.I.], v.95, p.645–690, 2015.

EGAN, T.J.; MARIO, A.; ZENOBI-WONG, M.; ZEILHOFER, H.U.; URECH, D. Effects of N-glycosylation of the human cation channel TRPA1 on agonist-sensitivity. **Biosci Rep**, [S.I.], v.36, p.1–12, 2016.

FABREGAS J.; MUÑOZ, A., LLOVO, J., CARRACEDO, A. Purification and partial characterization of tomentine. An N-acetylglucosamine-specific lectin from the green alga Codium tomentosum (Huds.) Stackh. **Journal of Experimental Marine Biology and Ecology**, [S.I.], v.124, p.21–30, 1988.

FANG, L. MILLER, Y.I. Emerging applications for zebrafish as a model organism to study oxidative mechanisms and their roles in inflammation and vascular accumulation of oxidized lipids. **Free Radic Biol Med**, [S.I.], v.53, p.1411–1420, 2012.

FEIZI, T., HALTIWANGER, R.S. Editorial overview: Carbohydrate–protein interactions and glycosylation: Glycan synthesis and recognition: finding the perfect partner in a sugar-coated life, **Current Opinion in Structural Biology**, [S.I.], v.34, p.7-9, 2015.

FIELDS, H.L. How expectations influence pain. **Pain**, [S.I.], v.159, p.03–10, 2018.

FIGUEIREDO, J.G.; BITENCOURT, F.S.; CUNHA, T.M.; LUZ, P.B.; NASCIMENTO, K.S.; MOTA, M.R.L.; SAMPAIO, A.H.; CAVADA, B.S.; CUNHA, F.Q.; ALENCAR, N.M.N. Agglutinin isolated from the red marine alga Hypnea cervicornis J. Agardh reduces inflammatory hypernociception: Involvement of nitric oxide. **Pharmacol Biochem Behav**, [S.I.], v.4, p.371-377, 2010.

FONTENELLE, T.P.C.; LIMA, G.C.; MESQUITA, J.X.; LOPES, J.L.S.; BRITO, T.V.; JÚNIOR, F.C.V.; SALES, A.B.; ARAGÃO, K.S.; SOUZA, M.H.L.P.; BARBOSA, A.L.R.; FREITAS, A.L.P. Lectin obtained from the red seaweed Bryothamnion triquetrum: Secondary structure and anti-inflammatory activity in mice. **Int J Biol Macromol**, [S.I.], v.112, p.1122–1130, 2018.

FORNASARI, D. Pain Mechanisms in Patients with Chronic Pain. **Clin Drug Investig**, [S.I.], v.32, p.45-52, 2012.

FUNDYTUS, M.E. Glutamate receptors and nociception: Implications for the drug treatment of pain. **CNS Drugs**, [S.I.], v.15, p.29–58, 2001.

GEPPETTI, P.; NASSINI, R.; MATERAZZI, S.; BENEMEI, S. The concept of neurogenic inflammation. **BJU Int**, [S.I.], v.101, p.2-6, 2008.

GONZÁLEZ-TRUJANO, M.E.; GUTIERREZ-VALENTINO, C.; HERNÁNDEZ-ARÁMBURO, M.Y.; DÍAZ-REVAL, M.I.; PELLICER, F. Identification of some bioactive metabolites and inhibitory receptors in the antinociceptive activity of Tagetes lucida Cav. **Life Sci,** [S.I.], v.231, p.116523, 2019.

GRAHAM, L.T. et al. Distribution of some synaptic transmitter suspects in cat spinal cord. **J Neurochem**, Ireland, v. 14, p.465-472, 1967.

GRANGER, D.N.; SENCHENKOVA, E. Colloquium Series on Integrated Systems Physiology: From Molecule to Function to Disease. *In:* Inflammation and the Microcirculation. San Rafael: **Morgan & Claypool Life Sciences**, 2010.

GREER, K.R.; HOYT, J.W. Pain: theory, anatomy, and physiology. **Crit Care Clin**, [S.I.], v.6, p.227-34, 1990.

GUIRY, M.D.; GUIRY, G.M. **Algaebase**: Listing the World's Algae. Available online: https://www.algaebase.org/ (acessado em dezembro 2020).

GUO, S.N.; ZHENG, J.L.; YUAN, S.S.; ZHU, Q.; WU, C. Immunosuppressive effects and associated compensatory responses in zebrafish after full life-cycle exposure to environmentally relevant concentrations of cadmium. **Aquat Toxicol**, [S.I.], v.188, p.64–71, 2017.

GUSTAVSSON, N.; WU, B.; HAN, W. Calcium sensing in exocytosis. **Adv Exp Med Biol**, [S.I.], v.740, p.731-757, 2006.

HAN, J. W. et al. Isolation and Characterization of a sex-specific lectinn in a marine red alga Aglaothamnion oosumienses Itono. **Applied and Environmental microbiology**, [S.I.], v.78, p.7283-7289, 2012.

HAN, J. W. et al. Purification and characterization of a D-mannose specific lectin from the green marine alga, Bryopsis plumose. **Phycological Research**, [S.I.], v.58, p.143-150, 2010.

HAN, J. W. et al. Purification and characterization of a lectin, BPL-3, from the marine green alga Bryopsis plumosa. **Journal Applied of Phycology**, [S.I.], v.23, p.745-753, 2011.

HANDY, D.E.; LOSCALZO, J. Redox regulation of mitochondrial function. **Antioxid Redox Signal**, Boston, v.6, p.1323–1367, 2012.

HAYASHI, H. Morphology of termination of small and large myelinated trigeminal primary afferent fibers in the cat. **J Comp Neurol**, [S.I.], v. 240, p.71-89, 1985.
HONG, C.; JEONG, B.; PARK, H.J.; CHUNG, J.Y.; LEE, J.E.; KIM, J.; SHIN, Y.; SO, I. TRP Channels as Emerging Therapeutic Targets for Neurodegenerative Diseases. **Frontiers in Physiology**, [S.I.], v.11, p.01-15, 2020.

HORI, K. et al. Strict specificity for high-mannose type N-glycans and primary structure of a red alga Eucheuma serra lectin. **Glycobiology**, UK, v.17, p.479-491, 2007.

HORI, K.; MATSUBARA, K.; MIYASAWA, K. Primary structures of two hemaglutinins from marine red alga Hypnea japonica. **Biochimica et Biophysica Acta**, [S.I.], v.1474, p.226-236, 2000.

HOWE, K. et al. The zebrafish reference genome sequence and its relationship to the human genome. **Nature**, [S.I.], v.496, p.498, 2013.

HUANG, J.; RAUSCHER, S.; NAWROCKI, G.; RAN, T.; FEIG, M.; DE GROOT, B.L.; GRUBMULLER, H.; JR, A.D.M. CHARMM36m: An Improved Force Field for Folded and Intrinsically Disordered Proteins. **Nature Methods**, [S.I.], v.14, p.71-73, 2016.

HUMPHREY, W.; DALKE, A.; SCHULTEN, K. VMD - Visual Molecular Dynamics, **J Molec Graphics**, [S.I.], v.14, p.33-38, 1996.

HYE, S.K.; HAE, Y.C.; JI, Y.K.; SON, B.W.; JUNG, H.A.; CHOI, J.S. Inhibitory phlorotannins from the edible brown alga Ecklonia stolonifera on total reactive oxygen species (ROS) generation. **Arch Pharm Res**, [S.I.], v.27, p.194–198, 2004.

ISHIHARA, K.; ARAI S.; SHIMADA, S. cDNA cloning of a lectin-like gene preferentially expressed in freshwater from macroalga Ulva limnetica (Ulcales, Chlorophyta). **Phycological Research**, Japan, v.57, p.104-110, 2009.

JAQUEMAR, D.; SCHENKER, T.; TRUEB, B. An ankyrin-like protein with transmembrane domains is specifically lost after oncogenic transformation of human fibroblasts. **J Biol Chem**, USA, v.274, p.7325–7333, 1999.

JULIUS, D.; BASBAUM, A. I. Molecular mechanisms of nociception. **Nature**, [S.I.], v.413, p. 203-210, 2001.

JULIUS, D. TRP channels and pain. **Annu Rev Cell Dev Biol**, [S.I.], v.29, p.355–384, 2013.

KÁDKOVÁ, A.; SYNYTSYA, V.; KRUSEK, J.; ZÍMOVÁ, L.; VLACHOVÁ, V. Molecular Basis of TRPA1 Regulation in Nociceptive Neurons. A Review. **Physiol Res**, Prague, v.66, p.425–439, 2017.

KANG, Y. H.; SHIN, J. A.; KIM, M. S.; CHUNG, I. K. A preliminary study of the bioremediation potential of Codium fragile applied to seaweed integrated multitrophic aquaculture (IMTA) during the summer. **Journal of Applied Phycology**, [S.I.], v.20, p.183–190, 2008.

KEITH, S. A.; KERSWELL, A. P.; CONNOLLY, S. R. Global diversity of marine macroalgae: environmental conditions explain less variation in the tropics. **Global ecology and biogeography**, [S.I.], v.23, p.517-529, 2014.

KICHKO, T.I.; NEUHUBER, W.; KOBAL, G.; REEH, P.W. The roles of TRPV1, TRPA1 and TRPM8 channels in chemical and thermal sensitivity of the mouse oral mucosa. **Eur J Neurosci**, [S.I.], v.47, p.201–210, 2018.

KIDGELL, J.T.; MAGNUSSON, M.; DE NYS, R.; GLASSON, C.R.K. Ulvan: A systematic review of extraction, composition and function. **Algal Res**, [S.I.], v.39, p.101-422, 2019.

KRAUSE, K.H. Aging: a revisited theory based on free radicals generated by NOX family NADPH oxidases. **Exp Gerontol**, [S.I.], v.42, p.256–262, 2007.

LAMBETH, J.D. NOX enzymes and the biology of reactive oxygen. **Nat Rev Immunol**, [S.I.], v.4, p.181–189, 2004.

LEE, I.; ELIZABETH, A.N.; NECKA, Y.A. Distinguishing pain from nociception, salience, and arousal: How autonomic nervous system activity can improve neuroimaging tests of specificity. **Neuroimage**, [S.I.], v.204, p.01-12, 2020.

LEPPANEN, A.; STOWELL, S. BLIXT, O.; CUMMINGS, R.D. Dimeric galectin-1 binds with high affinity to α2,3-sialylated and nonsialylated terminal N-acetyllactosamine units on surface-bound extended glycans. **J Biol Chem**, [S.I.], v.280, p.5549–5562, 2005.

LIESCHKE, G.J.; CURRIE, P.D. Animal models of human disease: zebrafish swim into view. **Nature Reviews Genetics**, [S.I.], v.8, p. 353–367, 2007.

LOESER, J. D.; MELZACK, R. Pain: an overview. **Lancet**, [S.I.], v. 353, p.1607-1609, 1999.

LOETCHUTINAT, C.; KOTHAN, S.; DECHSUPA, S.; MEESUNGNOEN, J.; JAY-GERIN, J.P.; MANKHETKORN, S. Spectrofluorometric determination of intracellular levels of reactive oxygen species in drug-sensitive and drug-resistant cancer cells using the 2′,7′-dichlorofluorescein diacetate assay. **Radiat Phys Chem**, [S.I.], v.72, p.323–331, 2005.

MAGALHÃES, F.E.A.; BATISTA, F.L.A.; LIMA, L.M.G.; ABRANTE, I.A.; BATISTA, F.L.A.; ABRANTE, I.A.; ARAÚJO, J.I.F.; SANTOS, S.A.A.R.; OLIVEIRA, B.A.; RAPOSO, R.S.; CAMPOS, A.R. Adult Zebrafish (Danio rerio) As a Model for the Study of Corneal Antinociceptive Compounds. **Zebrafish**, [S.I.], v.15, p.566–574, 2018.

MANNING, J.C.; ROMERO, A.; HABERMANN, F.A.; CABALLERO, G.G.; KALTNER, H.; GABIUS, H.J. Lectins: a primer for histochemists and cell biologists. Histochem. **Cell Biol**, [S.I.], v.147, p.199–222, 2017.

MCCURDY, C. R.; SCULLY, S. S. Analgesic substances derived from natural products (natureceuticals). **Life Sci**, USA, v.78, p.476-484, 2005.

MCDOUGALL, J. J. Peripheral analgesia: hitting pain where it hurts. **Biochim Biophys Acta**, [S.I.], v.1812, p.459-467, 2011.

MEDINA-RAMIREZ, G.; GIBBS, R.V.; CALVETE, J.J. Micro-heterogeneity and molecular assembly of the hemagglutinins from the red algae Bryothamnion seaforthii and B. triquetrum from the Caribbean Sea. **European Journal of Phycology**, UK, v.42, p.105-112, 2007.

MEENTS, J.E.; CIOTU, C.I.; FISCHER, M.J.M. TRPA1: a molecular view. **J Neurophysiol**, [S.I.], v.121, p.427–443, 2019.

MEIERS, J.; SIEBS, E., ZAHORSKA, E.; TITZ, A. Lectin antagonists in infection, immunity, and inflammation. **Current Opinion in Chemical Biology**, [S.I.], v.53, p.51–67, 2019.

MEYERS, J.R. Zebrafish: Development of a vertebrate model organism. **Current Protocols Essential Laboratory Techniques**, [S.I.], p.01–26, 2018.

MILLAN, M. J. The induction of pain: an integrative review. **Prog Neurobiol**, [S.I.], v.57, p.01-164, 1999.

MILLER, K.E. et al. Organization of glutamate like-immunoreactivity in the rat superficial dorsal horn: light and electron microscopic observations. **Synapse**, [S.I.], v. 2, p.28-36, 1988.

MITCHELL, S.W. **Researchs upon the venon of the Rattlesnake**.1860. Monography - Smithsonian Institute, Philadelphia, USA. Monography, 1860.

MITTAL, M.; SIDDIQUI, M.R.; TRAN, K.; REDDY, S.P.; MALIK, A.B. Reactive Oxygen Species in Inflammation and Tissue Injury. **Antioxidants & Redox Signaling**, [S.I.], v.20, p.1126-1166, 2014.

MONTELL, C.; RUBIN, G.M. Molecular characterization of the Drosophila TRP locus: a putative integral membrane protein required for phototransduction. **Neuron**, [S.I.], v.2, p.1313-1323, 1989.

MOORE, C.; GUPTA, R.; JORDT, S.E. Regulation of Pain and Itch by TRP Channels. **Neurosci Bull**, [S.I.], v.34, p.120–142, 2018.

MORAIS, T.; INÁCIO A.; COUTINHO, T.; MINISTRO, M.; COSTA, J.; PEREIRA, L.; BAHCEVANDZIEV, K. Seaweed Potential in the Animal Feed: A Review. **J Mar Sci Eng**, [S.I.], v.8, p.559, 2020.

MORAN, M.M. TRP Channels as Potential Drug Targets. **Annu Rev Pharmacol Toxicol**, USA, v.58, p.309-330, 2018.

MORI, T. et al. Isolation and characterization of griffithsin, a novel HIV-inactivating protein, from the red alga Griffithsia sp. **Journal Biology et Chemical**, USA, v.280, p.935-9353, 2005.

MOTTERLINI, R.; FORESTI, R.; BASSI, R.; GREEN, C. Curcumin, an antioxidant and anti-inflammatory agent, induces heme oxygenase-1 and protects endothelial cells against oxidative stress. **Free Radical Biology and Medicine**, [S.I.], v.28, p.1303-1312, 2000.

NAGANO C.S. et al. HCA and HML isolated from the red marine algae Hypnea cervicornis and Hypnea musciformis define a novel lectin family. **Protein Science**, [S.I.], v.14, p.2167-2176, 2005.

NAGAE, M.; NISHI, N.; MURATA, T.; USUI, T.; NAKAMURA, T.; WAKATSUKI, S.; KATO, R. Structural analysis of the recognition mechanism of poly-N-acetyllactosamine by the human galectin-9 N-terminal carbohydrate recognition domain. **Glycobiology**, UK, v.19, p.112–117, 2009.

NAGAE, M.; YAMAGUCHI, Y. Three-Dimensional Structural Aspects of Protein–Polysaccharide Interactions. **Int J Mol Sci**, [S.I.], v.15, p.3768-3783, 2014.

NASCIMENTO-NETO, L. G. et al. Characterization of isoforms of the lectin isolated from the red algae Bryothamnion seaforthii and its pro-healing effect. **Marine Drugs**, [S.I.], v.10, p.1936-1954, 2012.

NATHAN, C.; DING, A. Nonresolving Inflammation. **Cell**, [S.I.], v.140, p.871–882, 2010.

NILIUS, B.; PRENEN, J.; OWSIANIK, G. Irritating channels: the case of TRPA1. **J Physiol**, [S.I.], v.589, p.1543–1549, 2011.

NIU, J.F.; LU, F.; WANG, G.C.; ZHOU, B.C. Characterization of a new lectin involved in the protoplast regeneration of Bryopsis hypnoides. **Chinese Journal of Oceanology and Limnology**, [S.I.], v.27, p.502–512, 2009.

NOTOVA, S.; BONNARDEL, F.; LISACEK, F.D.R.; VARROT, A.; IMBERTY, A. Structure and engineering of tandem repeat lectins. **Current Opinion in Structural Biology**, [S.I.], v.47, p.62-39, 2020.

OECD. Guideline for Testing Acute Toxicity in Fishes. **OECD guideline for testin g of chemicals**. [S.I.], 1992. Disponível em: http://www.oecd.org/chemicalsafety/risk-assessment/1948241.pdf. Acesso em: 20 fev. 2020.

ONGARO, G.; KAPTCHUK, T.J. Symptom perception, placebo effects, and the Bayesian brain. **Pain**, [S.I.], v.160, p.1–4, 2019.

O'SULLIVAN, L.; MURPHY, B.; MCLOUGHLIN, P.; DUGGAN, P.; LAWLOR, P.G.; HUGHES, H.; GARDINER, G.E. Prebiotics from marine macroalgae for human and animal health applications. **Mar Drugs**, [S.I.], v.8, p.2038–2064, 2010.

OKUYAMA, S.et al. Strict Binding of small-sized Lectins from the Red Alga Hypnea japonica for Core (α1-6) Fucosylated N-Glycans. **Bioscience Biotechnology Biochemistry**, [S.I.], v.73, p.912-920, 2009.

PATEL, D.P.; CHRISTENSEN, M.B.; HOTALING, J.M.; PASTUSZAK, A.W. A review of inflammation and fibrosis: implications for the pathogenesis of Peyronie's disease. **World Journal of Urology**, [S.I.], v.38, p.253-261, 2020.

PAULSEN, C.E.; ARMACHE, J.G.A.O.Y.; CHENG, Y.; JULIUS, D. Structure of the TRPA1 ion channel suggests regulatorymechanisms. **Nature**, [S.I.], v.24, p.525-552, 2015.

PÉREZ, M.J.; FALQUÉ, E.; DOMÍNGUEZ, H. Antimicrobial Action of Compounds from Marine Seaweed. **Mar Drugs**, [S.I.], v.33, p.209-58, 1998.

PEUMANS, W.J.; VAN DAMME, E. J.N. Lectin as plant defense proteins. **Plant Phys**, [S.I.], v.109, p.347-352, 1995.
PEUMANS, W.J.; VAN DAMME, E.J.M. Plant lectins: specific tools for the identification, isolation, and characterization of O-linked glycans. Crit. Rev. **Biochem Mol Biol**, USA, v.33, p.209-58, 1998.

PHANG, S. et al. Marine algae of the South China Sea bordered by Indonesia, Malaysia. **The Raffles Bulletin of Zoology**, [S.I.], v.14, p.1–38, 2016.

PLIEGO-CORTÉS, A.; WIJESEKARA, I.; LANG, M.; BOURGOUGNON, N.; BEDOUXA, G. Current knowledge and challenges in extraction, characterization and bioactivity of seaweed protein and seaweed-derived proteins. **Advances in Botanical Research**, [S.I.], v.95, p.1-24, 2020.

PRASEPTIANGGA, D. Algal Lectins and their Potential Uses. **Squalen Bull of Mar & Fish Postharvest & Biotech**, [S.I.], v.10, p.89-98, 2015.

PRASEPTIANGGA, D.; HIRAYAMA, M.; HORI, K. Purification and characterization and c-DNA cloning of a novel lectin from the green alga Codium barbatum. Bioscience, Biotechnology, **Biochemistry**, [S.I.], v.76, p.805-811, 2012.

RAJA, S.N.; CARR, D.B.; COHEN, M.; FINNERUPD, N.B.; FLOR, H.; GIBSON, S.; KEEFE, F.J.; MOGIL, J.S.; RINGKAMP, M.; SLUKA, K.A.; SONG, X.; STEVENS, B.; SULLIVAN, M.D.; TUTELMAN, P.R.; USHIDA, T.; VADER, K. The revised International Association for the Stud of Pain definition of pain: concepts, challenges and compromises. **Pain**, [S.I.], v.161, p.1976-1982, 2020.

RIBEIRO, A.C.; FERREIRA, R.; FREITAS, R. Plant Lectins: Bioactivities and Bioapplications. **Studies in Natural Products Chemistry**, [S.I.], v.58, p.1-47, 2018.

RODRIGUES R. F. Purificação, **Caracterização de uma Lectina encontrada na alga marinha verde Codium isthmocladum (Vickers)**. 2011. Dissertação de Mestrado, Universidade Federal do Ceará, Fortaleza, 2011.

ROGERS D.J.; FLANGU H. Lectins from Codium species. **British Phycology Journal**, [S.I.], v.26, p.95-96, 1991.

ROGERS, D.J.; LOVELESS, R.W.; BALDING, P. Isolation and characterization of the lectins from sub-species of Codium fragile. In INTERNATIONAL LECTIN MEETING, **Berlin/New York**. Proceedings of the 7th Lectin Meeting. Berlin/New York : Walter de Gruyter, 1986. v.5, p.155-160, 1986.

ROGERS D.J.; SWAIN, L.; CARPENTER, B.G.; CRITCHLEY, A.T. Binding of N-acetyl-α-D-galactosamine by lectins from species of green marine alga genus, Codium. Lectins: Biology, Biochemistry, **Clinical Biochemistry**, [S.I.], v.10, p.162-165, 1994.

SAKAGUCHI, R.; MORI, Y. Transient receptor potential (TRP) channels: Biosensors for redox environmental stimuli and cellular status. **Free Radical Biology and Medicine**, [S.I.], v.146, p.36–44, 2020.

SALEHI, B.; SHARIFI-RAD, J.; SECA, A.M.L.; PINTO, D.C.G.A.; MICHALAK, I.; TRINCONE, A.; MISHRA, A.P.; NIGAM, M.; ZAM, W.; MARTINS, N. Current trends on seaweeds: Looking at chemical composition, phytopharmacology, and cosmetic applications. **Molecules**, [S.I.], v.24, p.4182, 2019.

SALTER, M.W. Cellular signalling pathways of spinal pain neuroplasticity as targets for analgesic development. **Curr Top Med Chem**, Canada, v.5, p.557-567, 2005.

SATO, Y. et al. High Mannose-binding Lectin with Preference for the Cluster of α1-2-Mannose from the Green Alga Boodlea coacta is a Potent Entry Inhibitor of HIV-1 and Influenza Viruses. **The journal of Biological Chemistry**, [S.I.], v.286, p.19446-19458, 2011.

SATO, Y.; SUZUKI, H.; SATO, T.; SUDA, T.; YODA, T.; IWAKURA, Y.; CHIDA, D. The role of endogenous glucocorticoids in lymphocyte development in melanocortin receptor 2-deficient mice. **Biochemical and Biophysical Research Communications**, [S.I.], v.403, p.253–257, 2010.

SCHAIBLE H.G.; RICHTER, F. Pathophysiology of pain. **Langenbecks Arch Surg**, [S.I.], v.389, p.237-43, 2004.

SILVA, L.M.R.; LIMA, J.D.S.S.; MAGALHÃES, F.E.A.; CAMPOS, A.R.; ARAÚJO, J.I.F.; BATISTA, F.L.A.; ARAÚJO, S.M.B.; SOUSA, P.H.M.; LIMA, G.C.; HOLANDA, D.K.R.; ROLIM, R.C.; FIGUEIREDO, E.A.T.; DUARTE, A.S.G.; RICARDO, N.M.P.S. Graviola Fruit Bar Added Acerola By-Product Extract Protects Against Inflammation and Nociception in Adult Zebrafish (Danio rerio). **J Med Food**, [S.I.], v.23, p.173–180, 2020.

SILVA, P. C. Historical review of attempts to decrease subjectivity in species identification, with particular regard to algae. **Protist**, [S.I.], v.159, p.153-161, 2008.

SIMPSON, D.S.A.; OLIVER, P.L. ROS Generation in Microglia: Understanding Oxidative Stress and Inflammation in Neurodegenerative Disease. **Antioxidants**, [S.I.], v.9, p.1-27, 2020.

SOSTRES, C.; GARGALHO, C.J.; ARROYO, M.T.; MEMBER, P.S.; LANAS, A. Adverse effects of non-steroidal anti-inflammatory drugs (NSAIDs, aspirin and coxibs) on upper gastrointestinal tract. **Best Practice & Research Clinical Gastroenterology**, Spain, v.24 p.121–132, 2010.

SOUZA, C.R.M.; BEZERRA, W.P.; SOUTO, J.T. Marine alkaloids with anti-inflammatory activity: Current knowledge and future perspectives. **Mar Drugs**, v.18, p.147, [S.I.], 2020.

STEINFELD, S.; BJØRKE, P.A. Results from a patient survey to acess gastrointestinal burden of non-steroidal anti-inflammatory drug therapy contrasted with a review of data from EVA to determine satisfaction with rofecoxib. **Rheumatology**, UK, v.4, p.35-42, 2002.

SUTTISRISUNG, S. et al. Identification and characterization of a novel legume-like lectin cDNA sequence from the red marine algae Gracilaria fisheri. **J Biosci**, [S.I.], v.36, p.833–843, 2011.

SZE, P. **A Biology of the algae**. 3. Ed. New York: McGraw-Hill. 1997. 278p.

TALAVERA, K.; STARTEK, J.B.; ALVAREZ-COLLAZO, J.; BOONEN, B.; ALPIZAR, Y.A.; SANCHEZ, A.; NAERT, R.; NILIUS, B. Mammalian transient receptor potential trpa1 channels: from structure to disease. **Physiol Rev**, [S.I.], v.100, p.725–803, 2020.

THANNICKAL, V.J.; FANBURG, B.L. Reactive oxygen species in cell signaling. **Am J Physiol Lung Cell Mol Physiol**, [S.I.], v.279, p.1005–1028, 2000.

TJØLSEN, A.; BERGE, D. G.; HUNSKAAR, S.; ROSLAND, J. H.; HOLE, K. The formalin test: an evaluation of the method. **Pain**, [S.I.], v.51, p.5-17, 1992.

TOBLIN, R.L.; MACK, K.A.; PERVEEN, G. PAULOZZI, L.J. A population-based survey of chronic pain and its treatment with prescription drugs. **Pain**, [S.I.], v.152, p.1249–1255, 2011.

TROTT, O.; OLSON, A.J. Software news and update AutoDock Vina: Improving the speed and accuracy of docking with a new scoring function, efficient optimization, and multithreading. **Journal of Computational Chemistry**, [S.I.], v.31, p.455-461, 2009.

TSANEVA, M.; VAN DAMME, E.J.M. 130 years of Plant Lectin Research. **Glycoconj J**, [S.I.], v.37, p.533–551, 2020.

VIANA, F. TRPA1 channels: molecular sentinels of cellular stress and tissue damage. **J Physiol**, [S.I.], v.594, p.4151–4169, 2016.

WANG, L.; WANG, J.; QIAO, X.; JU, D.; LIN, Z. Efect of ambient temperature on the micro-explosion characteristics of soybean oil droplet: the phenomenon of evaporation induced vapor cloud. **Int J Heat Mass Transf**, [S.I.], v.139, p.736–746, 2019.

WANG, S. et al. Molecular characterization of a new lectin from the marine alga Ulva pertusa. **Acta Biochimica et Biophysica Sinica**, [S.I.], v.36, p.111-117, 2004.

WELCH, C.J.; TALAGA, M.L.; KADAV, P.D.; EDWARDS, J.L.; BANDYOPADHYAY, P.; DAM, T.K. A capture and release method based on noncovalent ligand cross-linking and facile filtration for purification of lectins and glycoproteins. **J Biol Chem**, Nebraska, v.295, p.223–236, 2020.

WONGRAKPANICH, S.; WONGRAKPANICH, A; MELHADO, K.; RANGASWAMI, J. A Comprehensive Review of Non-Steroidal Anti-Inflammatory Drug Use in The Elderly. **Aging and Disease**, [S.I.], v.9, p.143-150, 2018.

WOO, C.W.; SCHMIDT, L.; KRISHNAN, A.; JEPMA, M.; ROY, M.; LINDQUIST, M.A.; ATLAS, L.Y.; WAGER, T.D. Quantifying cerebral contributions to pain beyond nociception. **Nat Commun**, [S.I.], p.01-14, 2017.

WOOLF, C.J. Pain: moving from symptom control toward mechanism-specific pharmacologic management. **Ann Intern Med**, USA, v.140, p.441-51, 2004.

WORBS, S.; SKIBA, M.; SÖDERSTRÖM, M.; RAPINOJA, M.; ZELENY, R.; RUSSAMANN, H.; SCHIMMEL, H.; VANNINEN, P.; FREDRIKSSON, S.; DORNER, B.G. Characterization of Ricin and R. communis Agglutinin Reference Materials. **Toxins**, [S.I.], v.7, p.4906-4934, 2015.

XIAO, T.S. Innate immunity and inflammation. **Cellular & molecular immunology**, [S.I.], v.14, p.1–3, 2017.

XIONG, G.; DENGB, Y.; CAOA, Z.; LIAOA, X.; ZHANGD, J.; LUA, H. The hepatoprotective effects of Salvia plebeia R. Br. extract in zebrafish (Danio rerio). **Fish and Shellfish Immunology**, [S.I.], v.95, p.399–410, 2019.

YANG, D.; KIM, J. Emerging role of transient receptor potential (TRP) channels in cancer progression. **BMB Rep**, [S.I.], v.53, p.125-132, 2020.

YOON, K. S. et al. Molecular Characterization of the Lectin, bryohealin, involved in protoplast regeneration of the Marine alga Bryopsis plumosa (Chlorophyta). **Journal of Phycology**, USA, v.44, p.103-112, 2008.

ZHANG, F.; YAN, X.; LI, J. Embedded Web Server for Hospital and Clinical Nursing Analysis of Cataract Anti-Inflammatory Drugs. **Microprocessors and Microsystems**, [S.I.], v.81, p.01–06, 2021.

ZHANG, H.; TSAO, R. Dietary polyphenols, oxidative stress and antioxidant and anti-inflammatory effects. **Current Opinion in Food Science**, [S.I.], v.8, p.33-42, 2016.

ZHANG, W.; ZHOU, Y.; LI, X.; XU, X.; CHEN, Y.; ZHU, R.; YIN, L. Macrophage-targeting and reactive oxygen species (ROS) responsive nanopolyplexes mediate anti-inflammatory siRNA delivery against acute liver failure (ALF). **Biomater Sci**, [S.I.], v.6, p.1986–1993, 2018.

ANEXO A- ARTIGO PUBLICADO EM 21 DE JULHO DE 2020

Journal of Applied Phycology
https://doi.org/10.1007/s10811-020-02198-x

New lectins from *Codium isthmocladum* Vickers show unique amino acid sequence and antibiofilm effect on pathogenic bacteria

Rômulo Farias Carneiro[1] · Philippe Lima Duarte[1] · Renata Pinheiro Chaves[1] · Suzete Roberta da Silva[2] · Ramon Rodrigues Feitosa[1] · Bruno Lopes de Sousa[3] · Antônio Willame da Silva Alves[4] · Mayron Alves de Vasconcelos[5,6] · Bruno Anderson Matias da Rocha[4] · Edson Holanda Teixeira[6] · Alexandre Holanda Sampaio[1] · Celso Shiniti Nagano[1]

Received: 24 March 2020 / Revised and accepted: 29 June 2020

Abstract
Two new lectins from the green alga *Codium isthmocladum* (CiL-1 and CiL-2) were isolated. Both lectins could agglutinate human and rabbit erythrocytes. Galactosides and fetuin showed inhibitory effect on CiL-1. CiL-2 was inhibited by GalNAc and porcine stomach mucin. CiL-1 was a monomeric protein of 12 kDa, whereas CiL-2 showed 12 kDa in SDS-PAGE and an oligomeric state in gel filtration. MALDI-ToF-MS of CiL-1 revealed a molecular mass of 12.027 ± 5 Da, while CiL-2 showed molecular mass of 12.264 ± 5 Da. Ninety-eight percent of CiL-1's primary structure was determined consisting of 112 residues placed in two repeated domains with approximately 60% of similarity. CiL-1 showed similarity with hypothetical proteins from aquatic pathogenic fungi. The N-terminal of CiL-2 showed no similarity to CiL-1 or to any known protein. The three-dimensional model of CiL-1 consists of four two-strand β-sheets disposed in a barrel-like arrangement, connected by loops of variable sizes, with a well-structured hydrophobic core. Binding site prediction suggests the existence of two independent monosaccharide binding sites in CiL-1. The lectins showed no antibacterial activity on Gram-positive and Gram-negative bacteria, but they were able to significantly inhibit the biofilm formation from *Staphylococcus aureus* and *Staphylococcus epidermidis*.

Keywords Lectin · Chlorophyta · Mass spectrometry · Antibiofilm · Structural modeling · Molecular docking

Introduction

In the last three decades, algal lectins have been isolated and characterized from several species. These lectins have proved to be important biotechnological tools. In particular, Griffithsin (GRFT), a high-mannose-binding lectin isolated from the marine red alga *Griffithsia* sp., is a potent antiviral agent able to act as a promising microbicidal

Electronic supplementary material The online version of this article (https://doi.org/10.1007/s10811-020-02198-x) contains supplementary material, which is available to authorized users.

✉ Celso Shiniti Nagano
naganocs@gmail.com

[1] Laboratório de Biotecnologia Marinha - BioMar-Lab, Departamento de Engenharia de Pesca, Universidade Federal do Ceará, Campus do Pici s/n, bloco 871, Av. Mister Hull, Box 6043, Fortaleza, Ceará 60440-970, Brazil

[2] Campus Monte Alegre, Universidade do Oeste do Pará, Av. Major Francisco Mariano s/n - Bairro Cidade Alta, Monte Alegre, PA 68220-000, Brazil

[3] Faculdade de Filosofia Dom Aureliano Matos, Universidade Estadual do Ceará, Av. Dom Aureliano Matos, 2060, Limoeiro do Norte, CE 62930-000, Brazil

[4] Departamento de Bioquímica e Biologia Molecular, Universidade Federal do Ceará, Campus do Pici s/n, bloco 871, Fortaleza, Ceará 60440-970, Brazil

[5] Departamento de Ciências Biológicas, Faculdade de Ciências Exatas e Naturais, Universidade do Estado do Rio Grande do Norte, Mossoró, Rio Grande do Norte 59625-620, Brazil

[6] Laboratório Integrado de Biomoléculas - LIBS, Departamento de Patologia e Medicina Legal, Universidade Federal do Ceará, Monsenhor Furtado, s/n, Fortaleza, Ceará 60430-160, Brazil

Published online: 21 July 2020

candidate to prevent HIV acquisition (Mori et al. 2005; Kouokam et al. 2016; Singh and Walia 2018). However, most studies have focused on marine red algae (Rhodophyta). Green marine algae have been little explored for the presence of lectins and their distribution. By comparison, marine red algae have had approximately 40 lectins isolated, whereas only about 20 lectins have been isolated from Chlorophyta. An even smaller number of articles have reported on structural characterization. To date, just eight lectins from green algae have had their primary structure determined (Kim et al. 2006; Han et al. 2010; Jung et al. 2010). Curiously, only low similarity was found among them. Furthermore, few biochemical characteristics are shared among chlorophyte lectins (Fabregas et al. 1988; Sampaio et al. 1998; Benevides et al. 2001; Praseptiangga et al. 2012).

As molecules with biotechnological potential, however, green algal lectins have demonstrated interesting properties. The lectin from *Caulerpa cupressoides* (CCL) showed antinociceptive and anti-inflammatory effects in rats, whereas lectins from *Boodlea coacta* (BCA) and *Halimeda renschii* (HRL-40) showed a marked effect against HIV and Influenza virus, respectively (Vanderlei et al. 2010; Sato et al. 2011; Mu et al. 2017).

Interestingly, most of the work involving lectins of green algae concentrates on those organisms with a coenocytic thallus (i.e., algae formed by one big and multinucleate cell; order Bryopsidales). For example, the genera *Bryopsis*, *Caulerpa, Codium*, and *Halimeda* have all had their lectins characterized (Benevides et al. 2001; Kim et al. 2006; Praseptiangga et al. 2012; Mu et al. 2017).

Codium isthmocladum Vickers is a coenocytic green alga widely distributed along the Brazilian northeast coast. Hemagglutinating activity was first observed in extracts of *C. isthmocladum* by Ainouz and Sampaio (1991). Here, we report isolation of two new lectins from *C. isthmocladum*, their antibiofilm potential and primary structure and modeling of one of them.

Methods

Algae collection

Codium isthmocladum specimens were collected on Paracuru Beach, Ceará, Brazil. Algae were transported in plastic bags to the lab; they were cleaned from epiphytes and frozen at − 20 °C.

All collections were authorized through our registration with SISBIO (Sistema de Autorização e Informação em Biodiversidade, ID: 33913-8) and SISGEN (Sistema Nacional de Gestão do Patrimônio Genético e do Conhecimento Tradicional Associado, ID: AC14AF9).

Lectin isolation

Algae were cut into small pieces and homogenized with three volumes of 50 mM sodium acetate buffer, pH 5, containing 1 M NaCl. The mixture was maintained under agitation for 16 h and then filtered and centrifuged at 8000×*g* for 20 min at 4 °C. Supernatant was named crude extract.

The crude extract was submitted to precipitation with 40% ammonium sulfate saturation. After 4 h at room temperature, precipitated proteins were pelleted by centrifugation and discarded. Supernatant was saturated with ammonium sulfate, left to stand for 4 h and then centrifuged. Precipitated proteins (F40-100) were recovered by addition of a small volume of 20 mM phosphate buffer, pH 7 (PB). The sample was dialyzed against PB, centrifuged, followed by loading the supernatant onto a DEAE-Sephacel column (1.0 × 10 cm), which was previously equilibrated with PB. The column was washed with the same buffer and eluted stepwise in NaCl (0.4, 0.5, and 1 M) in PB. Chromatography was conducted at a flow rate of 2 mL min^{-1} and monitored by measurement of absorbance at 280 nm. Three-milliliter fractions were collected. Both non-retained fractions (CiL-1) and retained fractions eluted with 0.4 M NaCl (F 0.4-DEAE) showed hemagglutinating activity.

F 0.4-DEAE was dialyzed, freeze-dried, and solubilized in a small volume of 20 mM Tris-HCl, pH 7.5, containing 150 mM NaCl and 5 mM $CaCl_2$ (TBS). This sample was centrifuged and loaded onto a BioSuite 250 HR SEC column (0.78 × 30 cm, 5-μm particle size, Waters Corp, USA) coupled to an Acquity UPLC system (Waters Corp), previously equilibrated with TBS. Chromatography was conducted at a flow rate of 0.4 mL min^{-1}. Active fractions (CiL-2) were pooled and stored at − 20 °C.

Hemagglutinating activity and inhibition assays

Hemagglutinating and inhibition assays were performed according to Sampaio et al. (1998). For the hemagglutinating assay, human (ABO) and rabbit erythrocytes were used in their native form and trypsin-treated.

The following sugars and glycoproteins were used in the inhibition test: D-xylose, D-ribose, L-fucose, L-arabinose, L-rhamnose, D-galactose, D-mannose, D-glucose, D-glucosamine, D-galactosamine, *N*-acetyl-D-glucosamine, *N*-acetyl-D-galactosamine, *N*-Acetyl-D-mannosamine (ManNAc), *N*-acetylneuraminic acid, D-galacturonic acid, methyl-α-D-galactoside, methyl-β-D-galactoside, methyl-α-D-mannoside, methyl-β-D-thiogalactoside, phenyl-β-D-galactoside, 4-nitrophenyl-α-D-galactoside, 4-nitrophenyl-β-D-galactoside, 2-nitrophenyl-β-D-galactoside, D-fructose, sucrose, melibiose, lactose, lactulose, maltose, raffinose, yeast mannan, bovine fetuin, asialofetuin, human transferrin,

porcine thyreoid tyroglubulin, bovine submaxillary mucin (BSM), and porcine stomach mucins (type 2 and 3 PSM).

The effects of temperature, pH, EDTA, and divalent cations on hemagglutination activity were evaluated as described in pre-established methods (Sampaio et al. 1998).

Molecular mass determination and homogeneity

Homogeneity of the lectins was investigated by SDS-PAGE (Laemmli 1970) in the presence and absence of 2-mercaptoethanol (2-ME). SigmaMarker low range (Sigma Aldrich, USA) was used as a protein marker.

Native molecular mass was estimated by size-exclusion chromatography (SEC) in a BEH SEC column, 1.7 μm (0.46 × 30 cm), coupled to an Acquity UPLC system (Waters Corp). Chromatography was conducted in PBS at a flow rate 0.3 mL min^{-1}. The column was previously calibrated with protein mix containing bovine thyroglobulin (669 kDa), apoferritin (443 kDa), β-amylase (200 kDa), alcohol dehydrogenase (150 kDa), BSA (66 kDa), carbonic anhydrase (29 kDa), and ribonuclease (14 kDa).

The average molecular mass of the lectins was determined by MALDI-ToF on an Autoflex MALDI-TOF/TOF mass spectrometer (Bruker Daltonics, Germany), using matrix solution (10 mg mL^{-1} of α-cyano-4-hydroxycinnamic acid on acetonitrile, water, trifluoroacetic acid (TFA); 50, 47, 3% v/v). The spectra were acquired in linear positive mode and processed with Flex Analysis 3.4 software (Bruker Daltonics, Germany). The experiments were performed in the Centro de Tecnologias Estratégicas do Nordeste (CETENE), Recife, PE, Brazil (www.cetene.gov.br).

N-terminal analysis

The lectins were reduced with dithiothreitol and alkylated with 4-vinylpyridine as described (Carneiro et al. 2017). After that, pyridylethylated (PE) lectins were submitted to reverse phase chromatography (RPC) coupled to the Acquity system (Waters Corp.). BEH C18 1.7 μm (0.21 × 5 cm) column (Waters) was equilibrated and washed with solution of 5% acetonitrile (ACN) containing 0.1% TFA at a flow rate of 0.4 mL min^{-1}. Retained proteins were recovered by elution through a gradient of 5 to 90% of ACN containing 0.1% TFA. Absorbance of the column eluates was monitored at 216 and 280 nm.

Determination of N-terminus was performed in a Shimadzu model PPSQ-31A protein sequencer (Shimadzu Corp., Japan) as described by Carneiro et al. (2015).

Amino acid sequencing and disulfide bridges assignment of CiL-1

CiL-1 was subjected to SDS-PAGE as described above. Protein spots were reduced and alkylated with dithiothreitol and iodoacetamide, respectively (Shevchenko et al. 2006). Then, carboxyamidomethylated (CAM)-CiL-1 was digested with trypsin, chymotrypsin, and endoproteinase Arg-C (all enzymes purchased from Roche, Switzerland). Digestion was performed in 50 mM ammonium bicarbonate at 1:100 (w/w) (enzyme/substrate) and maintained at 37 °C for 16 h. Peptides were extracted from gel according to (Shevchenko et al. 2006).

The peptides were separated on a reverse phase C18 nanocolumn (0.075 × 100 mm) coupled to a nanoAcquity system. The eluates were directly infused in a hybrid mass spectrometer (ESI-Q-ToF) (Synapt HDMS, Waters Corp). The instrument parameters were adjusted as described by (Carneiro et al. 2013). MS/MS spectra were manually interpreted, and sequenced peptides were searched online against NCBI and UniProt databanks.

To determine disulfide bridge assignment, non-reduced CiL-1 spots were digested with trypsin and chymotrypsin. Digestion products were processed as described above, and MS/MS spectra were manually interpreted.

Circular dichroism

Circular dichroism spectroscopy was performed on a Jasco J-815 spectropolarimeter (Jasco International Co., Japan) connected to a Peltier with controlled temperature. Lectins (0.2 mg mL^{-1} in 20 mM phosphate buffer, pH 7.0) were placed in a rectangular quartz cuvette with 1-mm path length. Spectra were acquired at a scan speed of 50 nm min^{-1} with a bandwidth of 1 nm. The acquisitions were performed at 190–240 nm (far-UV) at 20 °C with eight accumulations.

The analysis of structural data was performed by DICHROWEB web server (Whitmore and Wallace 2004).

Structural prediction

A suitable structural model for CiL-1 was obtained through the quality assessment of automatically generated structures produced by different modeling web servers, such as I-TASSER, Robetta, Phyre2, and SWISS-MODEL (Kim et al. 2004; Kelley et al. 2015; Yang et al. 2015; Waterhouse et al. 2018).

Prior to the adoption of this strategy, the primary structure of CiL-1 was used as input to search the Protein Data Bank (PDB) for experimentally determined structures with conserved or similar amino acid sequences, which, in turn, could be used as template for manual modeling with the Modeller suite (Webb and Sali 2016).

The final structures produced by each modeling server were submitted to the PROCESS web server (http://www.prosess.ca), which is designed to evaluate and validate protein structures (Berjanskii et al. 2010).

Molecular docking calculations

The structural basis for carbohydrate recognition by CiL-1 was explored through molecular docking calculations. To accomplish this, three different carbohydrates were selected based on experimental evidence, including α-D-galactose, α-neuraminic acid, and the tetrasaccharide α-Neu-(2-6)-α-D-GalNAc-(3-1)-α-D-Gal-(3-2)-α-Neu. The three-dimensional coordinates for α-D-galactose (CID, 6036) and α-neuraminic acid (CID, 441037) were obtained from the PubChem Substance and Compound database (Wang et al. 2009), while the oligosaccharide structure was designed with the Sweet tool, available on the glycoinformatics databases and tools web server (Bohne et al. 1998).

Initially, the most reliable carbohydrate-binding sites on the CiL-1 structure were identified by the DogSiteScorer tool (https://proteins.plus), which is a grid-based method that uses a difference of Gaussian filter to detect potential binding pockets (Volkamer et al. 2012). Afterwards, docking calculations were performed with AutoDock Vina, version 1.1.2 (Trott and Olson 2010), which applies an iterated local search global optimizer for the optimization procedure such that the succession of each step consists of a mutation and local optimization. The protein and carbohydrate ligands were treated as rigid and flexible molecules, respectively.

First, a blind docking strategy was applied using a search space defined by a 40 Å × 40 Å × 40 Å cube covering the whole protein surface. Then, a refined search was performed using a search space defined by a 20 Å × 20 Å × 20 Å cube centered on the spots elected as the most suitable carbohydrate-binding sites, as determined by the DogSiteScorer prediction and the blind docking results. For all calculations, exhaustiveness was set to 15, and all other parameters were used as default. For each docking, the ten top-ranked generations based on the predicted binding affinity (in kilocalories per mole) were analyzed.

Antibacterial effect

Evaluation of antibacterial activity

Staphylococcus aureus ATCC 25175, *Staphylococcus epidermidis* ATCC 12225, and *Escherichia coli* ATCC 11303 were obtained from American Type Culture Collection (ATCC; USA).

The antibacterial assay was evaluated by the microdilution method described by the Clinical and Laboratory Standards Institute—CLSI (2015) with modifications proposed by Vasconcelos et al. (2014).

Effect on bacterial biofilm

In order to evaluate the activity of the lectins on bacterial biofilm formation, lectins at different concentration from 500 to 7.8 μg mL^{-1} were added to a bacterial cells suspension (2×10^6 colony forming units (CFU) mL^{-1}) in 96-well polystyrene plates. The plates were incubated at 37 °C for 24 h. Afterwards, biofilm formation was assessed through total biomass and CFU quantification.

Total biomass quantification was evaluated by crystal violet staining. The biofilms were fixed using 200 μL of methanol for 15 min and then the plates were allowed to dry at 25 °C. The wells were stained with 200 μL of crystal violet (1%, v/v) for 5 min, the excess of crystal violet was removed, and the plates were washed with water. Two hundred microliters of acetic acid (33%, v/v) were then added into the wells to dissolve the crystal violet stain, and the optical density of each well was measured at 590 nm (OD_{590}) using a microplate reader (SpectraMax I3).

For determination of CFUs, the wells were washed with 200 μL water twice, and the biofilm-entrapped cells were removed from the wells by ultrasonic bath (10 min). The bacterial suspensions were vigorously vortexed to disaggregate cells from the biofilm matrix. In order to quantify the CFUs present in the biofilms, serial decimal dilutions from the bacterial suspensions were plated on TSA (Trypticase Soy Agar medium) plates for 24 h at 37 °C. The number of CFUs was determined and expressed as CFL mL^{-1}.

Results

Isolation of lectins

Two new lectins from *C. isthmocladum* (CiL-1 and CiL-2) were isolated by a combination of ammonium sulfate precipitation, ion-exchange (IEX) and size-exclusion chromatography. CiL-1 and CiL-2 were isolated 29 and 13 times from crude extract and presented minimal concentration to agglutinate of 0.17 and 0.37 μg mL^{-1}, respectively (Table 1).

Lectins present in the crude extract were concentrated in the F40-100. After IEX, non-retained fraction (CiL-1) and retained fraction eluted with NaCl 0.4 M in PB showed hemagglutinating activity (Fig. 1a). The final purification for CiL-2 was achieved by size-exclusion chromatography (Fig. 1b).

In SDS-PAGE (Fig. 1c), CiL-1 showed one single band of approximately 13 kDa in the presence of 2-ME and 12 kDa in the absence of 2-ME, respectively. CiL-2 showed a single band of approximately 13 kDa in the presence of 2-ME and

Table 1 Purification of *C. isthmocladum* lectins

Fraction	Volume (mL)	Titer (HU mL^{-1})	Protein total (mg)	Hemagglutinating activity total (HU)	Specific activity (HU mg^{-1})	Purification (fold)	Yield (%)	MAC* (μg mL^{-1})
Crude extract	1000	64	318	64,000	201	1.0	100.0	4.97
F 40-100	70	512	18.48	35,840	1939	9.6	56.0	0.52
P1 DEAE	202	128	4.444	25,856	5818	28.9	40.4	0.17
P2 DEAE	205	32	3.28	6560	2000	9.9	10.3	0.50
P SEC	12	128	0.564	1536	2723	13.5	2.4	0.37

**MAC*, minimal agglutinating concentration

three bands of 10, 24, and 34 kDa in the absence of reducing agent.

Hemagglutinating activity and inhibition assay

Both lectins were able to agglutinate human and rabbit erythrocytes with slight preference for trypsin-treated rabbit erythrocytes. CiL-1 hemagglutinating activity was slightly inhibited by galactosides and the glycoprotein fetuin. CiL-2 hemagglutinating activity was slightly inhibited by GalNAc and PSM (Table 2).

Optimal pH for hemagglutinating activity of both lectins was 6.0. CiL-1 activity was stable at temperatures below 60 °C, whereas the activity of CiL-2 remained unaltered up to 50 °C. Above these values, hemagglutinating activity for both lectins decreased and was abolished at 100 °C and 70 °C for CiL-1 and CiL-2, respectively.

EDTA and divalent cations had no effect on the activity of CiL-1. Since CiL-2 hemagglutinating activity was already significantly reduced by the presence of EDTA, hemagglutinating activity was recovered after Ca^{2+} addition, suggesting that CiL-2 is a calcium-dependent lectin.

Molecular mass determination

In native conditions, i.e., SEC, molecular mass of the lectins was 15 and 63 kDa for CiL-1 and CiL-2, respectively (data not shown). MALDI-ToF-MS of CiL-1 revealed a molecular mass of 12,027 ± 5 Da, while CiL-2 showed molecular mass of 12,264 ± 5 Da (Fig. 2).

N-terminal analysis and amino acid sequencing

CiL-1 showed no products after Edman degradation reactions. The first 17 amino acid residues of CiL-2 were identified by amino acid sequencing. The CiL-2 N-terminal sequence ^{1}FQIGQGSMGNKTITGVS^{17} showed no similarity to any known protein.

The bottom-up analysis allowed us to elucidate the primary structure of CiL-1. Peptides originated by digestion with proteolytic enzymes (Supplementary Table 1) were overlapped to secure an amino acid sequence of 112 residues (Fig. 3). The calculated molecular mass was 11,759 Da which is 268 Da below the molecular mass determined by MALDI-ToF (12,027 Da). This difference was attributed to the presence of two or three amino acids in C-terminal, which were not identified.

Four half-cystines were found to form two intrachain disulfide bonds. The correct pairing was determined through the analysis of non-reduced peptides and comparison with alkylated peptides. In particular, the cysteines found in tryptic peptide at m/z 670.26 and chymotryptic peptide at m/z 878.33 were observed in their oxidized form, i.e., involved in disulfide bonds. On the other hand, their CAM forms were found in tryptic peptide at m/z 708.93 and chymotryptic peptide at m/z 936.33, which were obtained after reduction and alkylation of the spots (Supplementary Figure 1). Together, these data indicated the following cysteine pairing: ^{17}Cys-Cys^{20} and ^{65}Cys-Cys^{68}.

The CiL-1 amino acid sequence consisted of two repeated domains of approximately 40 residues each: domain A (9–52) and domain B (57–101), showing 58% of similarity (Fig. 4). No glycosylation site was found in the sequence. The theoretical *pI* was 9.18.

CiL-1 showed no similarity with any lectin, but moderate similarity was found between CiL-1 and hypothetical proteins from several aquatic pathogenic microorganisms, including the fungi *Achlya hypogyna* (OQR97370.1), *Saprolegnia diclina* VS20 (XP_008611507.1), *S. parasitica* CBS 223.65 (XP_012209436.1), and *Aphanomyces astaci* (RHX96711.1). The sequence alignment is shown in Fig. 5.

Circular dichroism

Spectra of native CiL-1 in the far-UV showed two minima at 217 nm and maximum at 199 nm, whereas spectra of native CiL-2 showed minimum absorption at 222 nm and maximum at 199 nm (Supplementary Figure 2). According to the CONTIN prediction method (Van Stokkum et al. 1990), the theoretical secondary structure of CiL-1 consisted of 7% α-

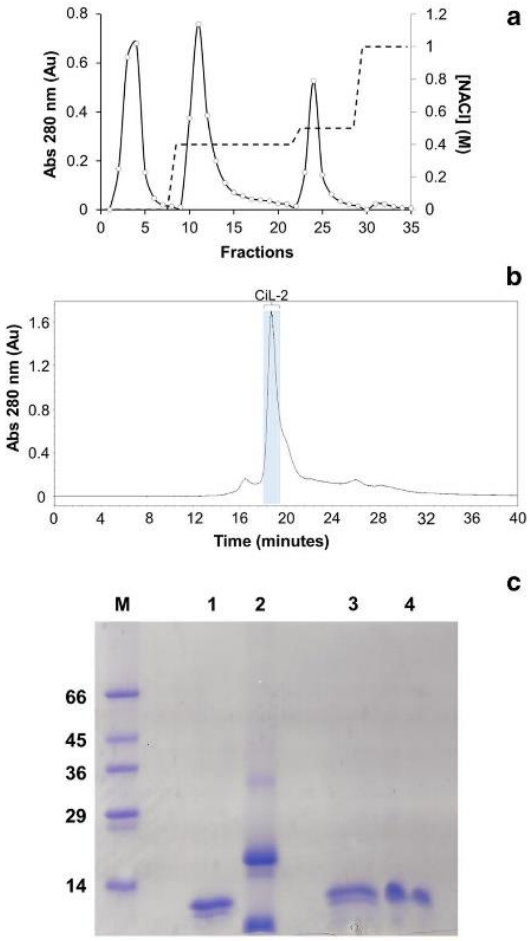

Fig. 1 Purification procedure. **a** Ion-exchange chromatography on DEAE-Sephacel column (1.0 × 10 cm), previously equilibrated with PB. The column was washed with the same buffer and eluted in steps of NaCl (0.4, 0.5, and 1 M) in PB. **b** Size-exclusion chromatography on BioSuite HR SEC column (0.78 × 30 cm, 5-μm particle size); the chromatography was conducted in TBS at 0.4 mL min^{-1}. **c** SDS-PAGE 12% of purified *C. isthmocladum* lectins. M, molecular marker; 1, CiL-1; 2, CiL-2; 3, CiL-1 in the presence of 2-ME; 4, CiL-2 in the presence of 2-ME

helix, 38% β-sheet, 22% turn, and 33% coil. The prediction values of CiL-2 were 6% α-helix, 39% β-sheet, 22% turn, and 33% coil.

CiL-1 structural prediction

Initially, the CiL-1 primary structure was used as input for the search of suitable template structures in the PDB database using the PSI-BLAST tool (Ding et al. 2014). PSI-BLAST produces a position-specific scoring matrix (PSSM) constructed from a multiple alignment of the highest scoring hits in an initial BLAST search. Nevertheless, no significant sequence similarity was found to any experimentally determined structure. Therefore, the current strategy based on

Table 2 Inhibitory effects of sugars and glycoproteins on the hemagglutinating activity of *C. isthmocladum* lectins

Sugar	MIC	
	CiL-1	CiL-2
D-galactose	50 mM	NI
D-glucose	NI	NI
D-mannose	NI	NI
D-xylose	NI	NI
D-ribose	NI	NI
L-fucose	NI	NI
L-rhamnose	NI	NI
L-arabinose	NI	NI
α-methyl-D-galactopyranoside	50 mM	NI
β-methyl-D-galactopyranoside	NI	NI
methyl-β-D-thiogalactose	100 mM	NI
D-galactosamine	50 mM	NI
D-glucosamine	NI	NI
N-Acetyl-D-galactosamine	NI	100 mM
N-Acetyl-D-glucosasamine	NI	NI
N-Acetyl-D-manosamine	NI	NI
N-acetylneuraminic acid	NI	NI
D-galacturonic acid	NI	NI
phenyl-β-D-galactopyranoside	NI	NI
2-nitrophenyl-β-D-galactoside	NI	NI
4-nitrophenyl-α-D-galactoside	NI	NI
4-nitrophenyl-β-D-galactoside	NI	NI
D-fructose	NI	NI
D-sacarose	NI	NI
α-lactose	50 mM	NI
β-lactose	NI	NI
D-maltose	NI	NI
Lactulose	NI	NI
Melibiose	NI	NI
Rafinose	NI	NI
Yeast mannan	NI	NI
Glycoproteins		
Bovine fetuin	62.5 μg mL^{-1}	NI
Asialofetuin	NI	NI
BSM	NI	NI
PSM type II	NI	500 μg mL^{-1}
Human transferrin	NI	NI
Porcine thyroid thyroglobulin	NI	NI

The initial concentrations of the inhibitors were 100 mM for sugars and 1 mg mL^{-1} for glycoproteins. *MIC*, minimal inhibitory concentration; *NI*, inhibition not observed

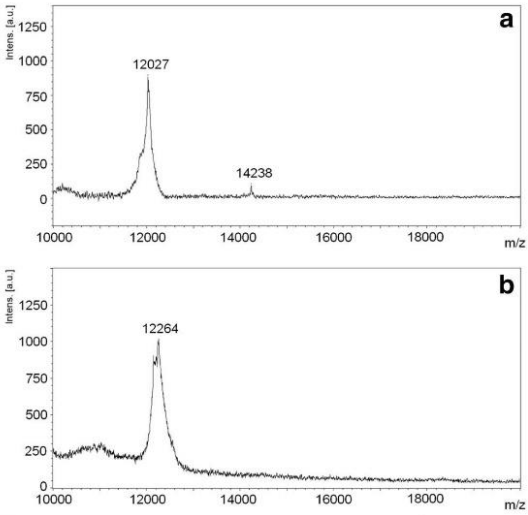

Fig. 2 Molecular mass determination of *C. isthmocladum* lectins by MALDI-ToF. Molecular masses of CiL-1 (**a**) and CiL-2 (**b**) were determined in native form. The spectra were acquired in linear positive mode and processed with Flex Analysis 3.4 software

automatically generated structures produced by different modeling web servers was adopted.

Five different structures obtained from each server were stereochemically analyzed by PROCESS, the most suitable structure produced by the Robetta web server, presenting 100% of amino acid residues disposed on allowed regions (98.2% on favored regions) of the Ramachandran plot (Supplementary Figure 3). The obtained CiL-1 model (110 amino acids) presents an overall structure composed of four two-strand β-sheets disposed in a barrel-like arrangement, connected by loops of variable sizes, with a well-structured hydrophobic core composed of aliphatic and/or aromatic residues belonging to each of these sheets (Fig. 6). Two disulfide bridges linking residues 17 to 20 and 65 to 68 were also present, stabilizing important loops involved in structuration of the binding sites, as described below.

A structural analysis performed with the 3D-Blast Structure Search Tool (http://3d-blast.life.nctu.edu.tw) indicated that CiL-1 shows important structural conservation with different proteins (Yang and Tung 2006), including different lectins and agglutinins such as the xylan binding protein from *Streptomyces lividans* (41.8%—PDB ID: 1KNM), the hemagglutinin component from the hemolytic lectin CEL-III from *Cucumaria echinata* (35.8%—PDB ID: 1VCL), the hemagglutinin component (HA1) from type C *Clostridium botulinum* (32.4%—PDB ID: 1QXM), the lectin from the mushroom *Marasmius oreades* (30.6%—PDB ID: 2IHO), and the agglutinin from *Amaranthus caudatus* (30.1%—PDB ID: 1JLX). Additionally, a CiL-1-predicted structure has significant resemblance with mytilec, a lectin from the mussel *Mytilus galloprovincialis* (PDB ID: 3WMV), despite this structure has not been identified by 3D-Blast Structure Search Tool (Wang et al. 2013). A structural alignment performed though the web server RaptorX (http://raptorx.uchicago.edu/) gave a root mean square deviation (RMSD) of 2.69 between the main chain atoms of CiL-1 and the xylan binding protein from *S. lividans*, which indicates 41.8% of structural conversation according to 3D-Blast tool, and a RMSD of 2.09 between CiL-1 and mytilec, attesting for this case an even higher degree of structural conservation (Terada et al. 2016). These data constitute an interesting find since structural conservation dissociated from primary structure similarity is indicative of convergent evolution.

Binding site characterization

Binding site prediction performed by the DogSiteScorer tool was aligned with the results obtained from AutoDockVina blind docking, both suggesting the existence of two independent monosaccharide binding sites (SI and SII) connected by a large extended site, divided here into two parts for purposes of clarity (EI and EII). These binding sites exhibit a horseshoe-like architecture, enabling CiL-1 to recognize different types of complex and simple carbohydrates (Fig. 7).

Monosaccharide binding site I (SI) comprises a cavity of approximately 147 Å^3 composed of residues Ala63, Arg64, Cys65, Asn66, Asn67, Cys68, Trp69, Glu82, Gln86, and Tyr88. Refined calculations with α-D-galactose and α-neuraminic acid over SI generated similar coordination, suggesting a conserved interaction pattern for monosaccharides (Fig. 8).

Similarly, a monosaccharide-binding site II (SII) is a pocket of approximately 140 Å^3 composed of residues Arg64,

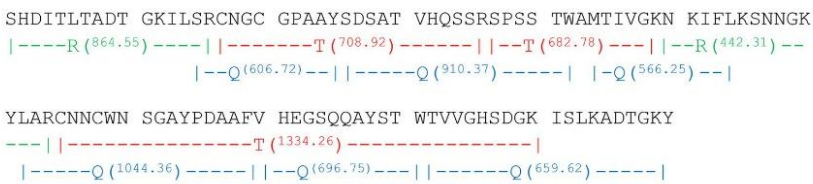

Fig. 3 Amino acid sequence of CiL-1. Primary structure of CiL-1 was determined by overlapping of peptides obtained by digestion with trypsin (*T*), chymotrypsin (*Q*), and Arg-C (*R*). m/z values determined by mass spectrometry are in parenthesis. Leucine and isoleucine were assigned according to chymotrypsin specificity

Fig. 4 Alignment of the repeated domains of CiL-1. Black and gray boxes represent identical and similar amino acids, respectively

Ala73, Tyr74, Pro75, Ala77, Asp76, Phe79, Gln109, and Tyr110. As for SI, the refined calculations with the selected monosaccharides over SII suggested a conserved interaction pattern for monosaccharides (Fig. 9).

On the other hand, the extended binding site (EI and EII) presents a total volume of approximately 220 $Å^3$ and is composed of residues Leu14, Cys17, Asn18, Tyr25, Asp27, Ser28, Ala29, Thr30, Val31, His32, Ala73, Ala78, Phe79, Val80, and Val105. A structural analysis of this extended site reveals a large shallow cavity that can be divided into 8 subsites for monosaccharide hosting, grouped here in EI and EII (Fig. 10). This complex site suggests an ability to interact with a broad spectrum of branched oligosaccharides, emphasizing those that present terminal galactose units and their derivatives, which would be better coordinated by the monosaccharide binding sites.

Antibacterial and antibiofilm effect of CiL-1 and CiL-2

CiL-1 and CiL-2 did not show any antibacterial activity on Gram-positive and Gram-negative bacteria. On the other hand, the lectins were able to significantly inhibit the biofilm formation from *S. aureus* and *S. epidermidis* (Fig. 11). The lectins did not present significant results against biofilm formation from *E. coli* (data not shown).

The *S. aureus* biofilm biomass was significantly reduced in the presence of CiL-1 and CiL-2 in all concentrations tested (Fig. 11a). A significant reduction of the CFU was observed on *S. aureus* biofilms formed in the presence of CiL-1, but not CiL-2 (Fig. 11b). Regarding *S. epidermidis* biofilm, CiL-1 reduced the biomass and CFU in the two highest concentrations tested (500 and 250 μg mL^{-1}), but antibiofilm activity of CiL-2 was not observed (Fig. 11c and d).

Discussion

In the 1980s and 1990s, several studies reported the presence of lectins in the *Codium* species (Fabregas et al. 1988; Rogers and Flangu 1991; Perez-Lorenzo et al. 1998). Some lectins from this genus have been isolated and characterized in distinct levels (Rogers et al. 1994; Praseptiangga et al. 2012). In general, these *Codium* lectins are low molecular mass proteins. They have affinity for GalNAc and glycoproteins containing galactosides, usually forming oligomeric structures through disulfide bonds, but they are not divalent ion-dependent (Rogers and Flangu 1991; Rogers et al. 1994;

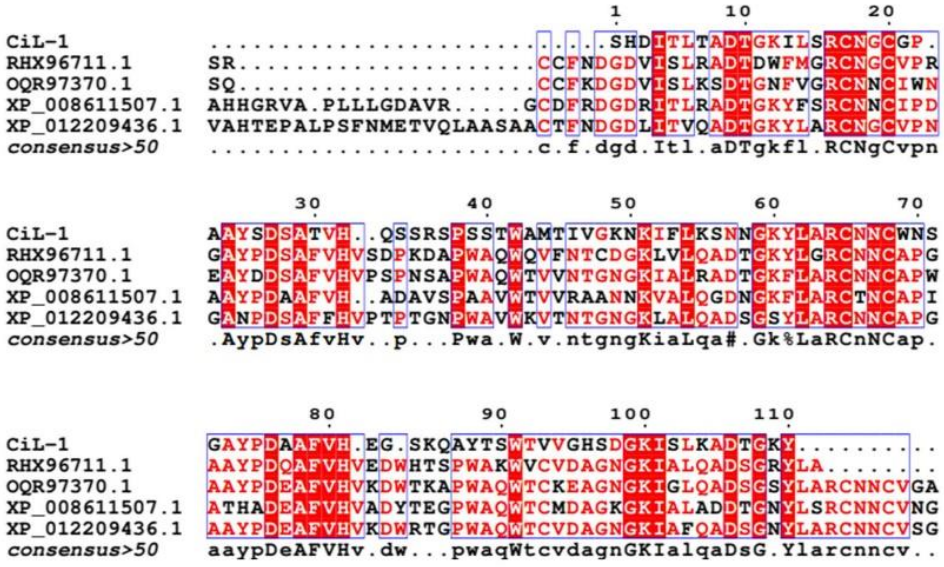

Fig. 5 Alignment of CiL-1 and hypothetical proteins from aquatic fungus. Amino acid sequence of CiL-1 was aligned with hypothetical proteins from *Achlya hypogyna* (OQR97370.1), *Saprolegnia diclina* VS20 (XP_008611507.1), and *Aphanomyces astaci* (RHX96711.1). Alignment realized by ESPript 3.0

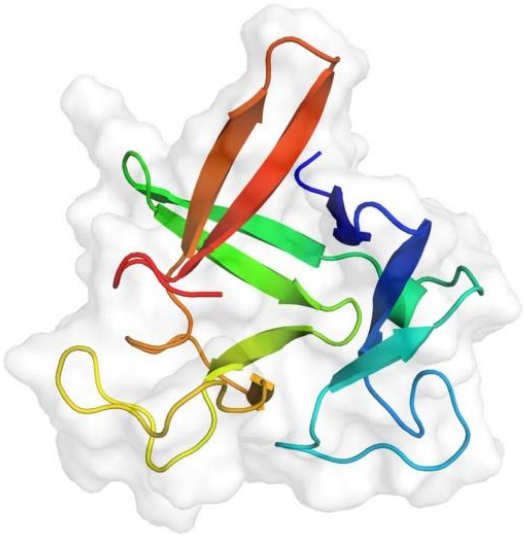

Fig. 6 Overall structure of CiL-1. The four two-stranded sheets are highlighted with different color shades in the cartoon representation.

Praseptiangga et al. 2012). In fact, some of these properties can be observed in the lectins isolated in this work, but some features of CiL-1 and -2 must be discussed in more detail.

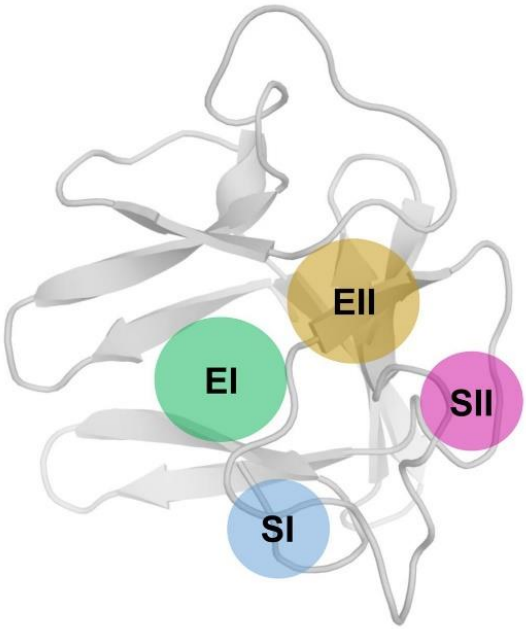

Fig. 7 Architecture of CiL-1 carbohydrate-binding sites. The overall protein structure is represented as light gray cartoon, while the carbohydrate-binding sites are shown as colored circles, highlighting the horseshoe-like distribution

First, the hemagglutinating activity and inhibition profile of the lectins isolated here are quite different from each other. The inhibition of CiL-1 by some galactosides indicated the involvement of the C-4 hydroxyls since glucose could not cause inhibition. Also, C-2 hydroxyls seem important in the interaction because galactosamine, a galactoside-containing small substituent group in this position, showed slight inhibition, while GalNAc, a galactoside with large substituent group, was not effective in inhibition.

Moreover, the influence of C-1 hydroxyl orientation was considered. A slight preference of CiL-1 for α anomers was observed since α-methyl-D-galactopyranoside could inhibit CiL-1, but not its β anomer. Galactosides containing large substituents in C-1, like 2- and 4-nitrophenyl-β-D-galactoside, were unable to cause inhibition, suggesting that large substituents in C-1 hydroxyl negatively affect interaction. Curiously, lactose was able to inhibit CiL-1, even presenting a large substituent in galactose C-1 hydroxyl (i.e., glucose).

Besides simple sugars, CiL-1 hemagglutinating activity was inhibited by bovine fetuin, a glycoprotein containing *N*- and *O*-glycans. Bovine fetuin is rich in α-neuraminic acid (NeuNAc), which is presented in both *N*- and *O*-glycan terminus. Additionally, bovine fetuin presents internal galactose residues. For instance, the tetrasaccharide α-Neu-(2-6)-α-D-GalNAc-(3-1)-α-D-Gal-(3-2)-α-Neu, which is present in fetuin (Edge and Spiro 1987), possesses galactose residue with free C-2 and C-4 hydroxyl, making it possible for CiL-1 to interact.

Interestingly, bovine fetuin in its asialo form was not able to inhibit CiL-1, attesting the importance of NeuNac in the interaction process. In fact, Perez-Lorenzo et al. (1998) observed that *C. ishtmocladum* crude extract hemagglutination was inhibited by NeuNAc (1 mM). However, hemagglutinating activity inhibition assay indicated that NeuNac (25 mM) did not inhibit CiL-1.

To shed light on this question, the interaction between CiL-1 and NeuNAc was evaluated by molecular docking calculations. As previous described, the CiL-1 predicted model presents two monosaccharide binding sites (SI and SII), which based on the computational analysis are both able to host and coordinate NeuNAc and α-galactose. This result, considered along with the inability of asialofetuin in inhibit CiL-1 hemagglutinating activity, suggests that terminal NeuNAc residues are essential for a proper CiL-1/fetuin interaction. Computational evidence also indicates that in view of its higher volume and specific configuration, NeuNAC can be proper coordinated by the monosaccharide-binding sites but poorly by the extended sites, which are shallower and mostly able to coordinate less bulky monosaccharides, as the tested galactosides, which effectively inhibited CiL-1 hemagglutinating activity. Therefore, complex

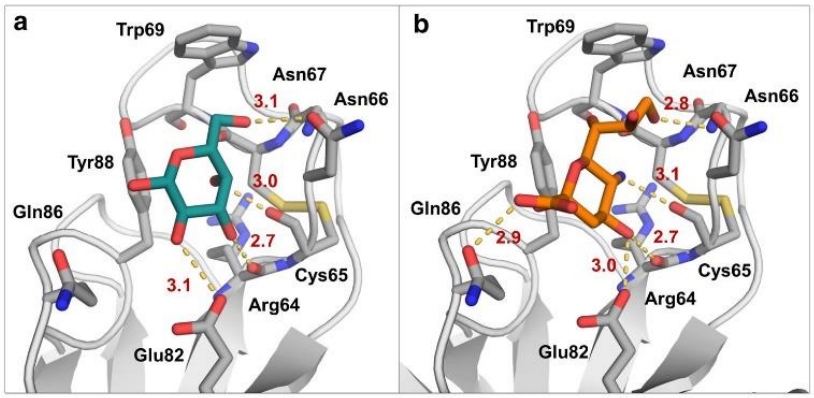

Fig. 8 Monosaccharide binding site I (SI). **a** α-D-galactose coordination. **b** α-neuraminic acid coordination. The protein backbone is represented as light gray cartoons, while residues involved in monosaccharide coordination are represented as gray sticks. Molecular interactions are represented in angstroms by yellow dashed lines. For the purpose of clarity, some residues and interactions involved in coordination were omitted

carbohydrates with terminal NeuNAc residues and not bulky galactosides are able to properly interact with CiL-1, as shown by the inhibition tests.

On the other hand, PSM and BSM were unable to cause inhibition of CiL-1. In PSM mucins, structures containing galactose with free C-2 and C-4 are usual, such as β-D-Gal-(1→3)-β-D-GalNAc-(1→O)-Ser/Thr (Karlsson et al. 1997). NeuNAc is also found in BSM mucins. From the BSM oligosaccharide portion, 85% consists of acidic *O*-linked chains, including a Sialyl Tn core (NeuAc α 2-6 GalNac α1Ser/Thr) (SAVAGE et al. 1990; CHAI et al. 1992); therefore, the reason why mucins were not able to inhibit CiL-1 is unclear.

Since CiL-2 was inhibited by PSM, Perez-Lorenzo et al. (1998) also observed that hemagglutination caused by *C. ishtmocladum* crude extract was inhibited by PSM, likely owing to the presence of a lectin with this specificity: CiL-2. Lectins isolated from *C. adherensis*, *C. arabicum*, *C. capitatum*, and *C. platylobium* also showed affinity for PSM. In all these cases, the inhibition of hemagglutinating activity by GalNAc, as well as in CiL-2, was observed (Rogers and Flangu 1991; Rogers et al. 1994).

Besides sugar specificity, CiL-1 and -2 diverge in their amino acid sequence. The first seventeen amino acids of CiL-2 showed no similarity with CiL-1.

Amino acid sequence of CiL-1 was determined by tandem mass spectrometry. Initially, trypsin and chymotrypsin digestion produced some overlapped peptides, but just this was not enough to complete the sequence. In particular, Arg-C digestion was crucial in determining the sequence of NH_2-terminal region, which did not produce reactions in Edman degradation for an unknown reason. Moreover, Arg-C digestion was important to confirm sequences in domain-A, as well as a linked region between the domains. However, amino acid composition of domain B and C-terminal does not allow us to obtain indubitable sequences using Arg-C. Thus, a significant difference (268 Da) was observed between molecular mass determined by MS and calculated molecular mass from sequenced peptides.

This difference was attributed to two or three unfound amino acids in the C-terminal. Since the chymotryptic peptide at m/z 659.62 was finished in Y^{110}, a specific site for chymotrypsin, it is possible to have at least two or three amino acids at the end of the polypeptide chain. Considering this, plausible sequences for this position would be $^{111}LR^{112}$ or $^{111}LGV^{113}$,

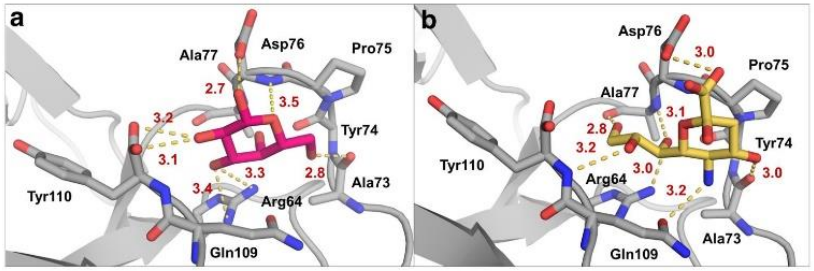

Fig. 9 Monosaccharide binding site II (SII). **a** α-D-galactose coordination. **b** α-neuraminic acid coordination. The protein backbone is represented as light gray cartoons, while residues involved in monosaccharide coordination are represented as gray sticks. Molecular interactions are represented in angstroms by yellow dashed lines. For the purpose of clarity, some residues and interactions involved in the coordination were omitted

Saprolegnia diclina VS20, *S. parasitica* CBS 223.65, and *Aphanomyces astaci*, respectively.

Interestingly, all these fungi are aquatic species. They all belong to the phylum Heterokontophyta, the same one that includes diatoms, kelps, and other brown algae. For purposes of lectinology, the relationship between green algae and aquatic fungus is unclear, but the existence of correlated molecules in such otherwise disparate taxonomic groups reveals a possible case of convergent evolution.

The CiL-1 three-dimensional model also showed structural conservation with lectins of distinct taxonomic groups, including bacterial, fungus, animal and plants, suggesting convergent evolution among these proteins. According to the model, CiL-1 assembles a barrel-like arrangement, possessing two sites for binding of monosaccharides. This fact explains how this monomeric lectin can agglutinate erythrocytes.

Moreover, an extended binding site was observed, likely able to host complex oligosaccharides. In fact, several algal lectins can interact with extended carbohydrates. For instance, lectins from the OAAH family, the members of which have of 13 to 27 kDa, showed affinity for high-mannose *N*-glycans (Chaves et al. 2018).

Antimicrobial activity of lectins isolated from several sources has been reported, including those from marine algae (Liao et al. 2003; Holanda et al. 2005; Vasconcelos et al. 2014). However, because of the greater number of isolated lectins, marine red algae have had a higher number of reported lectins with antimicrobial activity. The lectins isolated from the red algae *Galaxaura marginata* and *Eucheuma serra* strongly inhibited the growth of *Vibrio vulnificus* (Liao et al. 2003). Moreover, the lectin isolated from *Solieria filiformis* showed bacteriostatic effect against the Gram-negative bacteria *Serratia marcescens*, *Salmonella typhi*, *Klebsiella pneumoniae*, *Enterobacter aerogenes*, *Proteus* sp., and *Pseudomonas aeruginosa* (Holanda et al. 2005). The lectin from *Eucheuma denticulatum* inhibited the growth of *Vibrio alginolyticus* (Hirayama et al. 2015).

The antibacterial potential of the lectin isolated from the green alga *Bryopsis plumosa* was verified on several bacterial species, including *S. aureus* and *E. coli*, but no antimicrobial activity was observed (Han et al. 2010); similar results were observed in this study.

Although CiL-1 and CiL-2 did not show antibacterial activity, these lectins were able to inhibit the development of Staphylococcal biofilm, mainly *S. aureus* biofilm. According to (Otto 2019), *S. aureus* and *S. epidermides* are the most causative agents of nosocomial infections from biofilm formation in medical implants. In fact, biofilms are microbial communities that can cause serious medical problems since they present more resistance to antimicrobial agents (Singh et al. 2017). Over 65% of nosocomial infections and 80 % of all microbial infections are caused by formation and persistence of biofilms in the host or in medical hospital devices (Soto 2014).

Some algae lectins were shown to be potential molecules in inhibiting bacterial biofilm formation (Teixeira et al. 2007; Vasconcelos et al. 2014). The lectins isolated from *B. triquetrum* (BTL) and *B. seaforthii* (BSL) could significantly inhibit the formation of streptococci biofilms responsible for the development of dental caries in the early stages. (Vasconcelos et al. 2014) described a screening of antibacterial and antibiofilm activity from plants and algae lectins. The lectins from the marine red algae *B. seaforthii* (BSL) and *Hypnea musciformis* (HML) significantly reduced the biofilm formation of *S. aureus* and caused weak growth reductions in *S. aureus* and *S. epidermidis*.

Lectins may interact with carbohydrates of the biofilm matrix or glycans located on the *Staphylococcus* surface by carbohydrate recognition domain (CRD). The *S. aureus* cell wall is composed of peptidoglycan (PG) and wall teichoic acid (WTA) formed by GlcNAc, ManNAc, MurNAc, and teichoic acid (Romaniuk and Cegelski 2015) which might be recognized by CiL-1 and CiL-2 for antibiofilm activity.

In conclusion, we report two new lectins from the coenocytic green marine alga *Codium isthmocladum*. CiL-1 was characterized in detail, the results of which revealed a new type of lectin with a unique sequence, as well as an unusual fold by its three-dimensional model. Furthermore, the antibiofilm effect of the lectins isolated from *C. isthmocladum* in this study can be exploited for the prevention of infections caused by Staphylococcal biofilms.

Acknowledgments The authors would like to acknowledge the Centro de Tecnologias Estratégicas do Nordeste (CETENE) for providing equipment and technical support for experiments involving MALDI-ToF. The authors are grateful to Professor David Martin for helping in the English writing. A.H.S., and E.H.T. are senior investigators of CNPq. The authors dedicate this article to the memory of Professor David J. Rogers.

Funding information This work was supported by the Brazilian agencies CNPq (Conselho Nacional de Desenvolvimento Científico e Tecnológico), FUNCAP (Fundação Cearense de Apoio ao Desenvolvimento Científico e Tecnológico), and FINEP (Financiadora de Estudos e Projetos).

References

Ainouz IL, Sampaio AHJBM (1991) Screening of Brazilian marine algae for hemagglutinins. Bot Mar 34:211–214

Benevides N, Holanda M, Melo F, Pereira M, Monteiro A, Freitas AJBM (2001) Purification and partial characterization of the lectin from the marine green alga *Caulerpa cupressoides* (Vahl) C. Agardh. 44:17–22

Berjanskii M, Liang Y, Zhou J, Tang P, Stothard P, Zhou Y, Cruz J, MacDonell C, Lin G, Lu P, Wishart DS (2010) PROSESS: a protein structure evaluation suite and server. 38 (suppl 2):W633-W640

Bohne A, Lang E, von der Lieth C-W (1998) W_3-SWEET: carbohydrate modeling by internet. Molec Model Annu 4:33–43

Carneiro RF, de Melo AA, de Almeida AS, Moura Rda M, Chaves RP, de Sousa BL, do Nascimento KS, Sampaio SS, Lima JP, Cavada BS, Nagano CS, Sampaio AH (2013) II-3, a new lectin from the marine sponge *Haliclona caerulea*: purification and mass spectrometric characterization. Int J Biochem Cell Biol 45:2864–2873

Carneiro RF, de Almeida AS, de Melo AA, de Alencar DB, de Sousa OV, Delatorre P, do Nascimento KS, Saker-Sampaio S, Cavada BS, Nagano CS, Sampaio AH (2015) A chromophore-containing agglutinin from *Haliclona manglaris*: purification and biochemical characterization. Int J Biol Macromol 72:1368–1375

Carneiro RF, Lima PHP Jr, Chaves RP, Pereira R, Pereira AL, de Vasconcelos MA, Pinheiro U, Teixeira EH, Nagano CS, Sampaio AH (2017) Isolation, biochemical characterization and antibiofilm effect of a lectin from the marine sponge *Aplysina lactuca*. Int J Biol Macromol 99:213–222

Chai W, Hounsell EF, Cashmore Gc, Rosankiewicz Jr, Bauer Cj, Feeney J, Feizi T, Lawson AMJFjoh (1992) Neutral oligosaccharides of bovine submaxillary mucin: a combined mass spectrometry and ^{1}H-NMR study. Eur J Biochem 203 (1-2):257-268

Chaves RP, da Silva SR, da Silva JPFA, Carneiro RF, de Sousa BL, Abreu JO, de Carvalho FCT, Rocha CRC, Farias WRL, de Sousa OV, Silva ALC, Sampaio AH, Nagano CS (2018) *Meristiella echinocarpa* lectin (MEL): a new member of the OAAH-lectin family. J Appl Phycol 30:2629–2638

Ding S, Yan S, Qi S, Li Y, Yao YJ (2014) A protein structural classes prediction method based on PSI-BLAST profile. J Theor Biol 353: 19–23

Edge A, Spiro RG (1987) Presence of an O-glycosidically linked hexasaccharide in fetuin. J Biol Chem 262:16135–16141

Fabregas J, Muñoz A, Llovo J, Carracedo A (1988) Purification and partial characterization of tornentine, an N-acetylglucosamine-specific lectin from the green alga *Codium tomentosum* (Huds.) Stackh. J Exp Mar Biol Ecol 124:21–30

Han JW, Jung MG, Kim MJ, Yoon KS, Lee KP, Kim GH (2010) Purification and characterization of a D-mannose specific lectin from the green marine alga, *Bryopsis plumosa*. Phycol Rs 58:143–150

Hirayama M, Ly BM, Hori K (2015) Purification, primary structure, and biological activity of the high-mannose N-glycan-specific lectin from cultivated *Eucheuma denticulatum*. J Appl Phycol 27:1657–1669

Holanda ML, Melo VM, Silva LM, Amorim RC, Pereira MG, Benevides NM (2005) Differential activity of a lectin from *Solieria filiformis* against human pathogenic bacteria. Braz J Med Biol Res 38:1769–1773

Jung MG, Lee KP, Choi H-G, Kang S-H, Klochkova TA, Han JW, Kim GH (2010) Characterization of carbohydrate combining sites of Bryohealin, an algal lectin from *Bryopsis plumosa*. J Appl Phycol 22:793–802

Karlsson NG, Nordman H, Karlsson H, Carlstedt I, Hansson GC (1997) Glycosylation differences between pig gastric mucin populations: a comparative study of the neutral oligosaccharides using mass spectrometry. Biochem J 326:911–917

Kelley LA, Mezulis S, Yates CM, Wass MN, Sternberg MJE (2015) The Phyre2 web portal for protein modeling, prediction and analysis. Nature Protocols 10:845–858

Kim DE, Chivian D, Baker D (2004) Protein structure prediction and analysis using the Robetta server. Nucleic Acids Res 32:W526–W531

Kim GH, Klochkova TA, Yoon KS, Song YS, Lee KP (2006) Purification and characterization of a lectin, bryohealin, involved in the protoplast formation of a marine green alga *Bryopsis plumosa* (Chlorophyta). J Phycol 42:86–95

Kouokam JC, Lasnik AB, Palmer KE (2016) Studies in a murine model confirm the safety of griffithsin and advocate its further development as a microbicide targeting HIV-1 and other enveloped viruses. Viruses 8:311

Laemmli UK (1970) Cleavage of structural proteins during the assembly of the head of bacteriophage T4. Nature 227:680–685

Liao W-R, Lin J-Y, Shieh W-Y, Jeng W-L, Huang R (2003) Antibiotic activity of lectins from marine algae against marine vibrios. J Ind Microbiol Biotechnol 30:433–439

Mori T, O'Keefe BR, Sowder RC 2nd, Bringans S, Gardella R, Berg S, Cochran P, Turpin JA, Buckheit RW Jr, McMahon JB, Boyd MR (2005) Isolation and characterization of griffithsin, a novel HIV-inactivating protein, from the red alga *Griffithsia* sp. J Biol Chem 280:9345–9353

Mu J, Hirayama M, Sato Y, Morimoto K, Hori K (2017) A novel high-mannose specific lectin from the green alga *Halimeda renschii* exhibits a potent anti-influenza virus activity through high-affinity binding to the viral hemagglutinin. Mar Drugs 15

Otto M (2019) Staphylococcal biofilms. In: Fischetti VA, Novick RP, Ferretti JJ, Portnoy DA, Braunstein M, Rood JI (eds) Gram positive pathogens, 3rd edn. ASM Press, Washington DC, pp 699–711

Perez-Lorenzo S, Levy-Benshimol A, Gómez-Acevedo S (1998) Presencia de lectinas, taninos e inhibidores de proteasas en algas marinas de las costas Venezolanas. Acta Cient Venez 49:144–151

Praseptiangga D, Hirayama M, Hori K (2012) Purification, characterization, and cDNA cloning of a novel lectin from the green alga, *Codium barbatum*. Biosci Biotechnol Biochem 76:805–811

Rogers D, Flangu H (1991) Lectins from *Codium* species. Br Phycol J 26: 95–96

Rogers D, Swain L, Carpenter B, Critchley AT (1994) Binding of N-acetyl–D-galactosamine by lectins from species of the green marine algal genus, *Codium*. In: Van Driessche E, Fisher J, Beeckmans S, Bog-Hansen TC (eds). Lectins: Biology, Biochemistry, Clinical Biochemistry. Textop, Hellerup (Denmark) 10:162–165

Romaniuk JA, Cegelski L (2015) Bacterial cell wall composition and the influence of antibiotics by cell-wall and whole-cell NMR. Phil Trans Roy Soc B 370 (1679):20150024

Sampaio A, Rogers D, Barwell CJ (1998) Isolation and characterization of the lectin from the green marine alga *Ulva lactuca* L. Bot Mar 41: 427–434

Sato Y, Hirayama M, Morimoto K, Yamamoto N, Okuyama S, Hori K (2011) High mannose-binding lectin with preference for the cluster of alpha1-2-mannose from the green alga *Boodlea coacta* is a potent entry inhibitor of HIV-1 and influenza viruses. J Biol Chem 286: 19446–19458

Savage AV, Donohue JJ, Koeleman CA, van den EIJNDEN DH (1990) Structural characterization of sialylated tetrasaccharides and pentasaccharides with blood group H and Le^x activity isolated from bovine submaxillary mucin. Eur J Biochem 193:837–843

Shevchenko A, Tomas H, Havlis J, Olsen JV, Mann M (2006) In-gel digestion for mass spectrometric characterization of proteins and proteomes. Nat Protoc 1:2856–2860

Singh RS, Walia AK (2018) Lectins from red algae and their biomedical potential. J Appl Phycol 30:1833–1858

Singh S, Singh SK, Chowdhury I, Singh R (2017) Understanding the mechanism of bacterial biofilms resistance to antimicrobial agents. Open Microbiol J 11:53–62

Soto SMJA (2014) Importance of biofilms in urinary tract infections: new therapeutic approaches. Adv Biol 2014:543974

Teixeira E, Napimoga M, Carneiro V, De Oliveira T, Nascimento K, Nagano C, Souza J, Havt A, Pinto V, Gonçalves RB, Farias WRL, Saker-Sampaio S, Sampaio AH, Cavada BS (2007) In vitro inhibition of oral streptococci binding to the acquired pellicle by algal lectins. J Appl Microbiol 103:1001–1006

Terada D, Kawai F, Noguchi H, Unzai S, Hasan I, Fujii Y, Park SY, Ozeki Y, Tame JR (2016) Crystal structure of MytiLec, a galactose-binding lectin from the mussel *Mytilus galloprovincialis* with cytotoxicity against certain cancer cell types. Sci Rep 6:28344

Trott O, Olson AJ (2010) AutoDock Vina: improving the speed and accuracy of docking with a new scoring function, efficient optimization, and multithreading. J Comput Chem 31:455–461

Van Stokkum IH, Spoelder HJ, Bloemendal M, Van Grondelle R, Groen FC (1990) Estimation of protein secondary structure and error analysis from circular dichroism spectra. Anal Biochem 191:110–118

Vanderlei ES, Patoilo KK, Lima NA, Lima AP, Rodrigues JA, Silva LM, Lima ME, Lima V, Benevides NM (2010) Antinociceptive and anti-inflammatory activities of lectin from the marine green alga *Caulerpa cupressoides*. Int Immunopharmacol 10:1113–1118

Vasconcelos MA, Arruda FVS, Carneiro VA, Silva HC, Nascimento KS, Sampaio AH, Cavada B, Teixeira EH, Henriques M, Pereira MO (2014) Effect of algae and plant lectins on planktonic growth and biofilm formation in clinically relevant bacteria and yeasts. Biomed Res Int 2014:365272

Volkamer A, Kuhn D, Grombacher T, Rippmann F, Rarey M (2012) Combining global and local measures for structure-based druggability predictions. J Chem Inf Model 52:360–372

Wang Y, Xiao J, Suzek TO, Zhang J, Wang J, Bryant SH (2009) PubChem: a public information system for analyzing bioactivities of small molecules. Nucleic Acids Res 37:W623–W633

Wang S, Ma J, Peng J, Xu J (2013) Protein structure alignment beyond spatial proximity. Sci Rep 3:1448

Waterhouse A, Bertoni M, Bienert S, Studer G, Tauriello G, Gumienny R, Heer FT, de Beer TAP, Rempfer C, Bordoli L, Lepore R, Schwede T (2018) SWISS-MODEL: homology modelling of protein structures and complexes. Nucleic Acids Res 46:W296–W303

Webb B, Sali A (2016) Comparative protein structure modeling using MODELLER. Curr Protoc Bioinf 54:5.6.1–5.6.37

Whitmore L, Wallace BA (2004) DICHROWEB, an online server for protein secondary structure analyses from circular dichroism spectroscopic data. Nucleic Acids Res 32:W668–W673

Yang J-M, Tung C-H (2006) Protein structure database search and evolutionary classification. Nucleic Acids Res 34:3646–3659

Yang J, Yan R, Roy A, Xu D, Poisson J, Zhang Y (2015) The I-TASSER Suite: protein structure and function prediction. Nat Meth 12:7–8